12-14-2017

Development & Expression Of A Novel Synthetic Flagellin Fusion Protein Containing A Shigella Toxoid Subunit As A Potential Vaccine Against Shigellosis & Stec

Carlos Vazquez

DEVELOPMENT & EXPRESSION OF A NOVEL SYNTHETIC FLAGELLIN FUSION PROTEIN CONTAINING A SHIGELLA TOXOID SUBUNIT AS A POTENTIAL VACCINE AGAINST SHIGELLOSIS & STEC

by

CARLOS VAZQUEZ

Under the Direction of George E. Pierce, PhD

ABSTRACT

Currently, there is no vaccine for Shigellosis. The Shiga-like toxoid 2, by itself, is poorly immunogenic. Flagellin based fusion proteins, serving as toll like receptor agonists, have shown both activation of innate immunity and an increase in adaptive immune responses from normally poorly immunogenic microenvironments. A synthetic flagellin based construct was designed to allow the insertion of detoxified antigen sequences, allowing multivalent expression and antigen presentation. Specifically, subunit B of shiga-like toxin 2, an *Escherichia coli* O157 verocytotoxin, was chosen for co-expression alongside the construct for antigen specific

presentation. The fusion protein, FliC-Stx2B, contains the innate activating synthetic FliC construct along with the genetically modified Stx2B toxoid.

FliC-Stx2B amplicon DNA was produced through PCR while removing the associated signal peptide motif to prevent translocation and increase expression. Additionally, a hexa-histidine affinity tag was incorporated downstream of the amplicon to further aid in purification. Positive clones were induced with varying amounts of IPTG to determine solubility of expressed protein. A detergent wash method, using heavy detergents, was then used to resolubilize & isolate FliC-Stx2B from cell culture pellets. Purification was conducted using ÄKTA® FPLC systems utilizing nickel column affinity. FliC-Stx2B was then refolded while on-column to revert the fusion protein to an intrinsic state, then eluted. Biological activity was determined using Western Blot, ELISA, & TLR5 assays.

Over-expressed FliC-Stx2B was primarily found in insoluble fractions during culture induction studies. Non-desired proteins were removed from the induced insoluble cell pellet fractions during resolubilization, while also isolating FliC-Stx2B. The significant reduction in non-desired protein simplifies FliC-Stx2B purification further due to the addition of the hexa-histidine tag, allowing for nickel column affinity. Purification yields for FliC-Stx2B is reported between 45-70% across varying on-column incubation time points. Binding of anti-Stx2B mAbs, seen in both Western blot and indirect-ELISA assay, confirms that FliC-Stx2B biological activity is maintained following both insoluble protein resolubilization & purification. Preliminary TLR5 activity is seen in purified refolded FliC-Stx2B. These findings indicate that FliC-Stx2B retains its biological activity post-purification and could be a potential vaccine candidate.

INDEX WORDS: Vaccine, Flagellin, FliC, Tlr5, Shigella, Shigellosis, *Escherichia coli* O157:H7, STEC O157:H7, Resolubilization, Process Improvements

DEVELOPMENT & EXPRESSION OF A NOVEL SYNTHETIC FLAGELLIN FUSION PROTEIN CONTAINING A SHIGELLA TOXOID SUBUNIT AS A POTENTIAL VACCINE AGAINST SHIGELLOSIS & STEC

by

CARLOS VAZQUEZ

A Dissertation Submitted in Partial Fulfillment of the Requirements for the Degree of

Doctor of Philosophy

in the College of Arts and Sciences

Georgia State University

2017

DEVELOPMENT & EXPRESSION OF A NOVEL SYNTHETIC FLAGELLIN FUSION PROTEIN CONTAINING A SHIGELLA TOXOID SUBUNIT AS A POTENTIAL VACCINE AGAINST SHIGELLOSIS & STEC

by

CARLOS VAZQUEZ

Committee Chair: George Pierce

Committee: Sidney Crow

Eric Gilbert

Electronic Version Approved:

Office of Graduate Studies

College of Arts and Sciences

Georgia State University

Dec 2017

DEDICATION

I dedicate this dissertation to my wife and family, they are the pillars which support me.

ACKNOWLEDGEMENTS

I would like to thank Dr. George Pierce for his guidance and mentorship while allowing me to conduct research in his lab throughout both my undergraduate and graduate studies. Thank you for teaching me and being an example on what it means to be a professional, a leader, and an instructor. I would like to thank Dr. Sidney Crow for his consistent wisdom and guidance throughout my studies. Thank you for supporting me to go further. I would like to thank Dr. Eric Gilbert for his advice and genuine openness to discuss and aid my research. I would like to thank Dr. Sarah Boyd for mentoring me during the early years of my research. Without her mentorship, and genuine interest in my succeeding, I would not be on the same path that I am on today. Thanks to all of my lab mates throughout the years who have provided scientific & emotional support, guidance, and camaraderie. Thank you to those who have accompanied me during long nights and early mornings, many times in the same day, without complaint. Thank you, Dr. Sarah Boyd, Lionel McNamara, Joshua Renfroe, Dr. John Neville, Kelly Cannon, Maurice de la Croix, Dr. Shirley Belshazzar, Dr. Courtney Barlament, Dr. Trudy Tucker, Latara Northcutt, Michael Maulin,

Thank you to my parents and sister for their love and support as I strived for something not yet accomplished in our family. Lastly, I would like to thank my wife Christine Vazquez for being an endless amount of support and patience. Thank you for your believing in me and for being there through the highs and lows.

TABLE OF CONTENTS

x

LIST OF FIGURES

1 INTRODUCTION

1.1 Impact of *Shigella spp*. & Shigellosis

There are currently no approved vaccines against *Shigella spp.*, either cellular or subunit based. The Program for Appropriate Technology in Health (PATH, 2015) in their global report indicated that *Shigella spp.* & enterotoxigenic *Escherichia coli* based diseases may account for up to one billion cases of diarrheal episodes in both children and adults annually. The Centers for Disease Control (CDC, 2011) also estimates a minimum of 265,000 infections occur in the United States annually. Current detection methods are still being developed by the Global Enterics Multicenter Study (GEMS) foundation, amongst others, and infection rates may in fact be greater in number (Kotloff, *et al*., 2013). Investigators have recently shown that qualitative PCR (qPCR) methods indicated that the previously reported rate of 9.6% for *Shigella spp.* infections is actually considerably higher (Lindsay, *et al.*, 2013).

Shigella spp. based infections have been reported through GEMS to be one of four pathogens associated with moderate-to-severe diarrhea amongst children in sub-Saharan Africa and Southeast Asia; affecting all age groups but especially troublesome for children ages 5 and below, (Mani, *et al*., 2016; Ho, *et al.,* 2013; Mead, 1999). The Child Health Epidemiology Reference Group (CHERG) and the Institute for Health Metrics and Evaluation (IHME) have reported that in endemic areas STEC caused as many as 28,000 deaths in 2011 & 34,400 deaths in 2013 in children ages 5, respectfully, (Lanata, *et al*., 2013). In age groups above 5 years, meta-analysis suggests that an additional 40,000 deaths in these areas may also have been due to *Shigella spp.* infections. In older demographics, (Mani, *et al*., 2016; Lamberti, *et al*., 2014; Lanata, *et al*., 2013), STEC infections were in fact at a higher rate than both cholera and typhoid combined. In addition to people living in affected areas, travelers and military personnel are at

high risk when visiting these countries which also adds to the overall disease burden, (Mani, *et al*., 2016; Cohen, *et al*., 1988). Transmission is accomplished through person-to-person interactions or through the ingestion of contaminated food or water; there is no animal reservoir, (Mani, *et al*., 2016).

In addition to mortality rates, IHME (2010) also reported that the overall disability-adjusted life years (DALYs) estimates associated with shigellosis has risen to 7 million, while years lived with disability (YLDs) has been estimated to be around 744,000. These estimates, aided by recent advancements in screening analysis, represent 7.8% of all diarrheal DALYs & 9% of all diarrheal YLDs for disease burden.

1.2 Conjugate Shiga toxin-producing *Escherichia coli* (STEC) effects

Shigella spp. present other forms of issues as well, having the ability for horizontal gene transfer between species or sister-species, (Brussow, *et al*., 2004). Specifically, between *Escherichia coli* and its sister-species *Shigella dysenteriae;* a dysenteric Gram-negative rod which uses its' F-like pili to laterally transfer gene sequences between plasmids (Filloux, 2010; Miyake, 1962; Miyake & Demerec, 1959). This allows swapping of key genetic material amongst the related bacterium, further increasing its competitive evasiveness and complicating targeted vaccine development. When these bacteria conjugate, a Shiga-toxin producing strain of *E. coli* (STEC) is produced and may lead to shigellosis-like infections. It is also alternatively referred to as verocytotoxin-producing *E. coli* (VTEC).

The recent increase in detectable instances of shigellosis & shigellosis-like infections, from *Shigella spp*. & STEC, warrants further attention in ways to combat diarrheal infections. Especially, in areas where clean water, food, and cold chain storage options are not available due

to harsh environments or by economic means. Transmission of STEC *spp.* is accomplished through person-to-person interactions or through the ingestion of contaminated food or water (Mani, S. *et al*., 2016).

The effects of shiga toxin are similar in nature to that of *Ricinus communis* (Ricin toxin), causing malfunctions and alterations to ribosomes altering the production of protein (Sandvig, 2000). Young patients or those with compromised immune systems may also develop hemolytic uremic syndrome (HUS) leading to acute kidney failure due to the death of renal cells (Houdouin, *et al*., 2004).

HUS is characterized histologically through glomerular microvascular platelet adhesion aggregation/aggregation and the formation of fibrin polymers (Huang, *et al*., 2010). In addition, diarrhea associated HUS (D+HUS) also may include; thrombocytopenia, microangiopathic hemolytic anemia, acute renal failure. In the United States, acute renal failure affects children under the ages of 5 years old with a mortality rate of 3-5%, and is most commonly caused by D+HUS, (Huang *et al*., 2010; Tarr, *et al*., 2005; Garg, *et al*., 2003).

1.3 Shiga toxin structure & mode of action

The family of Shiga-like toxins expressed by STEC strains contain two groups designated Stx1 & Stx2. While only two groups exist, there are many sub-groups and serotypes. Stx2 has been shown epidemiologically to exhibit a higher rate of potency (100x) comparatively to Stx1 (Scheutz, *et al*., 2012; Fuller, *et al*., 2011). Furthermore, patients infected with STEC strains expressing shiga toxin type 2 generally have a higher rate of developing D+HUS than those with Stx1based infections. Due to this, Stx2 has become a target for directed vaccination therapy, focusing on pre-attachment disruption.

X-ray crystallography has revealed that the Shiga toxin structural configuration normally presents as an AB_5 complex (Fig. 1). A combination of the toxigenic A subunit (StxA) binds non-covalently to a B subunit (StxB) pentamer complex. The B subunit portion of the complex is associated with binding to cell surface receptors, specifically Globotriaosylceramide (Gb3), (Johannes & Römer, 2009; Fraser, *et al.,* 1994; Stein, *et al*., 1992). StxA/Stx2B holotoxin construction is accomplished by insertion of StxA's carboxyl terminus into the donut-shaped pentamer structure created by Stx2B formation during non-colavent assembly in the cell's periplasm, (Johannes & Römer, 2009).

Attachment of the holotoxin complex is vital for successful insertion into the host cell (Fig. 2). Shiga toxin AB_5 complex uses the B subunit to attach to Gb3 receptors (CD77) located on the cell surface, and will attach to these receptors even in the absence StxA, (Johannes & Römer, 2009). Following attachment, the holotoxin is taken up via endocytosis into the cell for subsequent retrograde transport to the endoplasmic reticulum (ER), (Johannes & Römer, 2009; Sandvig, 2000). Retrograde translocation of the holotoxin allows for the A subunit to be released into the cytoplasm. From there Stx2A may cleave an adenine base located on the α-sarcin loop in eukaryotic ribosomes, then use the altered ribosome as substrate. This cleavage event prevents tRNA binding preventing translation of protein, (Johannes & Römer, 2009).

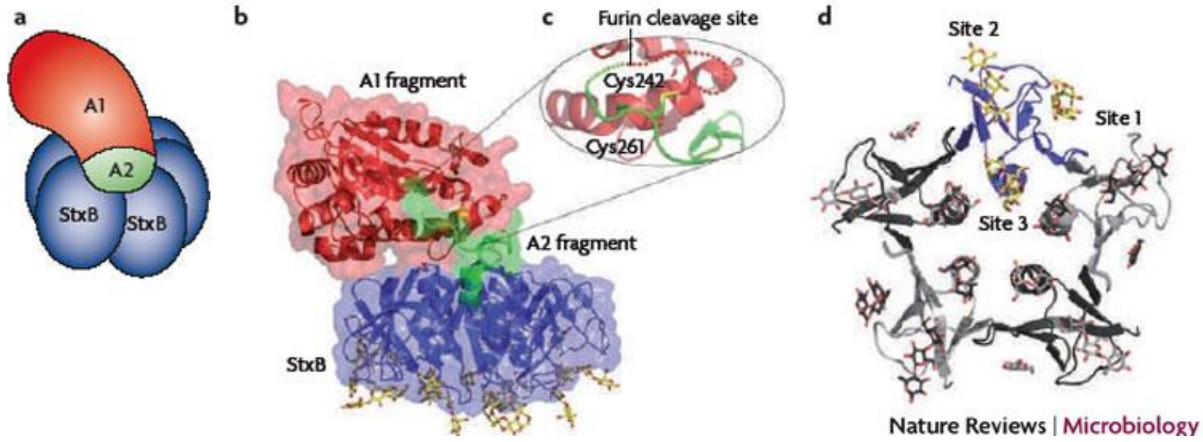

Figure 1.1 Shiga toxin AB_5 structures (Johannes & Römer, 2009)

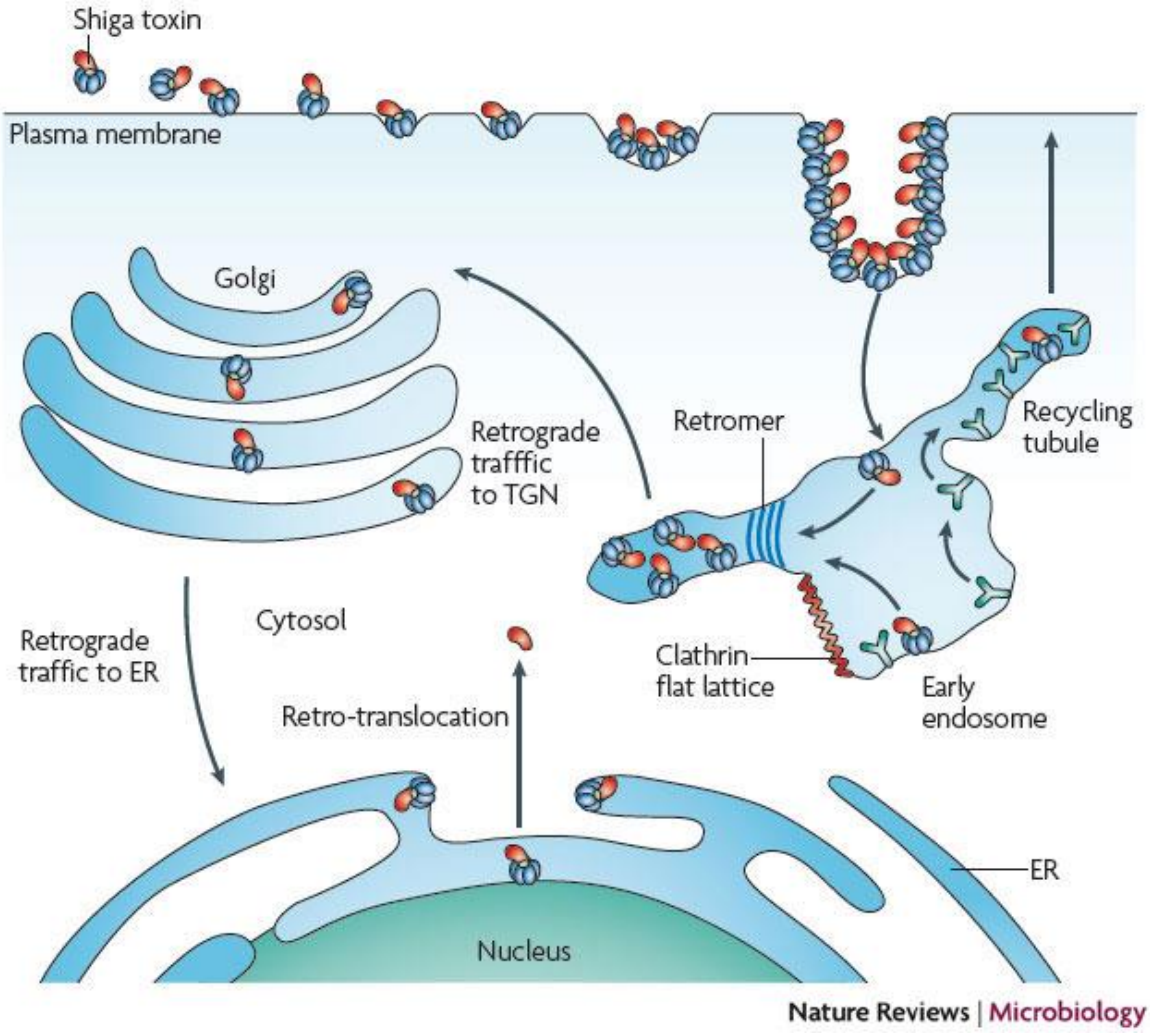

Figure 1.2 Shiga toxin mechanism of action (Johannes & Römer, 2009)

1.4 STEC foodborne-illness outbreak risks

A foodborne related outbreak is defined as an instance when two or more people get the same illness from the same contaminated food source, (CDC). More recently, foodborne related outbreaks have become more rampant due to the conjugative abilities of *Shigella spp.* and *E. coli* strains to produce the toxigenic strains of STEC. These strains, as mentioned previously, may illicit harmful symptoms such as; diarrhea, hemolytic uremic syndrome, fever, abdominal cramping, vomiting, and hemorrhagic colitis when infected, (Yang, *et al*., 2017; Kaper, *et al*., 2004). Because of STEC's ability to cause hemorrhagic colitis it is also commonly referred to as enterohemorrhagic *E. coli* (EHEC).

The primary mechanism for transmission of STEC strains is through the direct ingestion of contaminated foods, or contact with infected ruminant animals, (Yang, *et al*., 2017). Transmission of STEC strains, however, differ than *Shigella spp*. due to the fact that *Shigella spp*. do not have an animal reservoir. This fact makes STEC a further reaching threat in comparison to *Shigella spp.* producing the shiga toxin. This is especially concerning in farms dedicated to mass food crop production where detection methods may not be fully encompassing. It also is possible to transmit STEC through person-to-person interactions, however close proximity is required.

STEC infections are primarily foodborne and thrive over a wide range of temperatures, (Chaucheyras-Durand, *et al*. 2010). Infections are prevalent in cases where undercooked ground beef, raw milk, salads, raw leeks, vegetables, and fruits are the common food sources (Yang, *et al*., 2017; Herman, *et al.,* 2015; Feng, 2014). Moreover, the amount of STEC cells necessary to become infectious is relatively low (CDC, 2010). With STEC's ability to thrive in varying

temperatures, grow on common foods, and low ID50, the threat of STEC foodborne related outbreaks becomes increasingly problematic.

Due to the conjugative relationship between *Shigella spp*. & *E. coli* many forms of STEC can be produced as a result of variable chance. The most commonly associated serotypes include, O26, O111, and O157 (Pennington, 2010). STEC O157:H7, however, is the serotype mostly associated with foodborne-illness outbreaks in the world, (Yang, *et al*., 2017). It has evolved over time to include both the Stx1 and Stx2 genes and virulence factors such as; intimin, translocated intimin receptors, type III secretion system, and hemolysis, (Yang, *et al*., 2017; Saitoh, *et al*., 2008). Recent STEC O157:H7 outbreaks affecting certain food crops grown for mass food supply have infected numerous individuals and has been fatal for some. Specifically, serotypes O104:H4, O157 PT8, O111:NM, and *S. flexneri* serotype 2 have caused instances of fatal infections in those infected, (Yang, *et al*., 2017).

1.5 Current efforts against Shigellosis

As stated previously, there are currently no approved vaccines against Shigella, either cellular or subunit based. One of the factors adding to the growing need for vaccine development lies with effective sanitation & hygiene for diarrheal prevention. However, in areas where clean water and medication is not accessible other means for disease prevention is further warranted. Cost benefit analyses have shown that vaccination therapy in comparison to cost-prohibitive water and sanitation infrastructure development may be a more viable option, especially in low-income countries, (Mani, *et al*., 2016). *Shigella spp.* contain 50 different serotypes which all pose certain challenges when constructing a vaccine designed to be all-compassing, (Mani, et al.,

2016; Livio, *et al.,* 2014). A vaccine designed to have multivalent effects for high levels of protection is one way to increase overall coverage.

Currently, there are several types of vaccine candidates against *Shigella spp.* being developed; cellular, glycoconjugate, novel antigen, & subunit based (Mani, et al., 2016). Cellular candidates have reached phase II clinical trials using a mutated virG-based live attenuated strain, (Venkatesan & Ranallo, 2016). Glycoconjugate candidates using O polysaccharides covalently linked to carrier glycoconjugates have reached phase III trials, (Pozsgay, *et al*., 1999). Novel candidates generally have focused on immune system priming through addition of *Shigella spp.* LPS or outer membrane vesicles with some form of transportation mechanism, (Mani, et al., 2016). Candidates that use a subunit approach to illicit immune response represent the least amount of total vaccine candidates with only two reaching phase I clinical trials. PATH laboratories are currently testing a DB fusion protein that combines two T3SS antigens along with an invasion plasmid antigen, (Martinez-Becerra, *et al.,* 2012). Another subunit based approach is seen in the NICED produced 34kDa OmpA vaccine candidate, which utilizes conserved and cross reactive Omps from *Shigella flexneri* 2a, (Pore & Chakrabarti, 2013).

Subunit based candidates may also produce humoral protection, as they aim for antigen recognition during adaptive immune response, however have only been tested in animals. Specifically, PATH has been conducting trials on co-administration effects using a double-mutant toxin (dmLT) adjuvant in order to initiate innate immune system responses when paired with the DB fusion protein (Mani, et al., 2016; Martinez-Becerra, *et al.,* 2012).

1.6 Native Flagellin (FliC) background

A need for enhanced vaccine candidates has risen due to the increase in antigenic evasion within patients presenting with poorly immunogenic defense mechanisms. Flagellin based vaccines serving as toll like receptor (TLR) agonists have shown increased efficacy over the years in increasing danger signals against non-self antigens within poorly immunogenic microenvironments, (Leigh, et al., 2012). Flagellin/TLR5 receptor interactions initiate an innate immune response which may then activate and mature antigen presenting cells (APCs) creating pro-inflammatory responses (Leigh, *et al.* 2014; Osterhaus, 2014; Sabag & Lorberboum-Galski, 2014; Song, *et al.* 2014, Tarahomojoo, 2014). Specifically, modified multivalent flagellin platforms, FliC, that co-express detoxified antigenic sequences.

FliC is a monomer protein of the flagellar protofilament used to form the molecular motor that allows locomotion in bacteria. The subunit is comprised of four domain regions (D_0, D_1, D_2, and D_3) that form a hairpin turn, creating a linear structure that reads N - Terminus, D_0, D_1, D_2, D_3, D_2, D_1, D_0, C – Terminus (Fig. 3). It has been shown in previous research that Domains 1 & 2 contain high affinity with TLR5 receptors and are highly conserved in many Gram-negative bacteria such as *Salmonella spp.* (Song, *et al*., 2014; Mizel & Bates, 2010; Yoon, *et al*., 2012; Donnelly & Steiner, 2002). The D3 region is not conserved or necessary for TLR5, and is therefore called the hypervariable region, (Liu, *et al*., 2010).

By having high affinity for TLR5 receptors, FliC may initiate an innate immune response through activation and maturation of dendritic and natural killer cells, creating a pro-inflammatory cytokine response within the microenvironment. FliC has shown potential as a vaccine adjuvant within models where poor immunogenicity persists, (Leigh, *et al*., 2014; Osterhaus, 2014; Sabag & Lorberboum-Galski, 2014: Song, *et al*., 2014; Tarahomjoo, 2013).

Specifically, modified fusion FliC platforms that may co-express non-toxic or detoxified antigenic sequences.

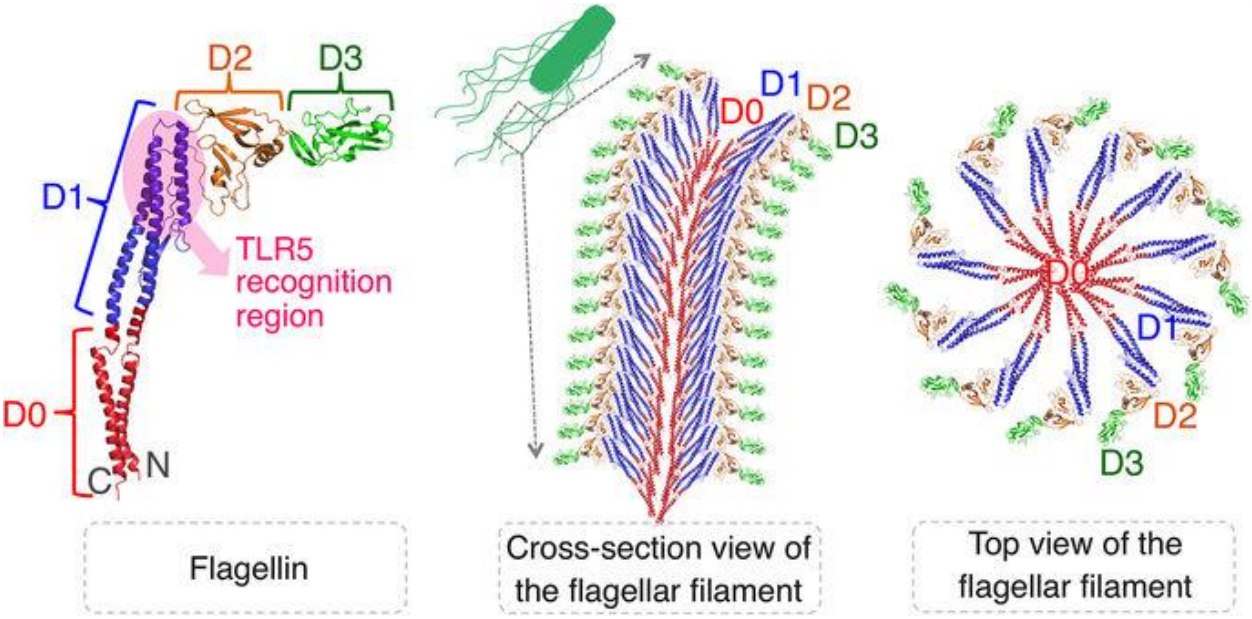

Figure 1.3 Native FliC structure, cross-section, and top view (Lu & Swartz, 2016)

1.7 Synthetic FliC platform

To utilize the innate cell activating FliC platform, modifications were made to the N & C terminal D_0 domains and the hypervariable D_3 domain so that specific sequences may be inserted for co-expression, (Boyd, 2014; Gupta, et al., 2014; Osterhaus, 2014; Sabag & Lorberboum-Galski, 2014; Song, *et al*., 2014). It has been shown in previous research that the FliC D_1 domain, and portions of the D_2 domain, were necessary for TLR5 activation whereas the D_0 domain of both the N & C termini were not (Yoon, *et al*., 2012; Andersen-Neissen, *et al*., 2005; Smith, *et al*., 2003; Donnelly & Steiner, 2002). The D_0 domain, therefore, was chosen to contain several

common restriction enzyme recognition sites for sequence insertions at either the N or C terminal ends of the modified FliC construct, (Boyd, 2014).

Other research reported that replacing the hypervariable region with a DNA sequence of equal size allowed for the same levels of inflammation as native FliC. However, when DNA larger than the original hyper variable sequence was inserted, inflammation responses decreased. The D_3 hypervariable domain aids in the spatial relationship of both D_1 and D_2 domains when interacting with TLR5 receptors. Therefore, changes in the hyper variable region for innate responses may be inhibited by size, (Liu, *et al.*, 2010; Donnelly & Steiner, 2002; Eaves-Pyles, *et al.*, 2001). Because of this, synthetic FliC contains a hypervariable D_3 region the same length as the wild type. Moreover, in synthetic FliC restriction enzyme cut sites totaling six base pairs long are placed every 15 nucleotides, allowing compensation for gene insertion sizes (Boyd, 2014). In order to determine construct stability following hypervariable domain gene insertion a monomeric fluorescent protein (mRFP) construct was designed and inserted into synthetic FliC.

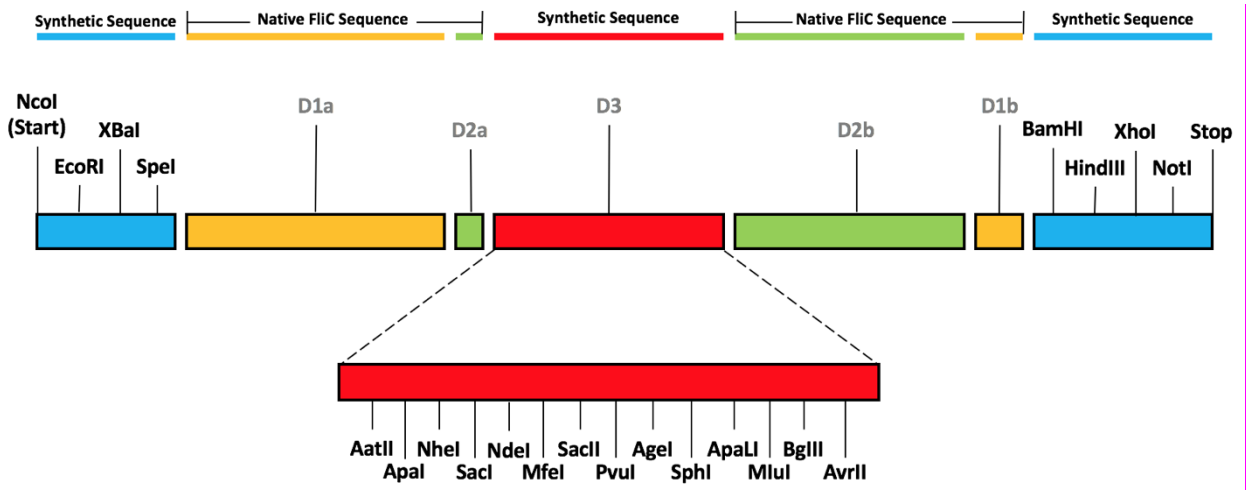

Figure 1.4 **Synthetic FliC cloning map (Boyd, 2014)**

1.8 Stx2B-1N rationale and design

As stated previously, flagellin based recombinant fusion protein vaccines serving as toll like receptor (TLR) agonists have shown increased efficacy in regard to generating an immune response. Because of this, the synthetic FliC platform was used in conjunction with the B-subunit of Shiga like toxoid 2 (Stx2B) to form Stx2B-1N, a bivalent recombinant based vaccine adjuvant candidate (Leigh, *et al*., 2014).

Stx2B was modified, *in silico*, so that it could be to be inserted into the N' terminal end of synthetic FliC, directly flanking the TLR5 activating D1 domain. In addition, to facilitate a more rapid purification of the desired recombinant protein a hexa-histidine tag was included into Stx2B-1N at the C' terminal (D0 domain) end, which has been previously shown not to alter the epitope binding site affinity (D1 & D2 domains) associated with immune system priming, (Yoon, *et al*., 2012; Andersen-Neissen, *et al*., 2005; Donnelly & Steiner, 2002).

1.9 FliC-Stx2B rationale and design

Empirically, it has been shown that Stx2B secretory mechanisms involved in its translocation can excrete the protein either extracellularly or in cell-associated fractions in phage induced *Enterohemorrhagic Escherichia coli* (EHEC) models, similarly to Stx1 secretion, (Shimizu, *et al.*, 2009). However, it also has been shown in previous studies that the addition of the type 3 secretion system (T3SS) signal peptide motif in both Stx A & B subunits may lead to excessive translocation of the protein into either membranous fractions or its' conditioned media (Leung, *et al*., 2002; Skinner & Jackson, 1998). Purification attempts using constructs containing the associated signal peptide (Stx2B-1N) produced low purified product yields. In order to help prevent translocation issues, post-translation, the associated signal peptide sequence

(MKKMFMAVLFALASVNAMA) from the toxoid STx2B gene sequence was removed through polymerase chain reaction. With the removal of the signal peptide, sequestration of the desired protein remains cytoplasmic. Over-expressed FliC-Stx2B is found in insoluble form, collecting in inclusion bodies which have lower endotoxin units when compared to soluble protein fractions. Furthermore, significant overexpression of FliC-Stx2B is also seen in comparison to constructs retaining the signal peptide sequence (Stx2B-1N).

In order to produce an industry level standard fusion protein to be used as a potential vaccine candidate, refolding of FliC-Stx2B is required due to it being insoluble. Refolding of FliC-Stx2B was designed to occur while on-column or during dialysis procedures. Refolding of the protein allows FliC-Stx2B to revert back to its' intrinsic nature, prior to purification. On-column refolding of the fusion protein also provides a more rapid purification process.

1.10 FliC-Stx2B protein process methodology

1.10.1 Enhanced cell clarification and protein isolation

Over expressed FliC-Stx2B is primarily found, at high yield, in insoluble inclusion body fractions following cell culture induction. In order to isolate the fusion protein from insoluble fractions a detergent based method is used to facilitate separation. This isolation significantly removes non-desired protein from the final resolubilized sample, improving sample yields for further downstream processing & purifications

1.10.2 Enhanced cell clarification and protein isolation

Resolubilized FliC-Stx2B on-column refolding is combined with AKTA® FPLC purification to enhance and streamline previous insoluble protein purification methodologies.

Once adhered to the column, resolubilized FliC-Stx2B sample is gradually introduced to a refolding buffer, using a stepwise gradient, then allowed to incubate over time. This refolding process gently refolds the fusion protein allowing for greater hexa-histidine tag presentation to further aid in column binding. Previous refolding procedures required liters of refolding buffer and hours of subjugation.

1.10.3 Biological activity profile characterization

Characterization of a novel fusion protein is vital for viability assessment prior to further pre-clinical or animal model studies. Verification analysis was accomplished qualitatively through SDS-PAGE & Western blot (anti-stx2b). To characterize FliC-Stx2B biological activity indirect-ELISA, tested over a certain concentration gradient, was used to identify high-and-low concentration thresholds.

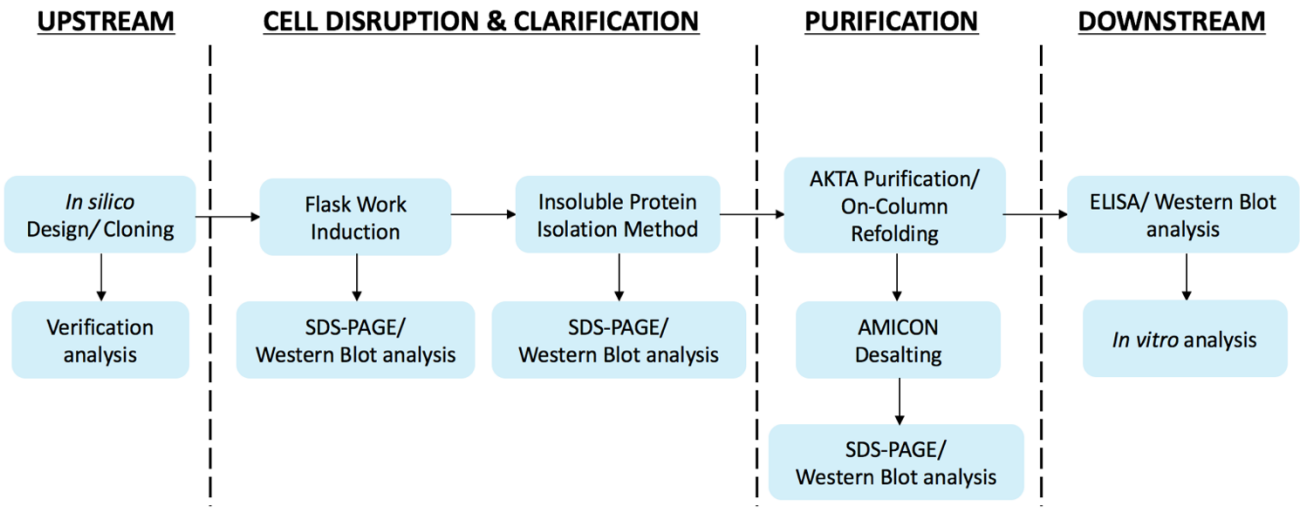

Figure 1.5 Process overview

1.11 Objectives

1.11.1 To design and develop a recombinant protein containing subunit B of shiga-like toxin 2 located in a synthetic FliC platform for overexpression

Genetic isolation of subunit B of shiga-like toxin 2 (Stx2B) from its origin AB_5 complex removes toxicity associated with the toxigenic A subunit. Concurrent genetic removal of Stx2B's TTSS signal peptide may produce an insoluble protein with toxoid classification.

1.11.2 To reach an approach to optimize and enhance current methods used for extraction and resolubilization of the insoluble recombinant protein FliC-Stx2B

By characterizing key factors involved with the insoluble extraction of FliC-Stx2B, an increase in yield may be obtained. These factors include: varying concentrations of urea used during detergent step washes, the amount of detergent washes utilized prior to resolubilization of the insoluble protein, and the intensity of shaking subjugated on the sample during the resolubilization phase.

1.11.3 To determine and further characterize the innate & adaptive biological activity profile of FliC-Stx2B utilizing epitope affinity

By design, FliC-Stx2B utilizes the Toll like receptor 5 activating synthetic FliC platform and the potentially humoral activating shiga-like toxin 2 subunit B. Through receptor affinity, TLR5 activation in HEK (human embryonic kidney) cells may be similar or equivalent to that of currently available protein standards used for academic and preclinical studies. Furthermore, utilizing resolubilization and refolding techniques, retention of biological activity against the Stx2B epitope domain may be similar to untreated samples.

2 METHODS & MATERIALS

2.1 *In silico* design

2.1.1 mRFP

In order to insert mRFP into the synthetic FliC construct, in silico work was conducted to make sure there were no frame shifts or added stop codon sequences, post insertion. This was done by isolating the mRFP gene sequence from the psB1AC3 host plasmid provided by the iGEM laboratory at Georgia State University, shown below highlighted.

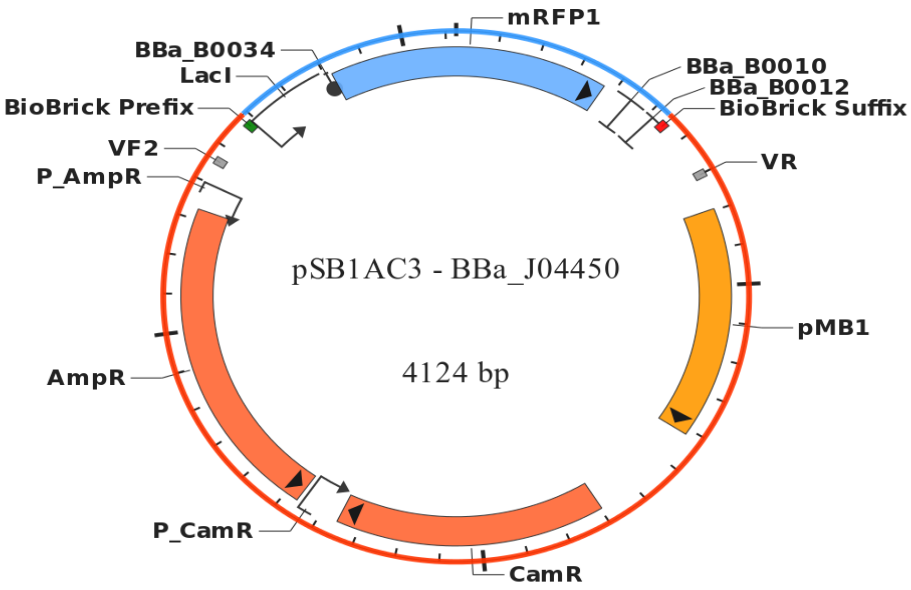

Figure 2.1 pSB1AC3 host plasmid containing mRFP construct BBa-J04450 (iGEM, 2009)

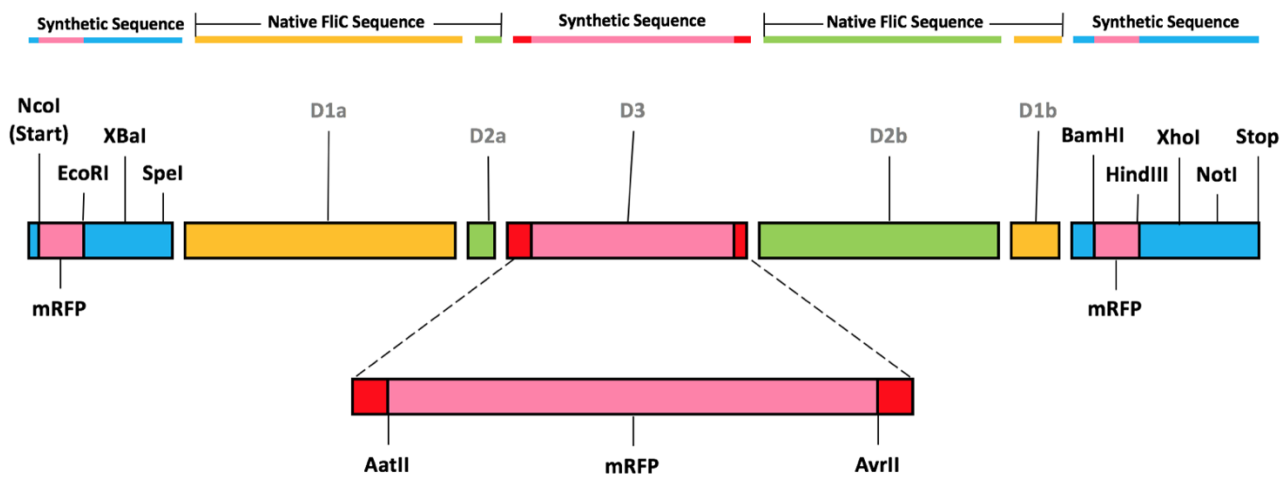

Figure 2.2 Possible cloning sites for mRFP at N' & C', and hyper variable regions on R2 construct

ATGGCTTCCTCCGAAGACGTTATCAAAGAGTTCATGCGTTTCAAAGTTCGTATGGAAGGTTCCGTTA
ACGGTCACGAGTTCGAAATCGAAGGTGAAGGTGAAGGTCGTCCGTACGAAGGTACCCAGACCGCTA
AACTGAAAGTTACCAAAGGTGGTCCGCTGCCGTTCGCTTGGGACATCCTGTCCCCGCAGTTCCAGTA
CGGTTCCAAAGCTTACGTTAAACACCCGGCTGACATCCCGGACTACCTGAAACTGTCCTTCCCGGAA
GGTTTCAAATGGGAACGTGTTATGAACTTCGAAGACGGTGGTGTTGTTACCGTTACCCAGGACTCCT
CCCTGCAAGACGGTGAGTTCATCTACAAAGTTAAACTGCGTGGTACCAACTTCCCGTCCGACGGTCC
GGTTATGCAGAAAAAAACCATGGGTTGGGAAGCTTCCACCGAACGTATGTACCCGGAAGACGGTGC
TCTGAAAGGTGAAATCAAAATGCGTCTGAAACTGAAAGACGGTGGTCACTACGACGCTGAAGTTAA
AACCACCTACATGGCTAAAAAACCGGTTCAGCTGCCGGGTGCTTACAAAACCGACATCAAACTGGA
CATCACCTCCCACAACGAAGACTACACCATCGTTGAACAGTACGAACGTGCTGAAGGTCGTCACTC
CACCGGTGCT

Figure 2.3 mRFP in host plasmid pSB1AC3 nucleotide sequence (675 bp)

Met A S S E D V I K E F **Met** R F K V R **Met** E G S V N G H E F E I E G E G E G R P Y E G T Q T A K L K
V T K G G P L P F A W D I L S P Q F Q Y G S K A Y V K H P A D I P D Y L K L S F P E G F K W E R
V **Met** N F E D G G V V T V T Q D S S L Q D G E F I Y K V K L R G T N F P S D G P V **Met** Q K K
T **Met** G W E A S T E R **Met** Y P E D G A L K G E I K **Met** R L K L K D G G H Y D A E V K T T Y **Met** A K
K P V Q L P G A Y K T D I K L D I T S H N E D Y T I V E Q Y E R A E G R H S T G A

Figure 2.4 mRFP amino acid sequence (225 amino acids)

To enhance mRFP DNA amplification for insertion into the host plasmid, primers were designed to contain specific N' terminal, C' terminal, and hypervariable region restriction enzyme cut sites. This would allow no further modifications to the isolated gene following PCR prior to restriction enzyme digest.

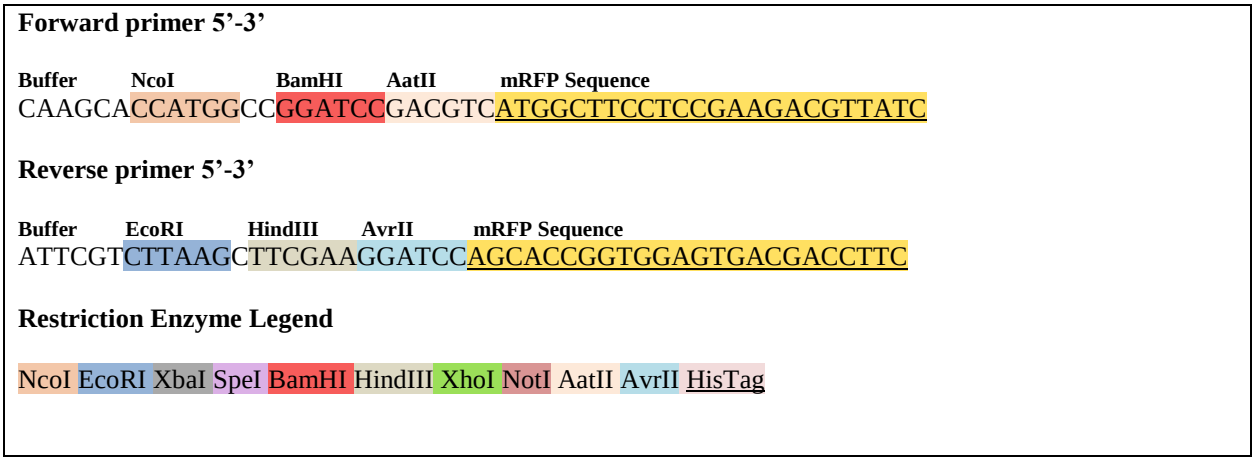

Figure 2.5 mRFP Primer Design

The isolated mRFP sequence was primarily designed to be inserted in between the restriction enzyme cut sites NcoI and EcoRI, located on the N' terminal domain of the synthetic FliC construct. The proposed gene sequence was ran through ExPasy® translation software in order to determine if stop codons were produced with the theorized insertion design.

AGGAGGTAAAACACCATGGCCGGATCCGACGTCATGGCTTCCTCCGAAGACGTTATCAAAGAGTTC
ATGCGTTTCAAAGTTCGTATGGAAGGTTCCGTTAACGGTCACGAGTTCGAAATCGAAGGTGAAGGT
GAAGGTCGTCCGTACGAAGGTACCCAGACCGCTAAACTGAAAGTTACCAAAGGTGGTCCGCTGCCG
TTCGCTTGGGACATCCTGTCCCCGCAGTTCCAGTACGGTTCCAAAGCTTACGTTAAACACCCGGCTG
ACATCCCGGACTACCTGAAACTGTCCTTCCCGGAAGGTTTCAAATGGGAACGTGTTATGAACTTCGA
AGACGGTGGTGTTGTTACCGTTACCCAGGACTCCTCCCTGCAAGACGGTGAGTTCATCTACAAAGTT
AAACTGCGTGGTACCAACTTCCCGTCCGACGGTCCGGTTATGCAGAAAAAAACCATGGGTTGGGAA
GCTTCCACCGAACGTATGTACCCGGAAGACGGTGCTCTGAAAGGTGAAATCAAAATGCGTCTGAAA
CTGAAAGACGGTGGTCACTACGACGCTGAAGTTAAAACCACCTACATGGCTAAAAAACCGGTTCAG
CTGCCGGGTGCTTACAAAACCGACATCAAACTGGACATCACCTCCCACAACGAAGACTACACCATC
GTTGAACAGTACGAACGTGCTGAAGGTCGTCACTCCACCGGTGCTCCTAGGAAGCTTCGAATTCGGT
CTAGAACTAGTGCAGCCGGCCAGGCGATTGCGAATCGTTTTACGGCGAACATCAAGGGTCTGACCC
AAGCCTCTCGTAATGCAAATGATGGTATTAGCATCGCACAAACCACCGAAGGCGCGCTGAACGAGA
TCAACAATAACTTGCAACGTGTCCGTGAGCTGGCAGTTCAGAGCGCGAACAGCACGAATAGCCAGT
CCGATTTGGACAGCATCCAGGCGGAGATTACGCAACGTTTGAACGAAATCGACCGCGTCAGCGGTC
AAACGCAGTTTAATGGTGTGAAAGTTCTGGCCCAGGATAACACCCTGACGATTCAGGTTGGCGCAA
ACGACGGTGAAACGATTGATATTGACCTGAAGCAGATCAACAGCCAAACCCTGGGTCTGGACACCC
TGAACGTGCAACAAAAGTATAAGGTGTCGGACACGGCCGCTACCGTGACCGGCGACGTCGATACTA
CGATTGCTGGGCCCAATAGTACTTTTAAAGCTAGCGCTACTGGTCTTGGTGAGCTCGACCAGAAAAT
TGATCATATGTTAAAATTTGATGATCAATTGGGAAAATATTACGCCCCGCGGACCGTTACGGGGGG
ACGATCGAAAGATGGCTATTATACCGGTTCCGTTGATAAGACGGCATGCGAGGTGACTCTTGCTGTG
CACGCGACTTCCCCGCTTACGCGTGGACTACCTGCGACAAGATCTGAGGATGTGAAAAATCCTAGG
GTTGCCAACGCTGACCTGACCGAGGCGAAAGCGGCGCTGACCGCAGCGGGCGTTACTGGTACCGCA
AGCGTTGTGAAAATGAGCTACACCGACAATAATGGTAAAACTATCGATGGCGGTCTGGCGGTCAAA
GTCGGCGACGACTACTATTCCGCCACCCAGAACAAAGACGGCAGCATCAGCATTAACACTACGAAA
TACACCGCAGATGACGGCACGAGCAAAACGGCACTGAATAAGCTGGGCGGTGCGGATGGTAAGAC
CGAAGTTGTTAGCATTGGTGGTAAAACCTATGCCGCGTCCAAGGCAGAGGGTCACAATTTCAAGGC
GCAGCCGGATCTGGCGGAAGCTGCAGCGACCACGACCGAGAATCCGTTGCAGAAGATTGATGCGGC
GCTGGCACAGGTCGATACGCTGCGCTCTGACCTGGGTGCCGTACAAAACCGTTTCAATAGCGCGAT
CACCAATCTGGGCAACACCGTGAACAATCTGACCTCTGCTCGCAGCCGTATTGAGGGATCCAAGCTT
CTCGAGTAGGCGGCCGCAAGC

Figure 2.6 Synthetic FliC construct with mRFP in N' terminus (2,007 bp)

R R **Stop** N T **Met** A G S D V **Met** A S S E D V I K E F **Met** R F K V R **Met** E G S V N G H E F E I E G E G E
G R P Y E G T Q T A K L K V T K G G P L P F A W D I L S P Q F Q Y G S K A Y V K H P A D I P D Y L K
L S F P E G F K W E R V **Met** N F E D G G V V T V T Q D S S L Q D G E F I Y K V K L R G T N F P S D G
P V **Met** Q K K T **Met** G W E A S T E R **Met** Y P E D G A L K G E I K **Met** R L K L K D G G H Y D A E V K
T T Y **Met** A K K P V Q L P G A Y K T D I K L D I T S H N E D Y T I V E Q Y E R A E G R H S T G A P R K
L R I R S R T S A A G Q A I A N R F T A N I K G L T Q A S R N A N D G I S I A Q T T E G A L N E I N N N
L Q R V R E L A V Q S A N S T N S Q S D L D S I Q A E I T Q R L N E I D R V S G Q T Q F N G V K V L A
Q D N T L T I Q V G A N D G E T I D I D L K Q I N S Q T L G L D T L N V Q Q K Y K V S D T A A T V T G
D V D T T I A G P N S T F K A S A T G L G E L D Q K I D H **Met** L K F D D Q L G K Y Y A P R T V T G G
R S K D G Y Y T G S V D K T A C E V T L A V H A T S P L T R G L P A T R S E D V K N P R V A N A D L
T E A K A A L T A A G V T G T A S V V K **Met** S Y T D N N G K T I D G G L A V K V G D D Y Y S A T Q
N K D G S I S I N T T K Y T A D D G T S K T A L N K L G G A D G K T E V V S I G G K T Y A A S K A E
G H N F K A Q P D L A E A A A T T T E N P L Q K I D A A L A Q V D T L R S D L G A V Q N R F N S A I
T N L G N T V N N L T S A R S R I E G S K L L E **Stop** A A A S

Figure 2.7 Synthetic FliC with mRFP amino acid sequence (661 amino acids)

2.1.2 Stx2B-1N stepwise PCR

Initially, primers were designed utilizing a step wise method, incorporating flanking DNA restriction enzyme cut sites during each round of PCR to produce insert DNA that may be incorporated into N' & C' terminal domains (Appendix A.1). The initial round of PCR added BamHI (C' terminal) and SpeI (N' terminal) restriction enzyme cut sites, while the second round added NcoI (N' terminal) and NotI (C' terminal). The third round of PCR added 12 buffer base pairs on both upstream and downstream ends of the Stx2B gene of interest.

2.1.3 Stx2B-1N single round PCR

In order to enhance Stx2B amplification from the pJ204 host plasmid, seen above with step wise PCR, primers specific of the gene of interest were redesigned for increased specificity. The following computational programs were used to assess and verify the *in silico* work for primer design; ExPASy© bioinformatic translation tool (for verification of frame shift errors), IDT optimized codon tool (highest optimization of nucleotide sequence for *E. coli)*, and NEBcutter® (restriction enzyme cut site finder).

STx2B nucleotide sequence (267 bp)

ATGAAGAAGATGTTTATGGCGGTTTTATTTGCATTAGCTTCTGTTAATGCAATGGCGGCGGATTGTG
CTAAAGGTAAAATTGAGTTTTCCAAGTATAATGAGGATGACACATTTACAGTGAAGGTTGACGGGA
AAGAATACTGGACCAGTCGCTGGAATCTGCAACCGTTACTGCAAAGTGCTCAGTTGACAGGAATGA
CTGTCACAATCAAATCCAGTACCTGTGAATCAGGCTCCGGATTTGCTGAAGTGCAGTTTAATAATGA
C

STx2B Translated sequence (89 Amino acids)

Met K K **Met** F **Met** A V L F A L A S V N A **Met** A A D C A K G K I E F S K Y N E D D T F T V K V D G K
E Y W T S R W N L Q P L L Q S A Q L T G **Met** T V T I K S S T C E S G S G F A E V Q F N N D

Figure 2.8 Stx2B nucleotide & amino acid sequences

Forward (STX2BFWDN)
CGCGCACCATGGTTATGAAGAAGATGTTTATGGCG

Reverse (STX2BREVN)
CGCCGCCGCACTAGTGTCATTATTAAACTGCACTTC

NcoI- CCATGG
SpeI- ACTAGT

Figure 2.9 Optimized Stx2B-1N primer design

AGGAGGTAAAACACCATGGTTATGAAGAAGATGTTTATGGCGGTTTTATTTGCATTAGCTTCTGTTA
ATGCAATGGCGGCGGATTGTGCTAAAGGTAAAATTGAGTTTTCCAAGTATAATGAGGATGACACAT
TTACAGTGAAGGTTGACGGGAAAGAATACTGGACCAGTCGCTGGAATCTGCAACCGTTACTGCAAA
GTGCTCAGTTGACAGGAATGACTGTCACAATCAAATCCAGTACCTGTGAATCAGGCTCCGGATTTGC
TGAAGTGCAGTTTAATAATGACACTAGTGCAGCCGGCCAGGCGATTGCGAATCGTTTTACGGCGAA
CATCAAGGGTCTGACCCAAGCCTCTCGTAATGCAAATGATGGTATTAGCATCGCACAAACCACCGA
AGGCGCGCTGAACGAGATCAACAATAACTTGCAACGTGTCCGTGAGCTGGCAGTTCAGAGCGCGAA
CAGCACGAATAGCCAGTCCGATTTGGACAGCATCCAGGCGGAGATTACGCAACGTTTGAACGAAAT
CGACCGCGTCAGCGGTCAAACGCAGTTTAATGGTGTGAAAGTTCTGGCCCAGGATAACACCCTGAC
GATTCAGGTTGGCGCAAACGACGGTGAAACGATTGATATTGACCTGAAGCAGATCAACAGCCAAAC
CCTGGGTCTGGACACCCTGAACGTGCAACAAAAGTATAAGGTGTCGGACACGGCCGCTACCGTGAC
CGGCGACGTCGATACTACGATTGCTGGGCCCAATAGTACTTTTAAAGCTAGCGCTACTGGTCTTGGT
GAGCTCGACCAGAAAATTGATCATATGTTAAAATTTGATGATCAATTGGGAAAATATTACGCCCCG
CGGACCGTTACGGGGGGACGATCGAAAGATGGCTATTATACCGGTTCCGTTGATAAGACGGCATGC
GAGGTGACTCTTGCTGTGCACGCGACTTCCCCGCTTACGCGTGGACTACCTGCGACAAGATCTGAGG
ATGTGAAAAATCCTAGGGTTGCCAACGCTGACCTGACCGAGGCGAAAGCGGCGCTGACCGCAGCGG
GCGTTACTGGTACCGCAAGCGTTGTGAAAATGAGCTACACCGACAATAATGGTAAAACTATCGATG
GCGGTCTGGCGGTCAAAGTCGGCGACGACTACTATTCCGCCACCCAGAACAAAGACGGCAGCATCA
GCATTAACACTACGAAATACACCGCAGATGACGGCACGAGCAAAACGGCACTGAATAAGCTGGGC
GGTGCGGATGGTAAGACCGAAGTTGTTAGCATTGGTGGTAAAACCTATGCCGCGTCCAAGGCAGAG
GGTCACAATTTCAAGGCGCAGCCGGATCTGGCGGAAGCTGCAGCGACCACGACCGAGAATCCGTTG
CAGAAGATTGATGCGGCGCTGGCACAGGTCGATACGCTGCGCTCTGACCTGGGTGCCGTACAAAAC
CGTTTCAATAGCGCGATCACCAATCTGGGCAACACCGTGAACAATCTGACCTCTGCTCGCAGCCGTA
TTGAGGGATCCCACCACCATCATCACCATCTCGAGTAGGCGGCCGCAAGC

Figure 2.10 Stx2B-1N nucleotide sequence containing hexa-histidine tag (1,572 bp)

R R **Stop** N T **Met** V **Met** K K **Met** F **Met** A V L F A L A S V N A **Met** A A D C A K G K I E F S K Y N E D D
T F T V K V D G K E Y W T S R W N L Q P L L Q S A Q L T G **Met** T V T I K S S T C E S G S G F A E V Q
F N N D T S A A G Q A I A N R F T A N I K G L T Q A S R N A N D G I S I A Q T T E G A L N E I N N N L
Q R V R E L A V Q S A N S T N S Q S D L D S I Q A E I T Q R L N E I D R V S G Q T Q F N G V K V L A Q
D N T L T I Q V G A N D G E T I D I D L K Q I N S Q T L G L D T L N V Q Q K Y K V S D T A A T V T G D
V D T T I A G P N S T F K A S A T G L G E L D Q K I D H **Met** L K F D D Q L G K Y Y A P R T V T G G R
S K D G Y Y T G S V D K T A C E V T L A V H A T S P L T R G L P A T R S E D V K N P R V A N A D L T
E A K A A L T A A G V T G T A S V V K **Met** S Y T D N N G K T I D G G L A V K V G D D Y Y S A T Q N
K D G S I S I N T T K Y T A D D G T S K T A L N K L G G A D G K T E V V S I G G K T Y A A S K A E G
H N F K A Q P D L A E A A A T T T E N P L Q K I D A A L A Q V D T L R S D L G A V Q N R F N S A I T
N L G N T V N N L T S A R S R I E G S H H H H H H L E **Stop** A A A S

Figure 2.11 Stx2B-1N containing hexa-histidine tag translated sequence (516 amino acids)

2.1.4 FliC-Stx2B

The gene of interest, Shiga-like toxoid 2 (Stx2B), was isolated from a genetically encoded host plasmid pJ204 (ATUM®), via polymerase chain reaction). Forward and reverse primers (Stx2B-1CF & Stx2B-1CR) were designed and synthesized with BamHI & XhoI restriction enzyme cut sites, respectfully, to amplify the toxoid gene Stx2B. The reverse primer Stx2B-1CR also incorporated a hexa-histidine tag, immediately flanked by restriction enzyme cut sites, to aid in downstream isolation and purification. Amplified Stx2B was designed to be inserted into vector pJ404 (ATUM®) which incorporates a pUC based origin of replication, a phage T5 derived inducible promoter, and ampicillin resistance (Appendix A.1, A4).

Previous Stx2B constructs utilizing the synthetic FliC platform, (Stx2B-1N), were analyzed in order to enhance the development & expression of the fusion protein (Appendix A.1). A signal peptide motif (MKKMFMAVLFALASVNAMA), associated with type three section systems (TTSS), was identified within the toxoid gene Stx2B and removed through deletion PCR to further enhance the expression and isolation of the fusion protein. Furthermore, Stx2b was inserted into the C-terminal end of the synthetic FliC platform to enhance Stx2B epitope presentation (Appendix A.1, A4).

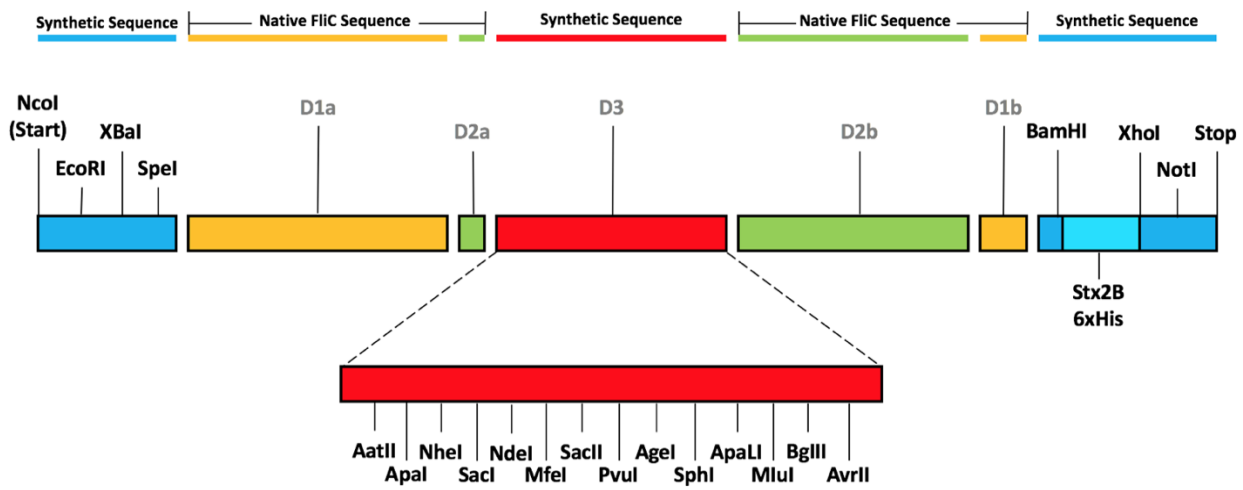

Figure 2.12 FliC-Stx2B cloning map

STx2B nucleotide sequence (267 bp)

GCGGATTGTGCTAAAGGTAAAATTGAGTTTTCCAAGTATAATGAGGATGACACATTTACAGTGAAG
GTTGACGGGAAAGAATACTGGACCAGTCGCTGGAATCTGCAACCGTTACTGCAAAGTGCTCAGTTG
ACAGGAATGACTGTCACAATCAAATCCAGTACCTGTGAATCAGGCTCCGGATTTGCTGAAGTGCAG
TTTAATAATGAC

STx2B Translated sequence (70 Amino acids)

A D C A K G K I E F S K Y N E D D T F T V K V D G K E Y W T S R W N L Q P L L Q S A Q L T G **Met** T V
T I K S S T C E S G S G F A E V Q F N N D

Figure 2.13 Stx2B nucleotide & amino acid sequences without signal peptide motif

Forward STX2B 1CF (with signal peptide) 51bp

GCGTACGGATCCGCGGATTGTGCTAAAGGTAAAATTGAGTTTTCCAAGTAT

Reverse STX2B 1CR (without signal peptide) 60 bp

TACGTGCTCGAGATGGTGATGATGGTGATGGTCATTATTAAACTGCACTTCAGCAAATCC

Restriction Enzyme Map

NcoI EcoRI XbaI SpeI BamHI HindIII XhoI NotI AatII AvrII HisTag

Figure 2.14 FliC-Stx2B primer design HisTag

AGGAGGTAAAACACCATGGGAATTCGGTCTAGAACTAGTGCAGCCGGCCAGGCGATTGCGAATCGT
TTTACGGCGAACATCAAGGGTCTGACCCAAGCCTCTCGTAATGCAAATGATGGTATTAGCATCGCAC
AAACCACCGAAGGCGCGCTGAACGAGATCAACAATAACTTGCAACGTGTCCGTGAGCTGGCAGTTC
AGAGCGCGAACAGCACGAATAGCCAGTCCGATTTGGACAGCATCCAGGCGGAGATTACGCAACGTT
TGAACGAAATCGACCGCGTCAGCGGTCAAACGCAGTTTAATGGTGTGAAAGTTCTGGCCCAGGATA
ACACCCTGACGATTCAGGTTGGCGCAAACGACGGTGAAACGATTGATATTGACCTGAAGCAGATCA
ACAGCCAAACCCTGGGTCTGGACACCCTGAACGTGCAACAAAAGTATAAGGTGTCGGACACGGCCG
CTACCGTGACCGGCGACGTCGATACTACGATTGCTGGGCCCAATAGTACTTTTAAAGCTAGCGCTAC
TGGTCTTGGTGAGCTCGACCAGAAAATTGATCATATGTTAAAATTTGATGATCAATTGGGAAAATAT
TACGCCCCGCGGACCGTTACGGGGGGACGATCGAAAGATGGCTATTATACCGGTTCCGTTGATAAG
ACGGCATGCGAGGTGACTCTTGCTGTGCACGCGACTTCCCCGCTTACGCGTGGACTACCTGCGACAA
GATCTGAGGATGTGAAAAATCCTAGGGTTGCCAACGCTGACCTGACCGAGGCGAAAGCGGCGCTGA
CCGCAGCGGGCGTTACTGGTACCGCAAGCGTTGTGAAAATGAGCTACACCGACAATAATGGTAAAA
CTATCGATGGCGGTCTGGCGGTCAAAGTCGGCGACGACTACTATTCCGCCACCCAGAACAAAGACG
GCAGCATCAGCATTAACACTACGAAATACACCGCAGATGACGGCACGAGCAAAACGGCACTGAAT
AAGCTGGGCGGTGCGGATGGTAAGACCGAAGTTGTTAGCATTGGTGGTAAAACCTATGCCGCGTCC
AAGGCAGAGGGTCACAATTTCAAGGCGCAGCCGGATCTGGCGGAAGCTGCAGCGACCACGACCGA
GAATCCGTTGCAGAAGATTGATGCGGCGCTGGCACAGGTCGATACGCTGCGCTCTGACCTGGGTGC
CGTACAAAACCGTTTCAATAGCGCGATCACCAATCTGGGCAACACCGTGAACAATCTGACCTCTGCT
CGCAGCCGTATTGAGGGATCCGCGGATTGTGCTAAAGGTAAAATTGAGTTTTCCAAGTATAATGAG
GATGACACATTTACAGTGAAGGTTGACGGGAAAGAATACTGGACCAGTCGCTGGAATCTGCAACCG
TTACTGCAAAGTGCTCAGTTGACAGGAATGACTGTCACAATCAAATCCAGTACCTGTGAATCAGGCT
CCGGATTTGCTGAAGTGCAGTTTAATAATGACCATCACCATCATCACCATCTCGAGTAGGCGGCCGC
AAGC

Figure 2.15 FliC-Stx2B without signal peptide nucleotide sequence (1527 bp)

R R **Stop** N T **Met** G I R S R T S A A G Q A I A N R F T A N I K G L T Q A S R N A N D G I S I A Q T T E G
A L N E I N N N L Q R V R E L A V Q S A N S T N S Q S D L D S I Q A E I T Q R L N E I D R V S G Q T Q
F N G V K V L A Q D N T L T I Q V G A N D G E T I D I D L K Q I N S Q T L G L D T L N V Q Q K Y K V
S D T A A T V T G D V D T T I A G P N S T F K A S A T G L G E L D Q K I D H **Met** L K F D D Q L G K Y
Y A P R T V T G G R S K D G Y Y T G S V D K T A C E V T L A V H A T S P L T R G L P A T R S E D V K
N P R V A N A D L T E A K A A L T A A G V T G T A S V V K **Met** S Y T D N N G K T I D G G L A V K V
G D D Y Y S A T Q N K D G S I S I N T T K Y T A D D G T S K T A L N K L G G A D G K T E V V S I G G
K T Y A A S K A E G H N F K A Q P D L A E A A A T T T E N P L Q K I D A A L A Q V D T L R S D L G A
V Q N R F N S A I T N L G N T V N N L T S A R S R I E G S A D C A K G K I E F S K Y N E D D T F T V K
V D G K E Y W T S R W N L Q P L L Q S A Q L T G **Met** T V T I K S S T C E S G S G F A E V Q F N N D H
H H H H H L E **Stop** A A A S

Figure 2.16 Translated FliC-Stx2B without signal peptide motif amino acid sequence (501 amino acids)

2.2 *Cloning*

Amplification of each gene of interest was conducted using Thermo Scientific® master mix kit & thermocycler conditions. Volumes used for each reaction are shown in Appendix A.2. The amplified samples were then loaded and ran on a 1% agarose DNA gel at 80V for 90 minutes in 1X TAE buffer, using Tridye® 1kb ladder for analytical comparison.

Restriction enzyme digests were conducted by incubating the isolated amplicon DNA samples with New England BioLabs® (NEB) restriction enzymes for 2.5 hours at 37°C, then placed on ice. In order to prevent over-cutting, a reaction clean-up was conducted on digest samples using a Qiagen® reaction clean-up kit to remove excess restriction enzymes and buffers. Digest samples were then subsequently quantified and ligated using Thermo Scientific rapid DNA ligation kit® (K1422) at an insert to vector ratio of either 1:3, 1:5, or 1:8.

Ligation samples were purified using a Qiagen® QIAquick gel extraction kit prior to transformation into New England BioLabs® *E. coli* (BL21) cells, which were made electro-competent. Two microliters of each insert to vector ratio sample was then mixed with 40µLs of electro-competent *E. coli* (BL21) cell suspension then electrically pulsed using a Bio-Rad MicroPulsar™. The samples were then allowed to recover in 1mL super optimal broth (SOB) medium at 37°C with gentle agitation (225 rpm). Recovered cells were then plated onto Luria Broth (LB) agar plates with 100µg/mL ampicillin to counter select against non-positive clones. Plates were grown at 37°C for 24-36 hours prior to analysis.

Conformational analysis was conducted using quadrant/colony PCR, restriction enzyme digest against BamHI & XhoI restriction enzymes, & DNA sequencing.

2.3 Protein work

2.3.1 Adaptation of Stx2B-1N & FliC-Stx2B expressing E. coli to adaptation media (ECAM)

Confirmed clones were adapted to synthetic *E. coli* adaptation media (ECAM), see Appendix A.4, through several culture passages. A 100mL Luria broth (LB, Appendix A.4) overnight culture with 100ug/mL ampicillin was inoculated with either Stx2B-1N or FliC-Stx2B positive clone and allowed to grow at 37°C with gentle agitation (225 rpm) until an OD_{600} of ~1.2-1.7 was reached. The overnight culture was then used as an inoculum for a 1st pass ECAM culture, to achieve an initial OD_{600} of 0.1. The 1st pass culture was again allowed to reach an OD_{600} of ~1.2-1.7 and was then used to inoculate the 2nd pass ECAM culture at a starting OD_{600} of 0.1. Once the OD_{600} of the 2nd pass reached 0.7, the culture was spun down and resuspended in sterile phosphate-buffered saline, then stored at -80°C.

2.3.2 Protein expression and sample processing

Cell culture for recombinant FliC-Stx2B protein expression was prepared by transferring confirmed transformant glycerol stocks onto fresh LB plates containing 100ug/mL ampicillin for bacterial counter-selectivity, then left in an incubator at 37°C overnight. A single colony from the LB plates was then used to inoculate an overnight culture of either Luria broth, Terrific broth (TB), or ECAM media (with 100µg/mL ampicillin), then left to incubate in an orbital shaker at 225rpm & 37°C. Overnight culture optical densities were then obtained and used to calculate the volume of inoculum to inoculate the working culture, containing the same media type and antibiotics as the overnight culture, to a starting OD_{600} of 0.1.

The working culture was subjected to the same culturing parameters as the overnight culture. Once an OD_{600} of 0.6-0.7 was reached in the working culture, it was induced with either 0.4mM or 1mM Isopropyl β-D-1-thiogalactopyranoside (IPTG) then left to incubate at 37°C and 225rpm for either 3, 6, or 18 hours. One culture flask receiving no IPTG was also grown alongside induced cultures to determine uninduced protein expression.

Samples were then centrifuged in a Beckman Coulter® Allegra 64R centrifuge for 10 minutes at 10k rpm at 4°C to remove media and cell debris. Following centrifugation, the supernatant was carefully decanted to isolate the cell pellet which was then resuspended in 10mL sterile PBS buffer and stored at -80°C. Insoluble and soluble protein fractions were separated following the addition of 0.142mL Roche® cOmplete mini (EDTA-Free) protease cocktail mixture, to prevent protein degradation, by sonication (3x) and subsequent centrifugation. The soluble fraction was then decanted and stored for future analysis, while the insoluble cell pellet was resuspended in equal volume lysis buffer (50mM Tris, 8M urea) and 0.142mL protease cocktail mix. Insoluble fractions were then sonicated three times and stored for analysis at -80°C.

2.3.3 Denaturing SDS-PAGE analysis

Induced and uninduced sonicated suspensions were quantified using Thermo Scientific® Pierce BCA protein assay kit. Quantified samples were then heated for 10 minutes at 95°C and centrifuged in an Eppendorf® 5415 D centrifuge at 13k rpm for five minutes to remove insoluble protein debris. To further denature the samples, 10µL of NuPAGE® 4x denaturing LDS dye was added to 30µL of protein sample. Samples were then loaded on a NuPAGE® 4-12% Bis-Tris gel and ran for one hour at a constant 200 volts, with 1X MOPS as the running buffer. The gel was stained with 150mL of 0.1% Coomassie Brilliant Blue R-250 working solution then heated in a

microwave, on full power, for 1 minute and left shaking (50rpm) for 15 minutes. Following Coomassie staining, the gel was transferred into 150mL destain solution and microwaved for 1 minute then placed on an orbital shaker at 50rpm.

2.3.4 Cell disruption & clarification using detergent wash method for insoluble protein resolubilization

Following induction of cells, the cell suspension was centrifuged to gather cell pellet then washed once with 10mL sterile PBS solution prior to freezing in liquid nitrogen. Frozen cell suspension was placed on ice and left at 4°C overnight to gently thaw and lyse the cells. After thawing overnight, cell suspension was centrifuged again (10k rpm at 4°C) for 10 minutes to collect the pellet, then resuspended with either 4mL or 40mL of resuspension buffer (20mM Tris-HCl, pH 8.0).

Resuspended cell suspensions were then sonicated three times for 10 second intervals (1 sec on/ 0.5 ½ off duty cycles), then subsequently centrifuged in a Beckman Coulter® Allegra 64R centrifuge for 10 minutes at 10k rpm and 4°C. The supernatant (containing the soluble protein fraction) was then decanted and stored for SDS-PAGE analysis.

The insoluble protein faction was then resuspended with either 3mL or 30mL of detergent based isolation buffer (2M urea, 20mM Tris-HCl, 0.5M NaCl, 2% Triton X-100, pH 8.0) at 4°C, then sonicated and centrifuged as done previously. The supernatant was then decanted and sampled for SDS-PAGE analysis. Detergent buffer wash step may then be repeated to further the isolation of FliC-Stx2B. Five milliliters, or 50mL, of Binding buffer solution (20mM Tris-HCl, 0.5M NaCl, 20mM Imidazole, 2M-6M guanidine hydrochloride, 1mM DTT, pH 8.0) was used to resolubilize the insoluble pellet, following detergent wash steps. Samples

were agitated on an orbital shaker (50-250rpm) at room temperature for 60 minutes, then centrifuged for 15 minutes at 10k rpm and 4°C. Prior to fast protein liquid chromatography (FPLC) purification, the resolubilized pellet sample was filtered through a 0.2uM filter and stored for later passage through a GE healthcare life sciences® HisTrap HP 1mL nickel column.

2.3.5 Dialysis refolding

Two milliliters of protein sample, resolubilized with 2M guanidine hydrochloride, was gently introduced into ~2 inches of Spectra/Por® molecularpourous membrane tubing which were clipped at the ends with Spectra/Por® closures. The dialysis tubing was then placed into beaker containing 400mL (200X of sample volume) refolding buffer (20mM Tris-HCl, 0.5M NaCl, 20mM Imidazole, 1mM DTT, 0-6M urea, pH 8.0) and a stir bar. The apparatus was stored at 4°C overnight and allowed to spin gently using the vortex produced through magnetic stirring. Guanidine hydrochloride removal was assessed through the addition of NuPAGE® LDS (lithium dodecyl sulfate) Sample Buffer.

2.3.6 Induced cell pellet preparation for Hydrophobic Interaction Column (HIC)

Induced cell pellet samples were resuspended in resuspension buffer then sonicated three times as described previously. Samples were then diluted using a 1:1 equal ratio of either lysis buffer B80 (50mM Tris, 125mM NaCl, 10mM EDTA, 4% sucrose) or Super Q equilibration buffer (100mM Tris 2.3M NaCl). Sample mix was then filtered through a 0.2-micron filter to prevent debris from entering AKTA® FPLC tubing.

2.3.7 Fermentation cell paste processing for AKTA® FPLC purification

Stx2B expressing *E. coli* fermentation paste was processed into a refined partially purified lysate by using the following steps: 1) homogenization, 2) PEG precipitation, and 3) Triton X-114 2-phase separation under the following parameters.

150 grams (wet wt.) of fermentation paste, harvested following a 5-hour induction using 1mM IPTG, was resuspended in 1L of B80 lysis buffer (Appendix A.4) and allowed to stir on ice for 30 minutes until the mixture became less turbid. Prior to the addition of the cell mixture, lysis buffer (B80) was added to the APV homogenizer to equilibrate it, while maintaining the pressure at 0 Bar. The lysate was then passed through the homogenizer three times at 720 bar, with the exception of the first pass which remained at 0 bar to ease the homogenization process on the cells. Between each pass, the lysate temperature was maintained at 4°C by placing it into pre-chilled 250mL bottles then submerging them into an ethanol ice bath.

Following homogenization, the cell lysate was centrifuged in a Beckman Coulter® Avanti J-20 XPI centrifuge at 10k rpm for 1 hour at 4°C to separate cell debris from the desired protein. The supernatant was collected and used for polyethylene glycol (PEG 3350) precipitation, while the pellet was resuspended in PBS and used for analysis. Four percent (w/v) PEG 3350 was added to the supernatant in a dual-beaker apparatus slowly, containing ice to maintain temperature, and allowed to dissolve fully and then stirred for 30 minutes. Lysate was then spun down for at 10k rpm for 1 hour at 4°C to separate out proteins. The supernatant volume was measured, and stored for later analysis. The pellet produced was then resuspended with pellet resuspension buffer (B57, Appendix A.4) at ½ the supernatant volume and stirred until fully dissolved. The lysate was then centrifuged in a Beckman Coulter® Allegra 64R at 10k rpm for 1 hour at 4°C. Supernatant and pellet fractions were separated for Triton X-114 treatment.

One percent (w/v) Triton X-114 was added to the supernatant which was then allowed to stir at room temperature for 30 minutes prior to being placed into a water bath set at 30°C for 10 minutes. The pellet produced was resuspended in 10mL PBS and stored for future analysis. Following the water bath, the lysate was then centrifuged in a Beckman Coulter® Allegra 64R at 10k rpm for 4 hours at room temperature with the brake to the centrifuge disabled, allowing for a slow regression in speed over time. After braking overnight, the aqueous phase top layer was extracted and filtered through a 0.2um PES filter, thus producing the refined lysate needed for AKTA® FPLC purification. The remaining pellet was again resuspended in 10mL PBS and stored for future analysis.

2.3.8 FPLC purification

Purification of recombinant FliC-Stx2B was conducted using a GE Healthcare and Life Sciences® HisTrap HP 1mL nickel column which has affinity for the hexa-histidine tag located on the C-terminal end of the construct.

Prior to sample loading, 10mL of binding buffer was used to equilibrate the column to increase the HisTrap HP nickel column's binding affinity. Three milliliters of filtered, resolubilized protein described above, was then loaded onto the column using a flow rate of 0.3mL/min being careful not to saturate the column. Ten milliliters of Solubilization buffer (20mM Tris-HCl, 0.5M NaCl, 20mM Imidazole, 1mM DTT, 6M urea, pH 8.0, Appendix A.4) was then added through the column at 0.3mL/min to wash away any unbound or non-specific proteins from the column.

Due to the nature of the protein being insoluble, a refolding step was included in order to purify protein with the highest intrinsic biological activity possible. A step-wise gradient of

refolding buffer (20mM Tris-HCl, 0.5M NaCl, 20mM Imidazole, 1mM DTT, 0-6M urea, pH 8.0, Appendix A.4) was applied starting from a concentration of 6M urea to 0M urea, using 0.3mL/min as the flow rate. Once the gradient reached 0M urea, the column containing bound FliC-Stx2B was allowed to incubate on-column for either 1, 2, 3, or 6 hours prior to a 5mL refolding buffer wash and an imidazole step-wise gradient elution.

Elution was conducted using 20mL of an elution buffer gradient (20mM Tris-HCl, 0.5M NaCl, 20-500mM Imidazole, 1mM DTT, pH 8.0, Appendix A.4) starting from 20mM imidazole and ending at 500mM imidazole with a flow rate of 0.3mL/min. Samples were collected in 20% increments of the step-wise gradient and stored in 2mL aliquots to be analyzed by SDS-PAGE.

2.3.9 Western blot analysis

Prior to nitrocellulose membrane transfer, a denaturing SDS-PAGE was conducted using the same parameters described in denaturing SDS-PAGE analysis. Upon completion of the gel, a filter paper sandwich was assembled consisting of Novex® Nitrocellulose membrane filter paper sandwich and the SDS-PAGE gel.

Protein transfer from the SDS-PAGE gel to the nitrocellulose membrane was conducted using NuPAGE® transfer buffer & an Invitrogen® XCell II blot module set at a constant 30V for 1 hour under cold temperature. The nitrocellulose membrane was removed following the protein transfer and placed into 100mL of (1X) TBST milk solution (20mM Tris-HCl, 0.15mM NaCl, 1% Triton X-100, 5% nonfat dry milk) then left overnight on an orbital shaker (50rpm) at 4°C. Following overnight shaking, the membrane was washed using room temperature (1X) TBST for 10 minutes (3x) at 70rpm.

Primary antibodies were diluted in (1X) TBST milk solution at a working ratio of 1: 1,000. The antibody mixture was then applied while shaking at 50rpm for 1 hour at room temperature, then subsequently washed again with (1X) TBST milk solution at 70rpm. Diluted secondary antibody, prepared the same way as the primary solution, was applied for 1 hour at 50rpm then washed again with 1X TBST three times. The membrane was then coated with PerkinElmer™ Western Lightning® ECL Pro chemiluminescence substrate, and incubated in the dark for 5 minutes. ImagineQuant® LAS 4000 mini software systems were used to visualize chemilluminescence reactions.

2.3.10 Indirect ELISA analysis

In order to characterize FliC-Stx2B epitope activity, an ELISA assay was conducted using a protein concentration range of 250ng-3.9ng. Following diluting samples in ELISA coating buffer (0.5M Carbaonate-Bicarbonate, pH 9.6, Appendix A.4), 50µL of each desired sample concentration was then plated on a Costar® 96 well plate, in triplicate, and incubated at 4°C overnight. Samples were then aspirated by gently, but swiftly, inverting the plate to remove any liquids from the wells. Each well was then washed with 150µL PBST (0.05% Tween 20 in Phosphate-buffered saline) three times, to remove any unbound proteins. 60µL of blocking buffer (PBST with 5% nonfat dry milk, Appendix A.4) was then added to each well following aspiration and allowed to incubate at 37°C for 1 hour.

After incubation, the wells were aspirated and washed as described previously. Primary antibody, at a working concentration of 1:2000 in blocking buffer, was then added to each well and allowed to incubate at 37°C for 1.5 hours. The plate was then aspirated and washed again to prepare for the addition of the secondary antibody mix using the same parameters as the primary

antibody wash. A final wash step was conducted prior to the addition of 100µL/well eBioscience® (1X) TMB ELISA substrate solution, then allowed to incubate at room temperature for three minutes in the dark. The reaction was then stopped with the addition of 100uL/well 1M phosphoric acid and read on a Wallac® Victor^2 1420 multilabel counter at an optical density of 450nm.

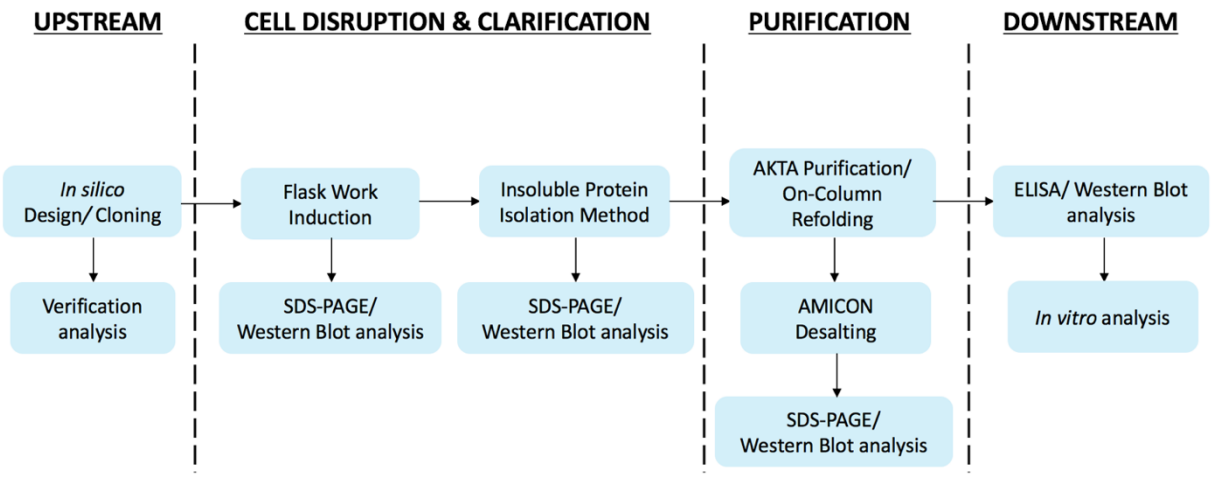

Figure 2.17 Process Overview

3 RESULTS

3.1 Amplification of mRFP

Following amplification of mRFP via polymerase chain reaction (PCR), subsequent DNA was then ran on a 1% DNA Agarose gel to determine whether in silico primer design was accurate. mRFP is 760bp in length with the addition of both forward and reverse primers. mRFP amplicon DNA bands were seen between 0.5 kilobases and 1.0 kilobases when compared to Tridye® DNA ladder. In Fig. 3.1, it is seen in the highlighted region that amplified mRFP migrates towards ~700bp.

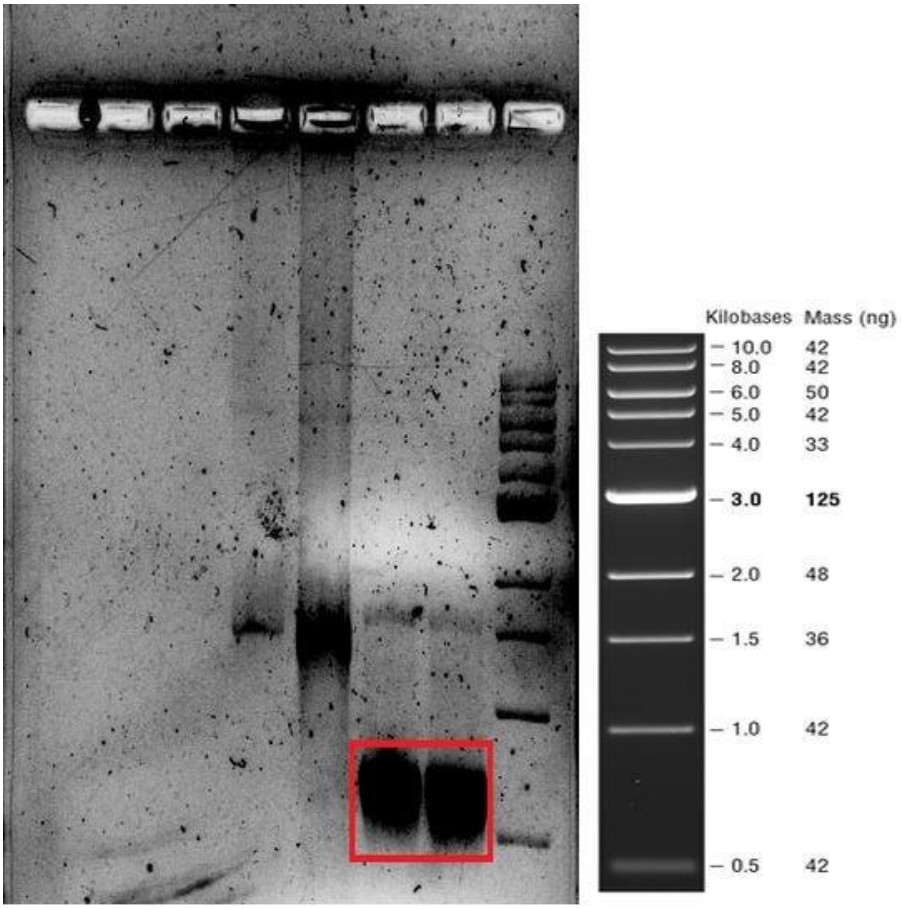

Figure 3.1 mRFP amplified DNA from host plasmid pJ204

3.2 Transformation of mRFP into electro-competent *E. coli*

Following inoculation of the transformed cell mixture onto antibiotic-selective Luria broth plates containing ampicillin, colony growth began to occur after 24 hours of incubation at 37°C. The colonies were off white in color and spherical in shape, much like the control competent *E. coli* colonies that were grown on LB plates without antibiotics. Control plates did not show growth of competent *E. coli* indicating transformants (Fig. 3.2) contained the antibiotic resistance encoding pJ404 plasmid.

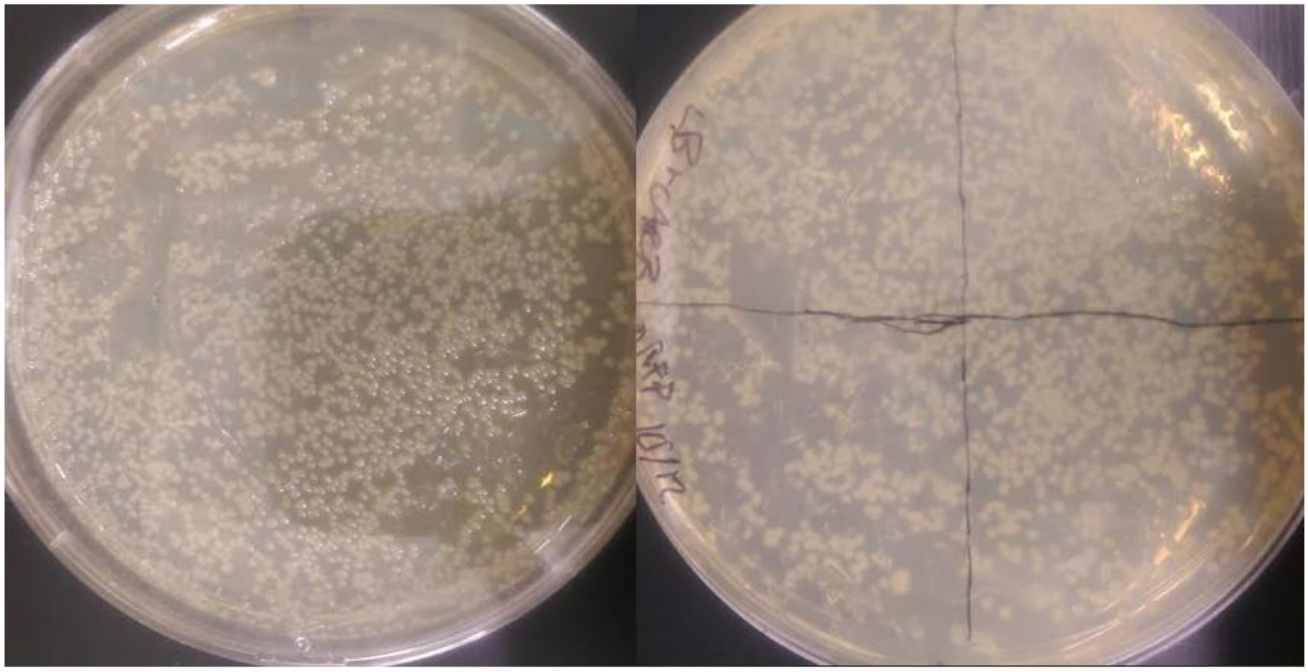

Figure 3.2 mRFP transformant colony growth 24 hours post transformation on LB ampicillin (100µg) plates

Putative transformant colonies were carefully isolated using a sterile toothpick then resuspended in 50µL diH2O prior to colony PCR. The samples were then ran on a 1% DNA Agarose gel in 1X TAE (Appendix A.4) for insert confirmation. It is seen in Fig. 3.3 that test samples in lanes 2-20, putative transformant colonies containing mRFP/pJ404, showed banding at ~ 0.7 kilobases when compared to Tridye® 1kb ladder. Primer dimer formation is also seen towards the bottom of the DNA agarose gel. Lanes 22-26 showed no banding in control samples containing nuclease free water and forward and reverse primers. Lanes 27 and 28 contained amplified mRFP DNA from the previous PCR (Fig. 3.1) and presented with the same banding patterns at ~0.7 kilobases.

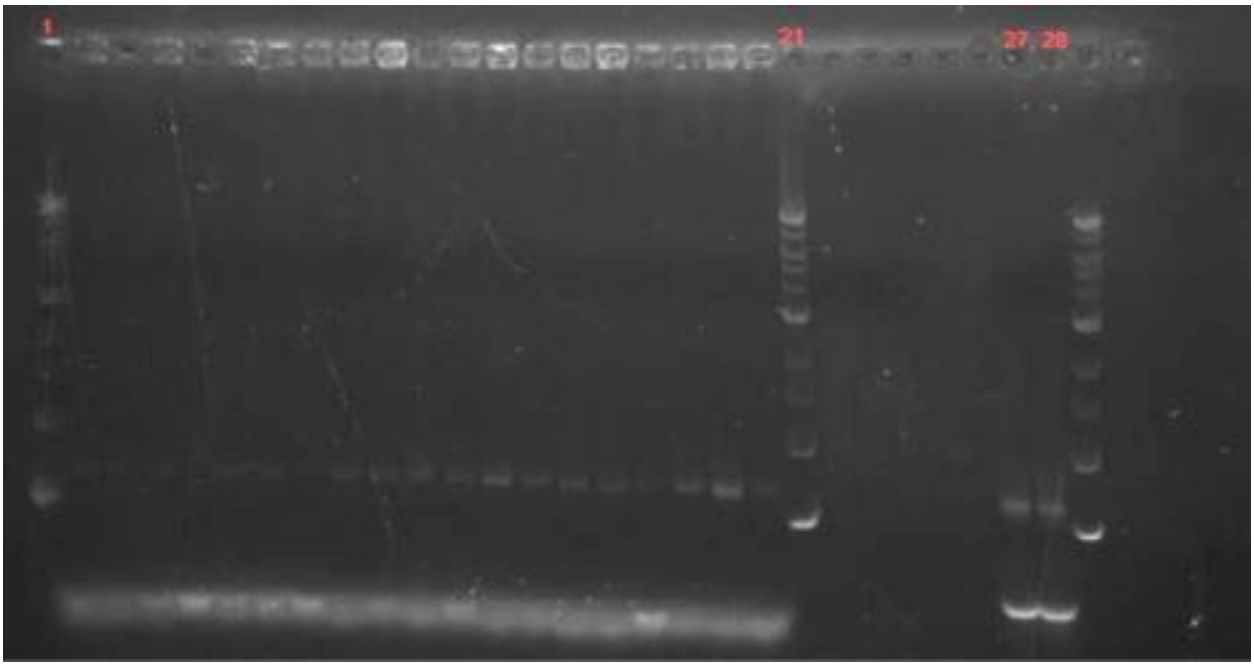

Figure 3.3 Colony PCR on mRFP transformant colonies
Lanes 1, 21, 29) Ladder. Lanes 2-20) Transformant colonies expressing mRFP. Lanes 22-26) Nuclease free water with primers. Lanes 27, 28: Previously amplified mRFP DNA.

3.3 Amplification & restriction digest verification of Stx2B-1N

Previous attempts at amplifying the toxoid gene Stx2B from its host plasmid pJ204 proved troublesome and produced insufficient DNA yields. Therefore, primers redesigned for optimal adherence & specificity were incubated with varying concentrations of template DNA to produce higher yields of amplified DNA (Fig. 3.4). As it is seen in Fig. 3.4 the varying concentrations of template DNA illustrated a gradient like effect on the amplification of Stx2B from pJ204. In Fig. 3.4 (lanes 2 and 3) amplification of Stx2B can be seen, however in lane 3 a non-specific band appears at ~1.5 kilobases. This same band is seen more prominently in lane 4, as template DNA concentration increases, while the ~300bp Stx2B band seen in previous lanes disappears.

Restriction digest products for Stx2B and synthetic FliC (in host plasmid pJ404), seen in Fig. 3.5, showed expected band migration for both double cut pJ404 plasmid and amplified Stx2B DNA.

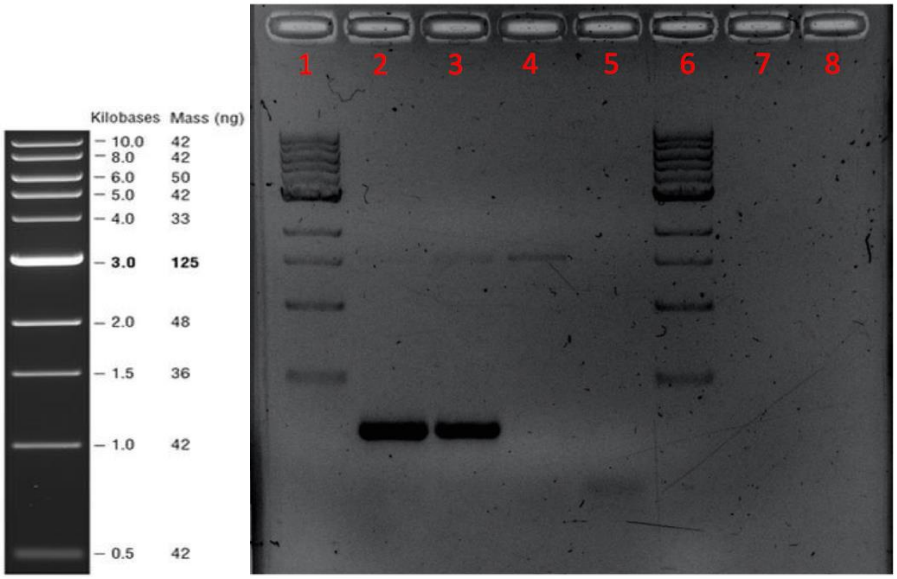

Figure 3.4 Optimized Stx2B-1N PCR conducted using varying levels of template DNA
Lanes 1-8) Tridye 1kb DNA ladder. Lane 2) 100ng template DNA. Lane 3) 300ng template DNA. Lane 4) 500ng template DNA.

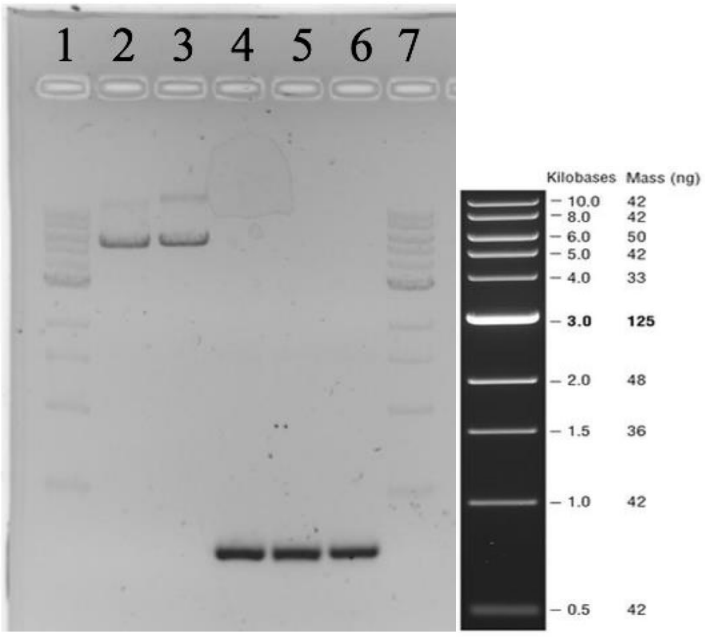

Figure 3.5 Restriction digest on Stx2B host plasmid pJ204 and synthetic FliC
Lanes 1 & 7) Tri-dye DNA ladder. Lanes 2 & 3) Double digest pJ404/R2. Lanes 4-6) Double digest Stx2B.

3.4 Transformation of Stx2B-1N into electro-competent *E. coli* -

Using restriction Stx2B & pJ404 restriction digest products, ligation and transformation was conducted and grew transformant colonies on antibiotic-selective Luria broth plates containing ampicillin. No growth was seen on control plates containing transformed digested vector plasmid with no DNA ligase, and with samples transformed solely with the electro-competent *E. coli* cells. Colonies were cream in color, indicative of previous *E. coli* colonies seen before (Fig. 3.2). Colony forming units for the plates inoculated with either 1:3 or 1:8 molar ratio ligations ranged in number, forming more colonies on the higher insert to vector ratio reactions.

Quadrant colony PCR, performed on various colonies per quadrant, yielded amplified Stx2B insert DNA from each sample set as seen (Fig. 3.6A & 3.6B). Due to these results, isolated colony PCR was conducted (Fig. 3.7) in order to isolate and verify colonies for subsequent verification analysis. Similar to Fig. 3.5, all tested transformant colonies showed the amplification of the gene of interest.

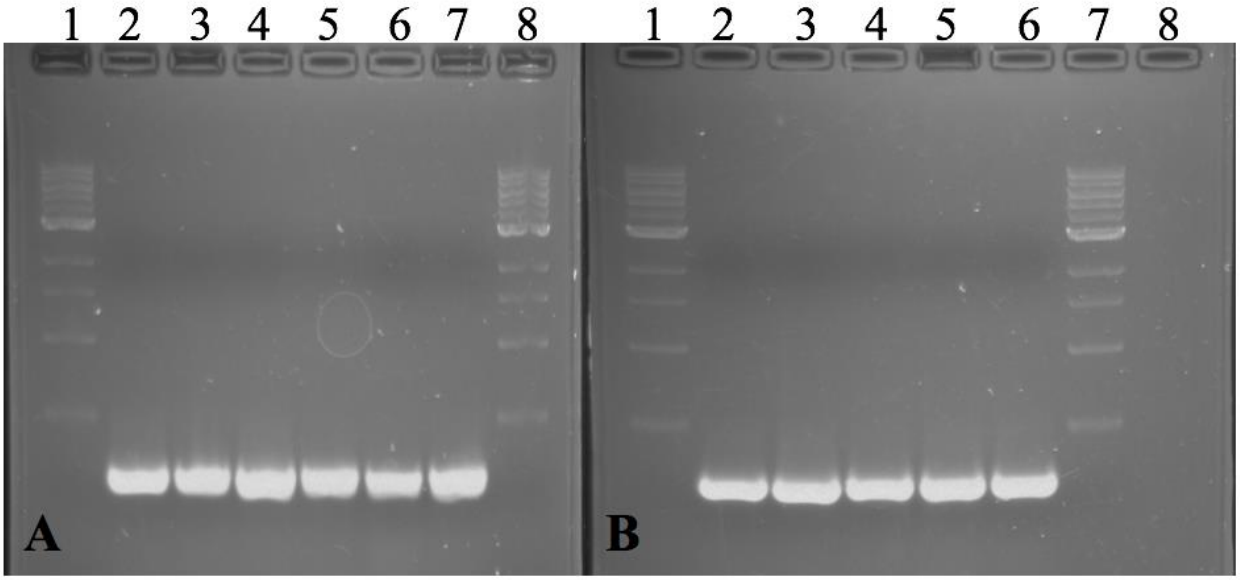

Figure 3.6 Quadrant colony PCR conducted on Stx2B-1N transformant colonies for both 1:3 and 1:8 molar ratio ligations

(A) *Lanes 1 and 8) Tri-dye DNA ladder. Lanes 2-4) 1:3 ligation ratio with 100*µ*L inoculum. Lanes 5-7) 1:8 ligations with 50*µ*L inoculum.* ***(B)*** *Lanes 1 and 7) Tri-dye DNA ladder. Lane 2) 1:8 ligation with 50*µ*L ligation inoculum. Lanes 3-6) 1:8 ligations with 100*µ*L inoculum.*

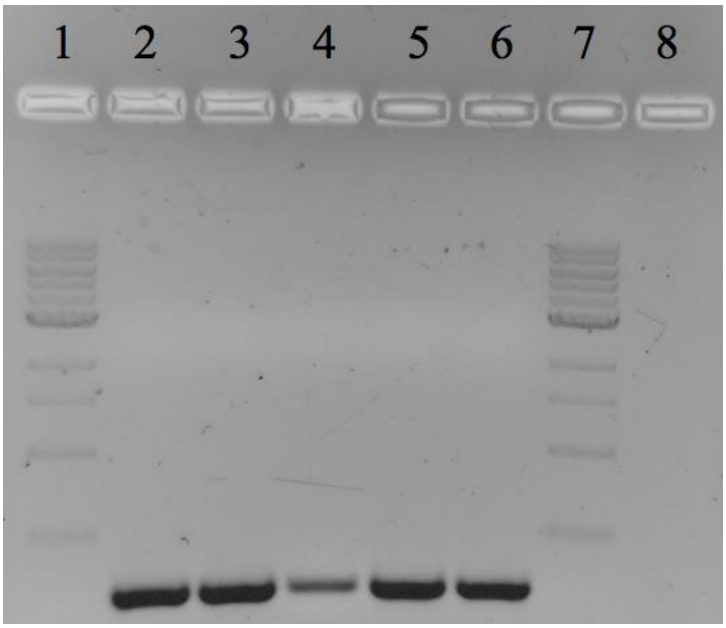

Figure 3.7 Isolated colony PCR conducted on Stx2B-1N transformant colonies
Lanes 1 and 7) Tri-dye DNA ladder. Lanes 2-6) isolated colony PCR samples chosen from positive quadrant PCR.

3.5 Initial Stx2B-1N nickel column purification

Following Stx2B-1N protein expression (Appendix A.3, A12-A14), cell lysate samples were analyzed for the solubility of the recombinant protein before and after passage through a nickel column in both soluble and insoluble fractions (Fig. 3.8).

Presence of Stx2B-1N is shown to be associated more with soluble cell fractions (supernatant & treated pellet lanes) in comparison to the insoluble pellet samples (untreated pellet & resuspension lanes). Stx2B-1N recombinant protein collects predominately in elution fraction lanes 3 & 4, however excess protein banding persists albeit reduced in comparison to flow through lanes.

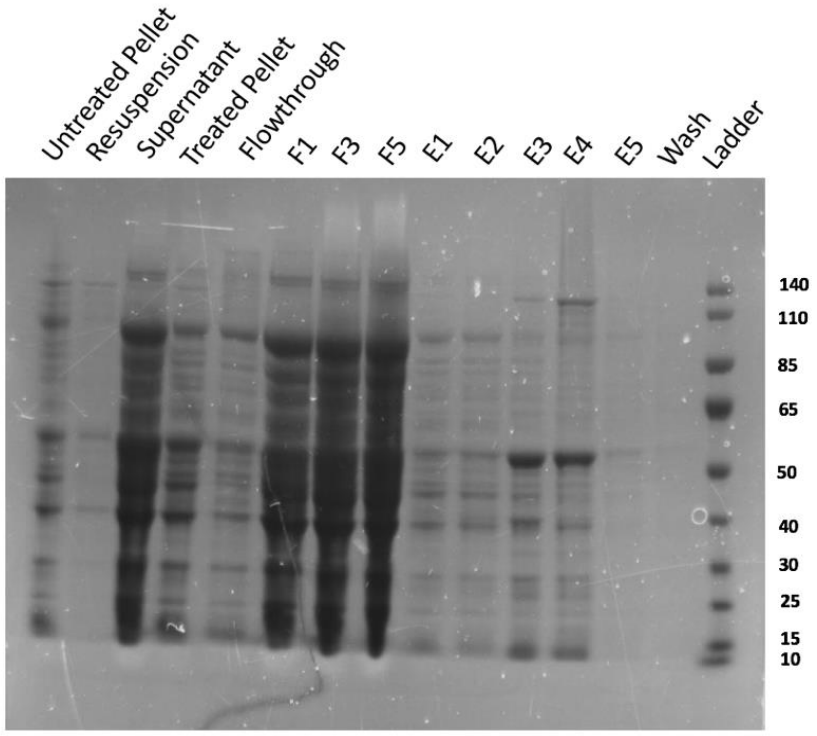

Figure 3.8 Initial Stx2B-1N FPLC nickel column purification
Lane 1) thawed cell pellet sample alone. Lane 2) resuspended cell pellet from lane 1. Lane 3) cell pellet supernatant following centrifugation prior to purification Lane 4) cell pellet prior to purification. Lane 5) AKTA© flow through. Lanes 6-8) flow through fractions 1 & 3. Lanes 9-13) Eluted fractions.

Due to the excess of non-desired protein banding in the eluted fractions (Fig. 3.8) optimization of imidazole concentrations within the binding buffer was conducted (Fig. 3.9). Binding buffers containing varying concentrations of imidazole were used (5mM & 20mM respectfully) in order to inhibit competitive binding of non-desired proteins to the HisTrap column during AKTA® FPLC. Purification using binding buffer with an imidazole concentration at 5mM (Fig. 3.9A) showed elution of excess proteins and Stx2B-1N more prominently than the initial purification (Fig. 3.8). When using binding buffer with an imidazole concentration at 20mM, however, excess non-desired protein banding decreased but still remained (Fig. 3.9B).

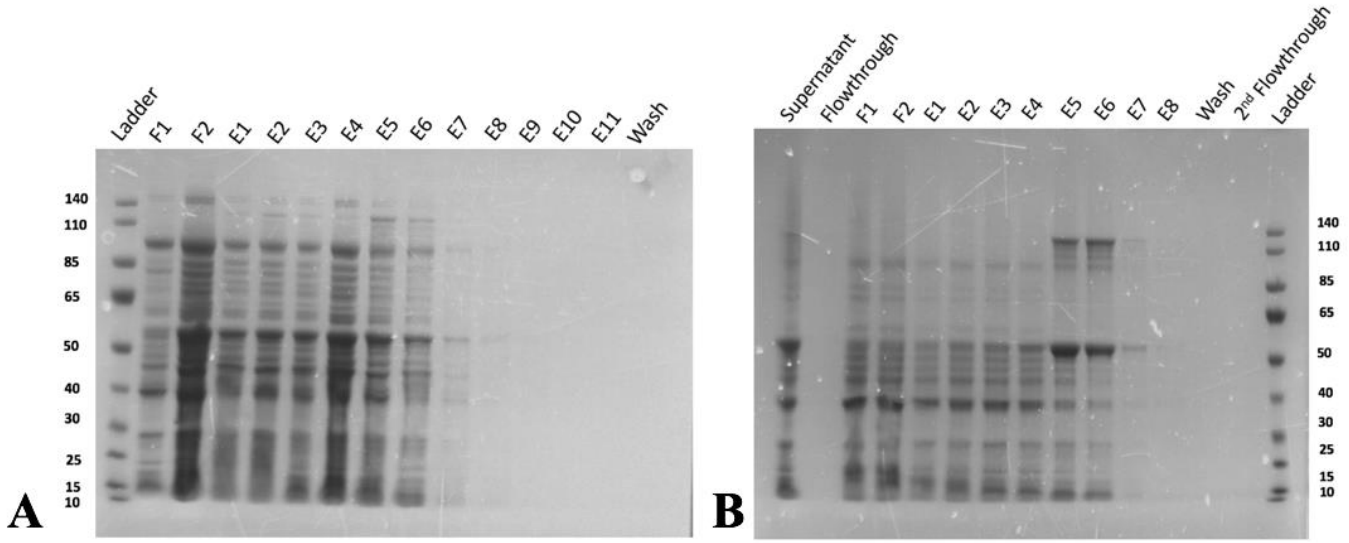

Figure 3.9 Stx2B-1N nickel column purification using varying concentrations of imidazole during binding
(A) *AKTA© purification using 5mM (left) &* ***(B)*** *20mM imidazole (right) for binding activity respectfully.*

3.6 Stx2B-1N fermentation paste refined lysate fraction analysis

Prior to protein purification, fermentation cell paste was produced, harvested, and processed into a refined lysate in order to prevent blocking of AKTA® FPLC capillary tubes. The refined lysate also acts to further isolate and remove excess non-desired protein and cell debris. As it is seen in the Western blot (Fig. 3.10B), the appearance of a protein with a molecular weight at ~38kDa is still the most abundantly present. Interestingly, a second protein band is also present at ~60kDa in the PEG 3350 and Triton X-114 treated samples as the excess non-desired protein bands decrease. This ~60kDa protein is also seen during cell sample processing prior to producing the refined lysate (Fig. 3.10).

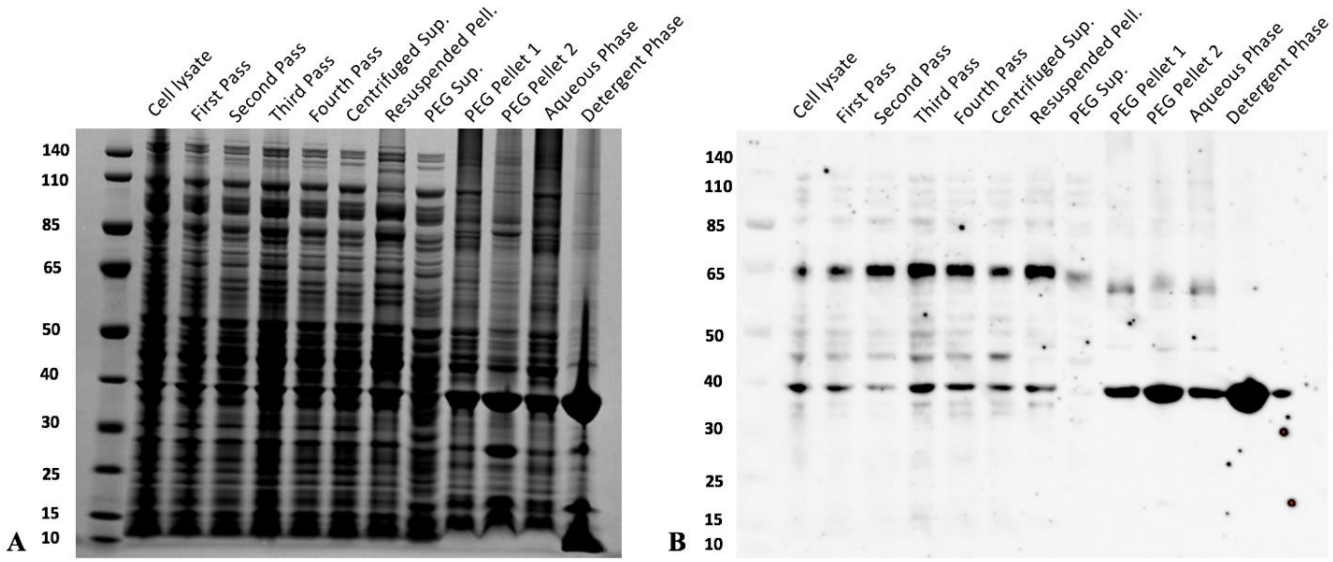

Figure 3.10 Stx2B-1N refined lysate SDS-PAGE & Western blot analysis (anti-FliC ab)
(A) *Lane 1) Page Ruler Ladder. Lane 2) Cell lysate prior to homogenization. Lane 3) First pass through homogenizer. Lane 4-6) 2nd – 4th pass. Lane 7) Centrifuged supernatant. Lane 8) Resuspended pellet following centrifugation. Lane 9) PEG centrifuged supernatant. Lane 10) Resuspended PEG pellet 1. Lane 11) Resuspended PEG pellet 2. Lane 12) Aqueous phase. Lane 13) Detergent phase. Lane 15) Magic Mark Protein Standard.* ***(B)*** *Anti-FliC Western Blot using the same lane designations as figure (A).*

3.7 Transformation & analysis of FliC-Stx2B into electro-competent *E. coli*

Putative transformant colonies produced through restriction digest, ligation, and subsequent transformation via electroporation, were subjugated to colony PCR (Fig. 3.11). Individual transformant colony DNA, incubated with both forward and reverse primers specific for the toxoid gene Stx2B, showed amplification of Stx2B in all fractions tested (Fig. 3.11, lanes 2-8).

PCR confirmed transformant colonies were then subjected to restriction enzyme digest to verify the insertion of Stx2B, using both BamHI & XhoI restriction cut sites for both single & double restriction digest (Fig. 3.12). As it is seen in Fig. 3.12 (lanes 5 & 6) restriction double digest conducted on plasmid DNA isolated from transformant colonies produced the ~300bp Stx2B inserted gene. Isolated plasmid DNA cut with BamHI (Fig. 3.12, lane 7) showed one single band, similar to the control single digest (Fig. 3.12, lane 2).

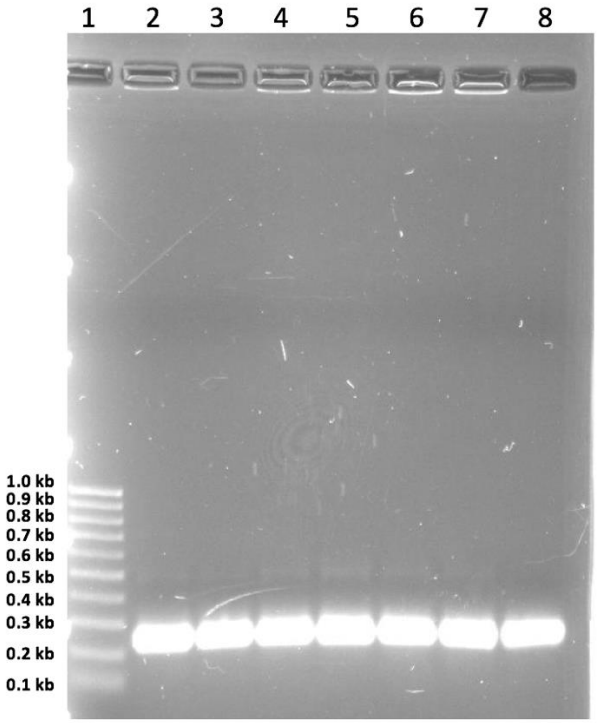

Figure 3.11 Isolated colony PCR conducted on FliC-Stx2B transformant colonies
Lanes 1) Tri-dye DNA ladder. Lanes 2-8) Isolated FliC-Stx2B transformant colonies subjected to PCR.

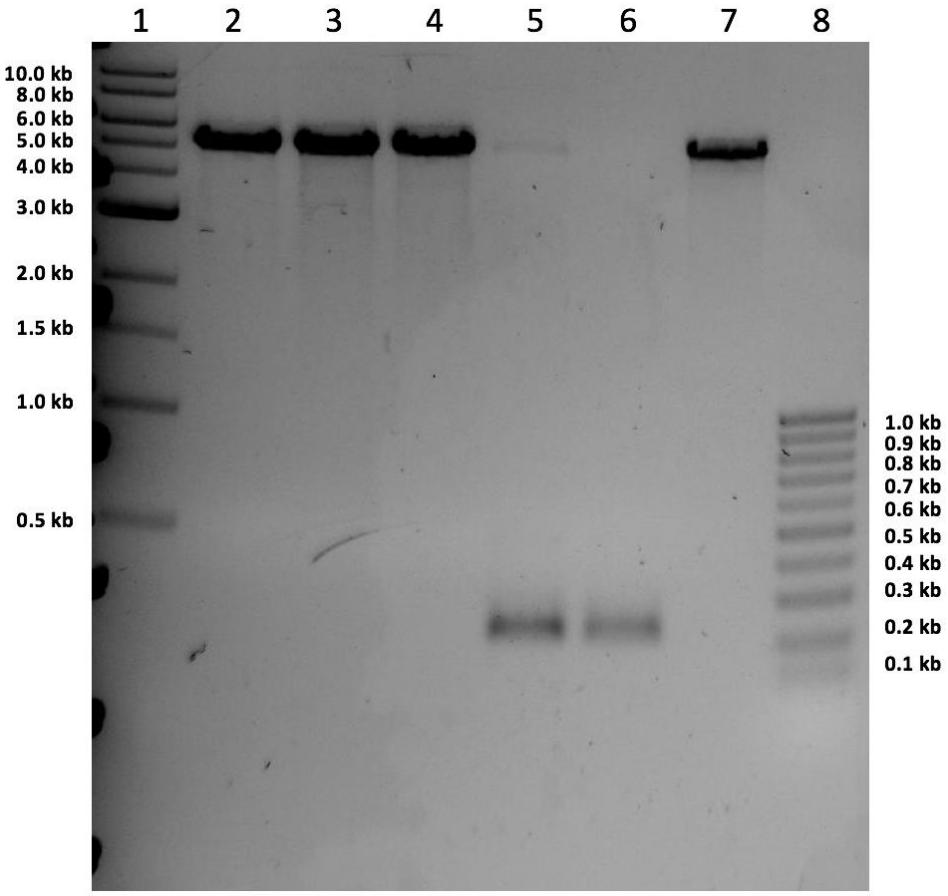

Figure 3.12 Restriction enzyme digest verification on FliC-Stx2B & pJ404
Lane 1) Tridye® 1kb ladder. Lane 2) pJ404 single digest. Lane 3 & 4) pJ404 double digest. Lane 5) FliC-Stx2B double digest. Lane 6) FliC-Stx2B double digest. Lane 7) FliC-Stx2B uncut plasmid. Lane 8) 100bp ladder.

3.8 FliC-Stx2B Expression

Following molecular cloning and verification procedures, induction studies were conducted on both Stx2B-1N & FliC-Stx2B constructs to determine if exclusion of the signal peptide motif, associated with the Stx2B toxoid, has an effect on protein expression (Fig. 3.13). Stx2B-1N contains the detoxified STx2B gene with its' signal peptide motif inserted into the N – terminus of the synthetic FliC construct, whereas FliC-Stx2B contains no signal peptide motif and is cloned into the C – terminus. The induced insoluble fractions (Fig. 3.13, lanes 3 & 4) show expression of both Stx2B-1N & FliC-Stx2B recombinant proteins, in comparison to the

uninduced fractions. However, the level of expression seen in FliC-Stx2B is more significant in comparison to Stx2B-1N. Expression is also seen in the soluble protein fractions in lanes 6 & 7, however slight.

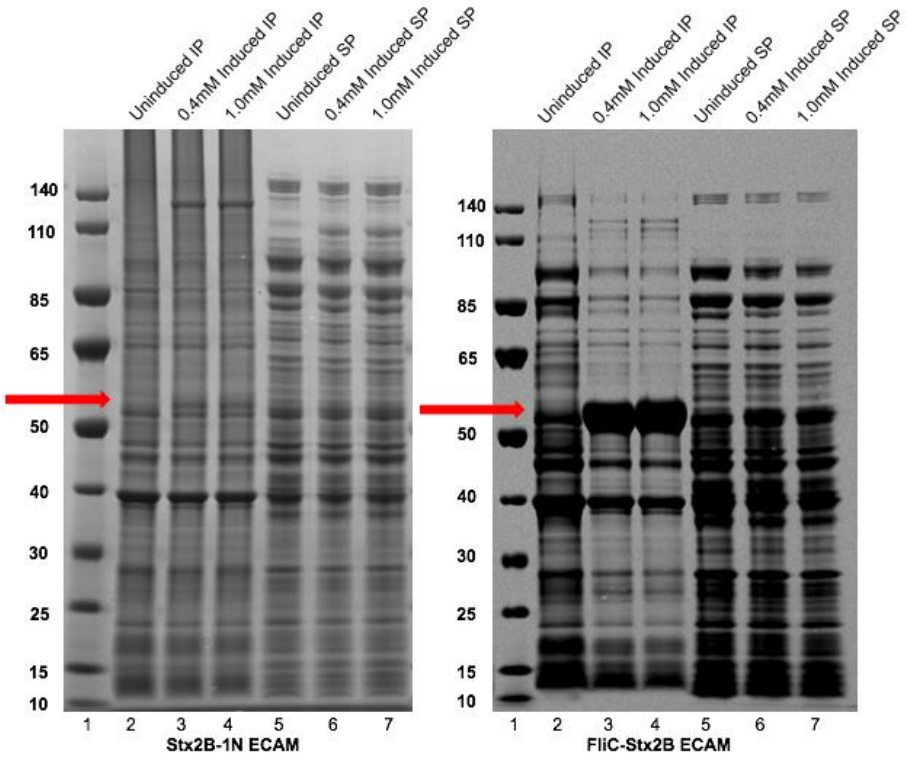

Figure 3.13 Stx2B-1N & FliC-Stx2B E. coli 3-hour induction in E. coli adaptation media ***Stx2B-1N:*** *Lane 1) Page-Ruler Protein Ladder. Lane 2-4) uninduced & induced (0.4mM, 1.0mM IPTG) insoluble protein fractions. Lane 5-7) uninduced & induced (0.4mM, 1.0mM IPTG) soluble protein fractions. All lanes loaded with 5ug of protein.* ***FliC-Stx2B:*** *Lane designations and protein fractions same as Stx2B-1N. Stx2B-1N & FliC-Stx2B molecular weight ~ 53kDa.*

Because of the significant expression seen with the FliC-Stx2B construct, an induction trial utilizing three media types (Luria Broth, Terrific Broth, & ECAM minimal media, Appendix A.4) was conducted (Fig. 3.14). The same parameters used in Fig. 3.13 were also used for this study. The level of expression shown with FliC-Stx2B is present within the insoluble fractions

(Fig. 3.14, lanes 3 & 4) in each of the three mediums tested, however expression levels were lower in Luria-Broth cultures. Reduction in non-FliC-Stx2B proteins in expressed lanes 3 & 4 is also shown in comparison to the uninduced insoluble fractions (Fig. 3.14, lane 1) and the uninduced & induced soluble fractions (Fig. 3.14, lanes 5-7). Each 100mL culture yielded ~1.0g (wet wt.) of cell pellet.

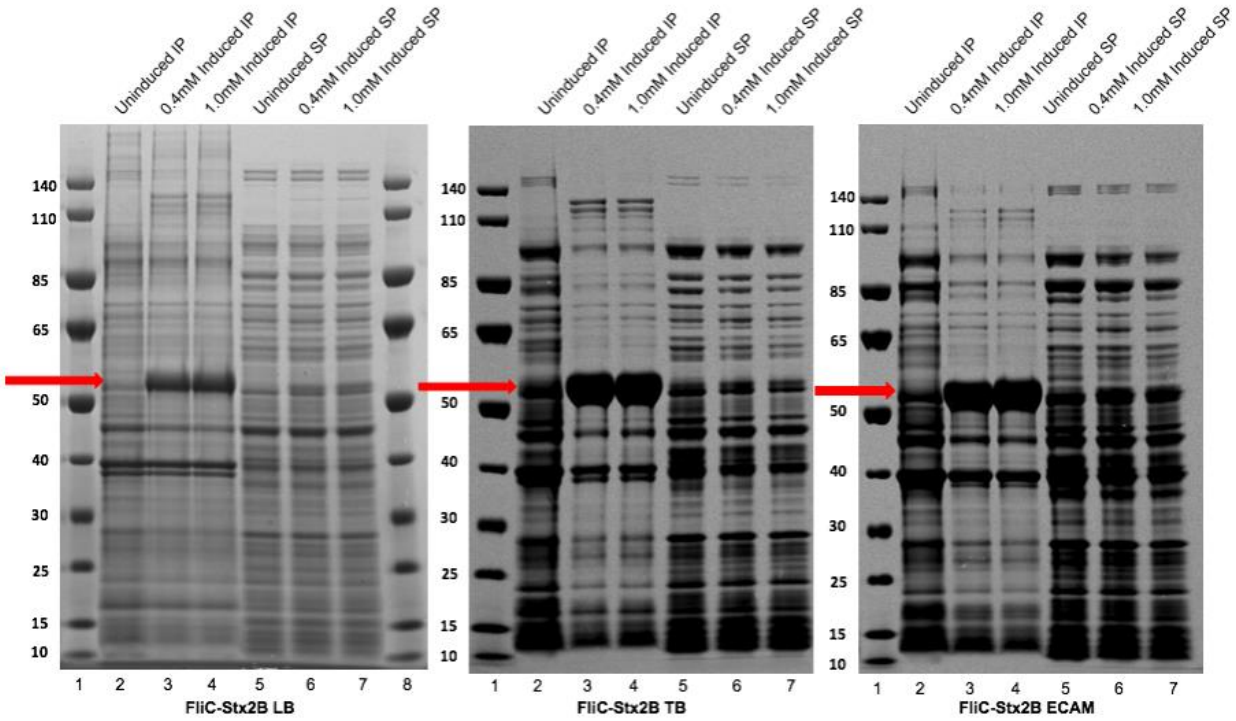

Figure 3.14 FliC-Stx2B E. coli 3-hour induction samples in LB, TB, & ECAM media ***FliC-Stx2B LB.*** *Lanes 1 & 8) Page-Ruler Protein Ladder. Lanes 2-4) uninduced & induced (0.4mM, 1.0mM IPTG) insoluble protein fractions. Lane 5-7) Uninduced & induced (0.4mM, 1.0mM IPTG) soluble protein fractions.* ***FliC-Stx2B TB & ECAM:*** *Lane designations and protein fractions consistent with FliC-Stx2B LB.*

3.9 Insoluble FliC-Stx2B clarification & resolubilization -

Due to the insolubility of FliC-Stx2B, a modified detergent wash method was utilized containing both urea (pellet wash steps) and guanidine hydrochloride (resolubilization step) detergents, in order to isolate FliC-Stx2B from insoluble inclusion bodies immediately following

cell disruption (Fig. 3.15). For both TB media & ECAM culture samples, an incremental reduction in non-desired protein is observed against the soluble protein fractions (Fig. 3.15, lanes 2-4, 7-10). Resolubilized pellet lanes also show greater reduction of non-desired proteins following pellet detergent wash steps. Resolubilized sample bands (Fig. 3.15, lanes 5 & 10) also appear curved due to the addition of guanidine hydrochloride.

To determine the applicability of the modified detergent wash method, tested culture volumes were increased to 100mL & 1L, respectfully, in comparison to small-scale 10mL cultures (Fig. 3.16). Similar to Fig. 3.15, the up-scaled modified detergent wash method shown in Fig. 3.16 shows a significant reduction in non-desired protein banding, along with significant isolation of FliC-Stx2B from the insoluble inclusion body pellet. The corresponding Western blot also indicates the presence of biologically active FliC-Stx2B (Fig. 3.16B, lanes 3-6 & 9-12). This is seen not only at the predicted molecular weight, but in higher molecular weight polymer bands.

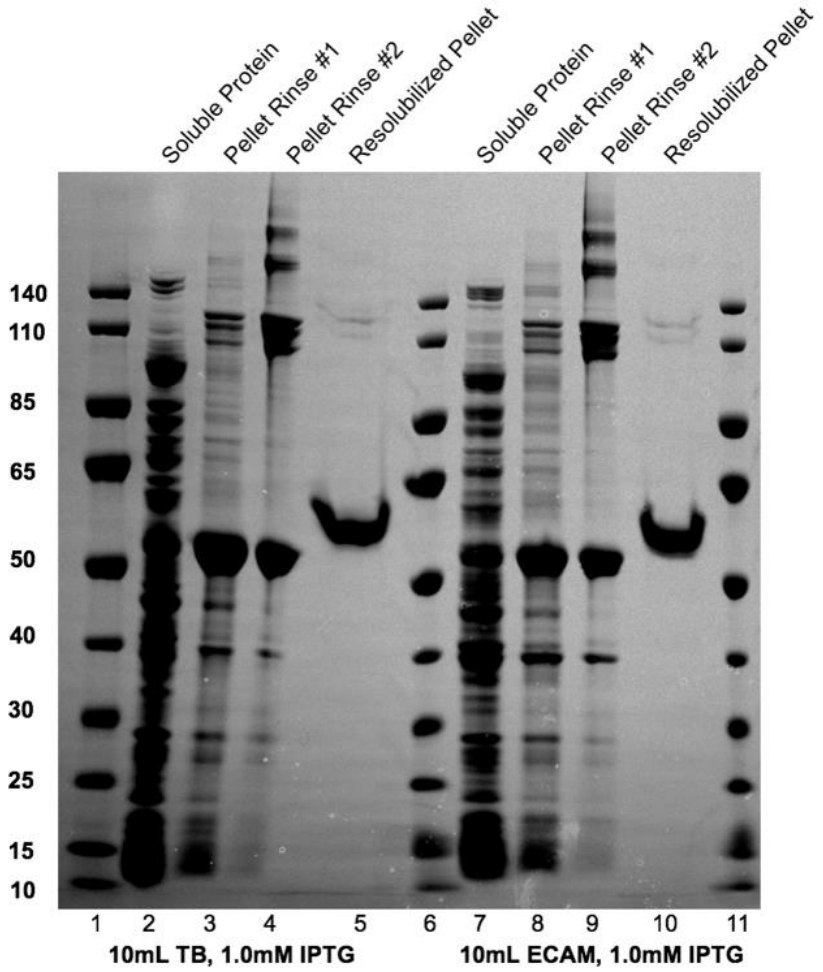

Figure 3.15 FliC-Stx2B Cell Clarification & Detergent Wash in Terrific Broth and ECAM
Lanes 1, 6, & 11) Page-Ruler protein ladder. Lanes 2 & 7) Soluble protein fraction. Lanes 3,4 & 8,9) Pellet detergent wash fractions. Lanes 5 & 10) Resolubilized FliC-Stx2B insoluble protein.

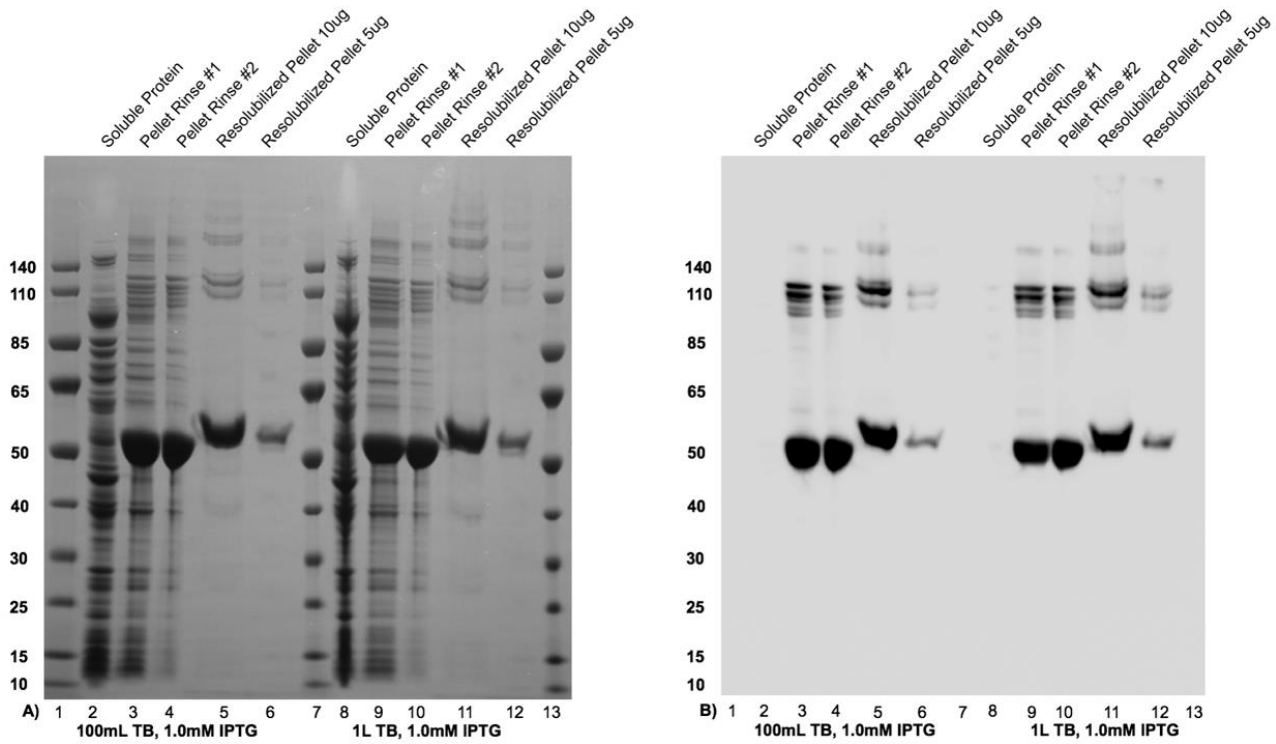

Figure 3.16 SDS-PAGE & Western Blot on FliC-Stx2B Cell Clarification using 100mL & 1L Culture Pellets in Terrific Broth
(A) *Lanes 1, 7, & 13) Page-Ruler protein ladder. Lanes 2 & 8) Soluble protein fraction. Lanes 3,4 & 9,10) Pellet detergent wash fractions. Lanes 5 & 11) Resolubilized FliC-Stx2B insoluble protein (10ug). Lanes 6 & 12) Resolubilized FliC-Stx2B insoluble protein (5ug).* ***(B)*** *All lanes correspond to (A). Anti-Stx2B primary mAb was used at a ratio of 1: 1,000.*

3.10 FliC-Stx2B on-column purification with biological activity analysis

In order to refold resolubilized FliC-Stx2B back to its intrinsic form, an on-column purification procedure was utilized using AKTA® FPLC systems. The step-wise refolding & elution gradient washes (Fig. 3.17, lanes 4, 5, 7, & 14) show no removal of the bound His-tagged FliC-Stx2B from the nickel column. Moreover, refolded FliC-Stx2B was eluted at both 60% & 80% increments during the step-wise elution gradient (Fig. 3.17, lanes 10 & 11).

Following AKTA© FPLC purification and refolding, purified FliC-Stx2B was then de-salted using Amicon filters with a molecular weight cut off of 30kDa. An Enzyme Linked

Imunno Absorbent assay was then conducted on both pre-AKTA© (resolubilized) and purified FliC-Stx2B samples to determine whether or not the on-column refolding step proved efficacious in maintaining anti-Stx2B biological activity. As it is shown in Fig. 3.18, purified FliC-Stx2B shows a higher rate of activity in almost all samples tested. The activity profile seen with pre-AKTA© samples also contain ~50% less total activity in comparison to refolded samples.

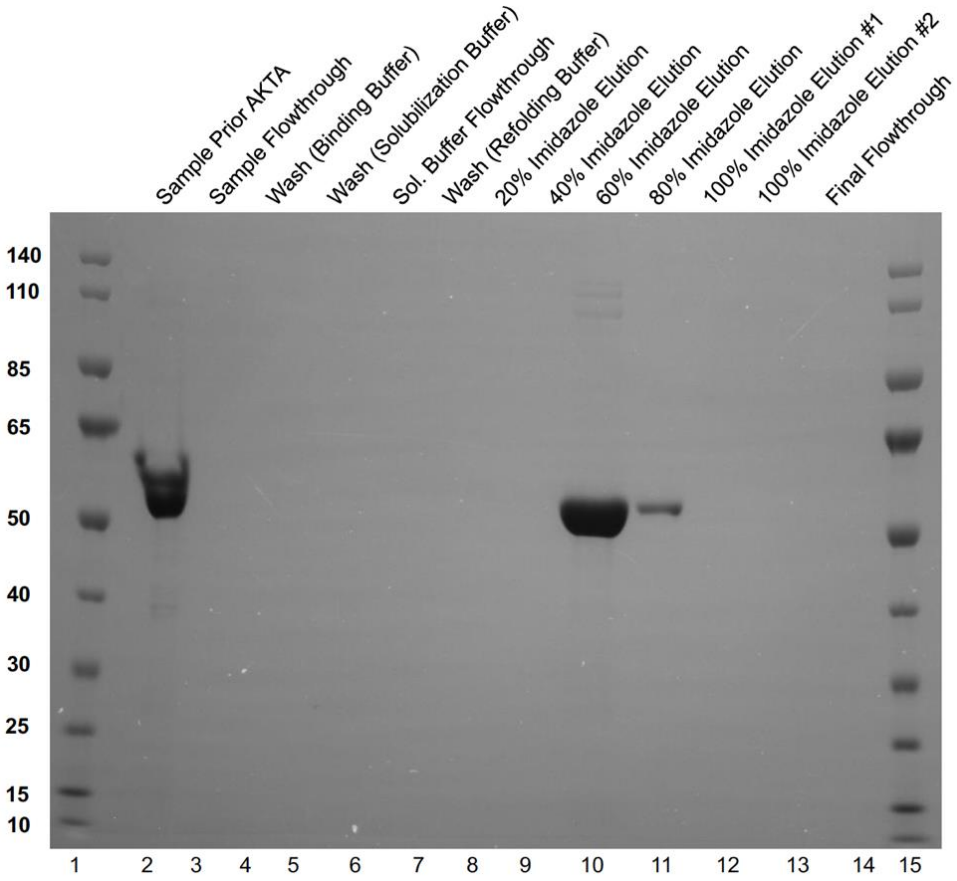

Figure 3.17 FliC-Stx2B FPLC Purification
Lanes 1 & 15) Page-Ruler protein ladder. Lane 2) Resolubilized FliC-Stx2B insoluble protein. Lane 9) Purified FliC-Stx2B at 60% imidazole elution. Lane 10) Purified FliC-Stx2B at 80% imidazole elution.

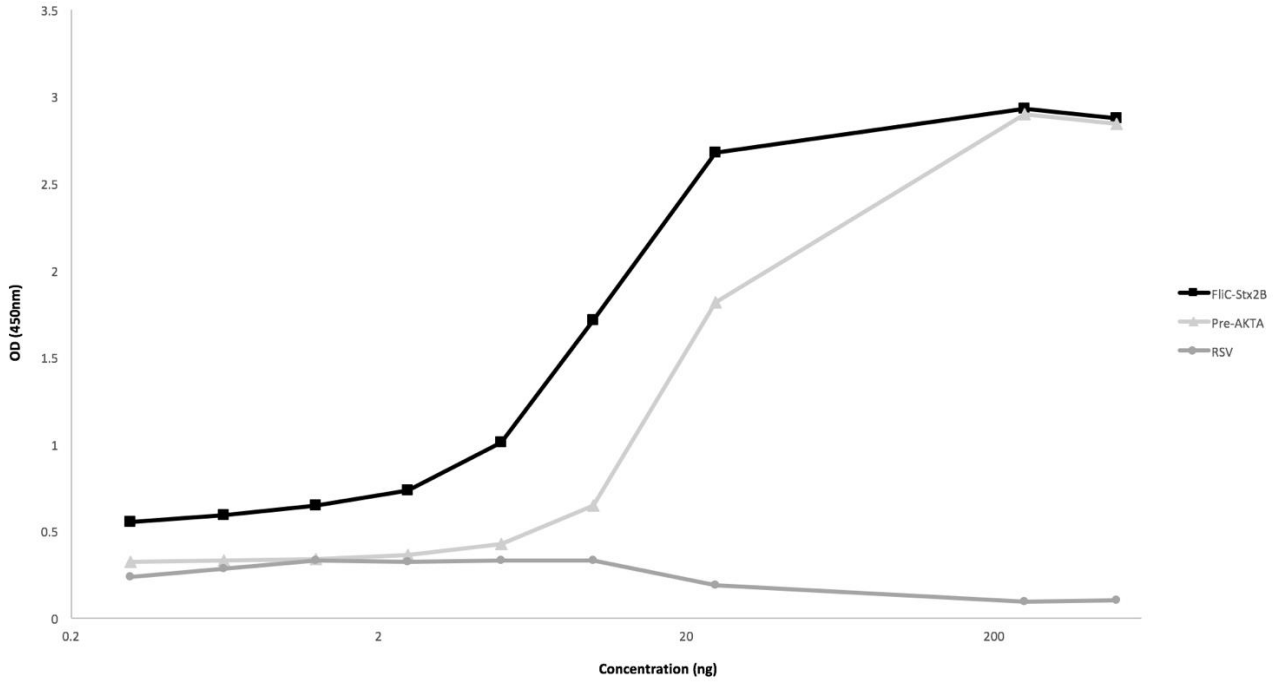

Figure 3.18 FliC-Stx2B resolubilized & purified Indirect-ELISA
Purified FliC-Stx2B samples tested over a concentration range of 3ng to 500ng.

3.11 FliC-Stx2B on-column refolding time study & biological activity analysis

To determine the optimal incubation period for FliC-Stx2B on-column refolding, a time study was conducted using three separate 1mL HisTrap Nickel columns in alternating lines using AKTA® FPLC systems concurrently (Fig. 3.19A). Purified & refolded FliC-Stx2B was eluted again in a step-wise gradient at both 60% & 80% increments, further characterizing elution conditions (Fig. 3.17). Higher molecular weight FliC-Stx2B polymer proteins, identified in Fig. 3.16B, was also positively identified in the corresponding Western blot, indicating the presence of biologically active FliC-Stx2B throughout each refolding time-point.

A Western blot & indirect ELISA, specifically targeting the Stx2B epitope domain, was conducted using purified FliC-Stx2B samples from the 1 and 6-hour on-column refolding incubation (Fig. 3.19A & 3.19B) with a concentration range of 250ng-3.9ng for *in vitro* analysis (Fig. 3.20). There was little difference seen between 1-hour and 6-hour on-column incubation

samples, however at each tested concentration set the 1-hour incubated FliC-Stx2B samples contained higher biological activity in comparison to 6 hours of incubation.

Preliminary *in vitro* analysis comparing FliC-Stx2B's ability to activate innate immunity associated TLR5 receptors, expressed in HEK293 cells, against control FljB protein is seen in Fig. 3.21. Tested samples were added to confluent HEK293 cells, then observed at an optical density of 630nm after a time period of ten minutes.

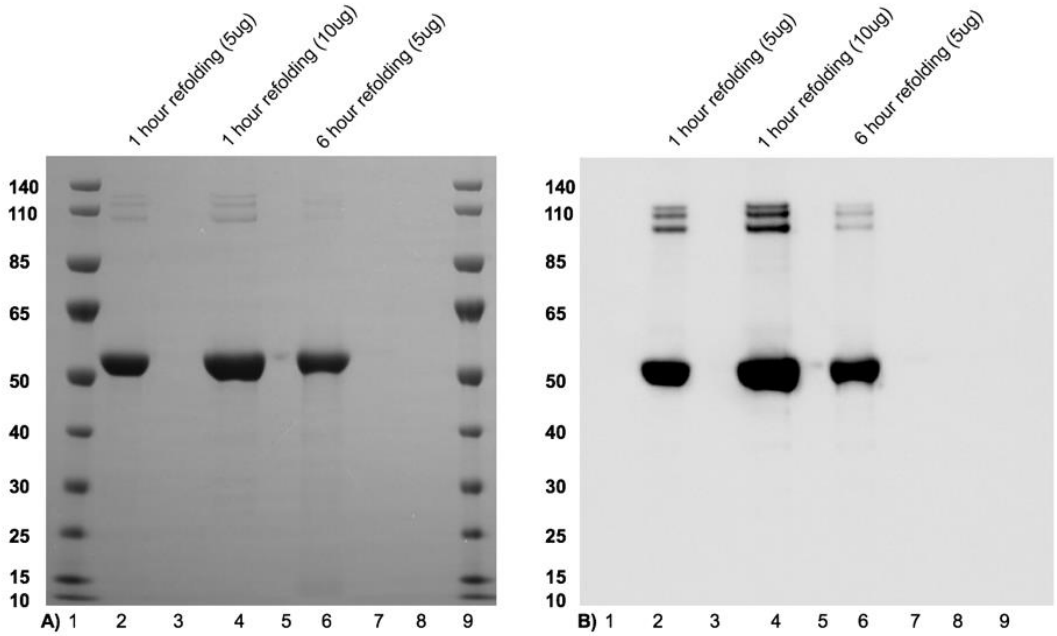

Figure 3.19 SDS-PAGE & Western Blot for FliC-Stx2B FPLC purified protein
(A) *Lanes 1 & 9) Page-Ruler protein ladder. Lane 2) 1-hour incubated FliC-Stx2B purified protein loaded with 5ug. Lane 4) 1-hour incubated FliC-Stx2B purified protein loaded with 10ug. Lane 6) 6-hour incubated FliC-Stx2B purified protein loaded with 10ug.* ***(B)*** *All lanes correspond to (A). Anti-Stx2B primary mAb was used at a ratio of 1: 1,000.*

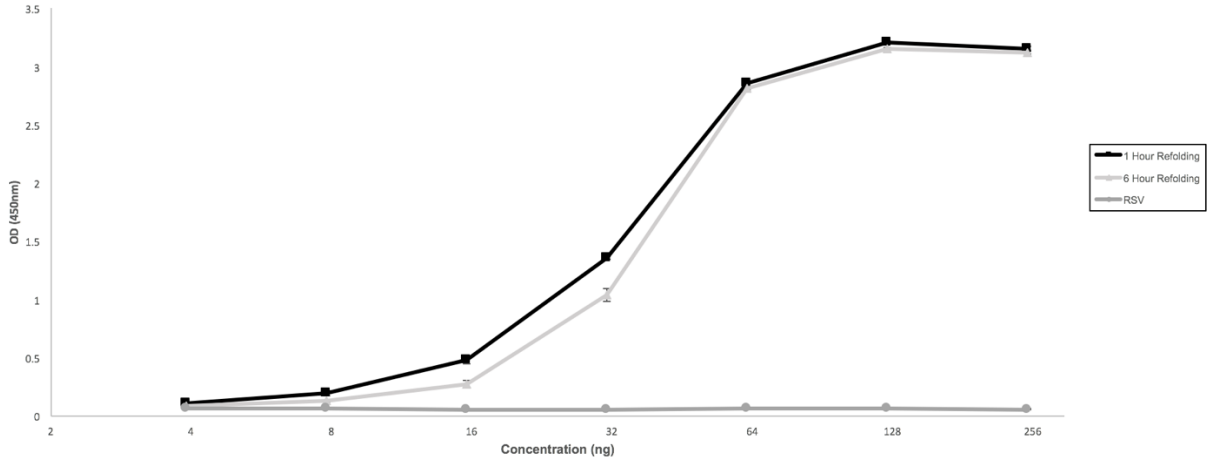

Figure 3.20 FliC-Stx2B refolding study ELISA
1 & 6-hour purified FliC-Stx2B protein tested over a concentration range of 250ng-3.9ng

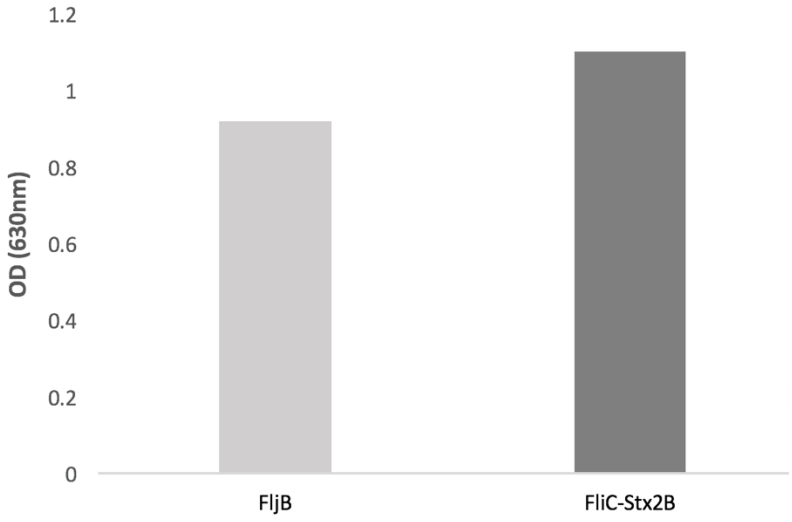

Figure 3.21 FliC-Stx2B TLR5* in vitro *assay
1-hour purified FliC-Stx2B fusion protein, & control FljB, TLR5 activity against TLR5 receptor expressing human embryonic kidney cells (HEK293). Tested samples observed at OD630 after 10 minutes.

3.12 FliC-Stx2B dialysis refolding

Treated cell culture pellet samples were induced, clarified, and processed in order to isolate the insoluble fusion protein FliC-Stx2B (Fig. 3.22). Following separation of both soluble and insoluble fractions, FliC-Stx2B remains primarily in the insoluble pellet rinse fraction (Fig. 3.22, lanes 2 & 3). This retention is shown throughout both pellet rinse washes and the resolubilized protein fraction (Fig. 3.22, lanes 3-5). Removal of non-desired proteins is also seen in the final resolubilized protein fraction (Fig. 3.22A & 3.22B).

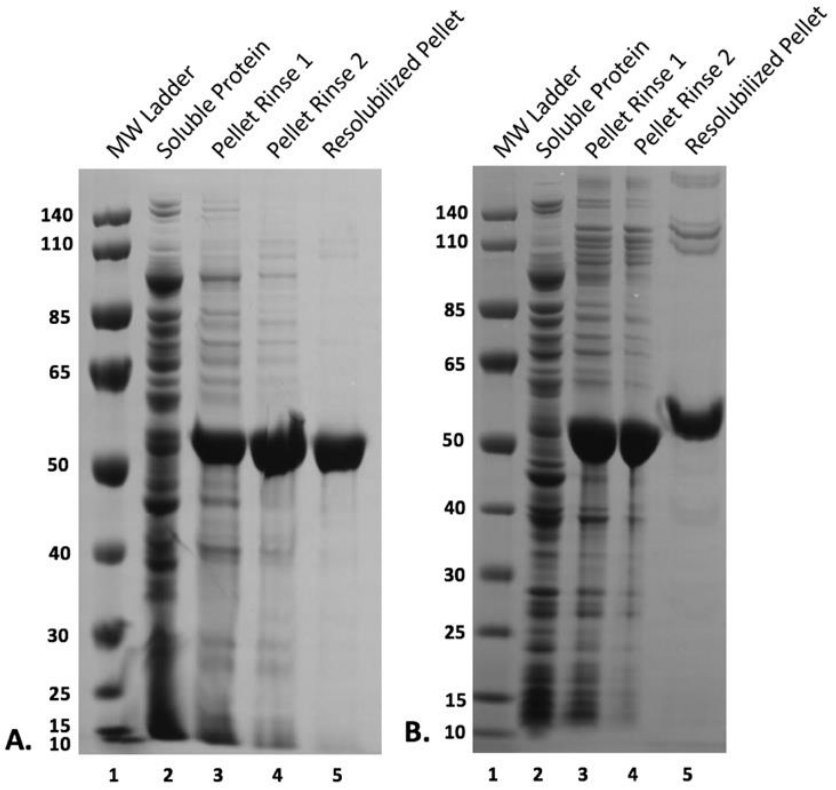

Figure 3.22 FliC-Stx2B expression, cell clarification, & isolation using varying concentrations of detergent

(A) 2M Guanidine hydrochloride. *Lane 1) Page-Ruler Protein Ladder. Lane 2) Soluble protein fraction. Lane 3 & 4) Insoluble protein fraction from pellet rinse washes using 2M Urea. Lane 5) Resolubilized insoluble protein fraction using 2M Guanidine hydrochloride.* ***(B) 6M Guanidine hydrochloride.*** *Lane 1) Page-Ruler Protein Ladder. Lane 2) Soluble protein fraction. Lane 3 & 4) Insoluble protein fraction from pellet rinse washes using 2M Urea. Lane 5) Resolubilized insoluble protein fraction using 6M Guanidine hydrochloride.*

Following resolubilization of insoluble FliC-Stx2B, dialysis refolding using a refolding buffer devoid of guanidine hydrochloride was conducted to return the protein to a more intrinsic form (Fig. 3.23A). FliC-Stx2B (Fig. 3.23A, lane 5) shows an increase in band presence overall, however did not contain guanidine hydrochloride unlike in the resolubilized FliC-Stx2B sample. Both resolubilized and dialyzed FliC-Stx2B samples however showed similar banding patterns when compared to on-column purified samples, specifically polymerized protein bands located at ~105-120kda (Fig. 3.23). Refolded FliC-Stx2B was then subsequently purified using nickel column affinity under the same parameters as on-column purification with the exception of on-column incubation (Figs 3.17 & 3.19) in Fig. 3.24.

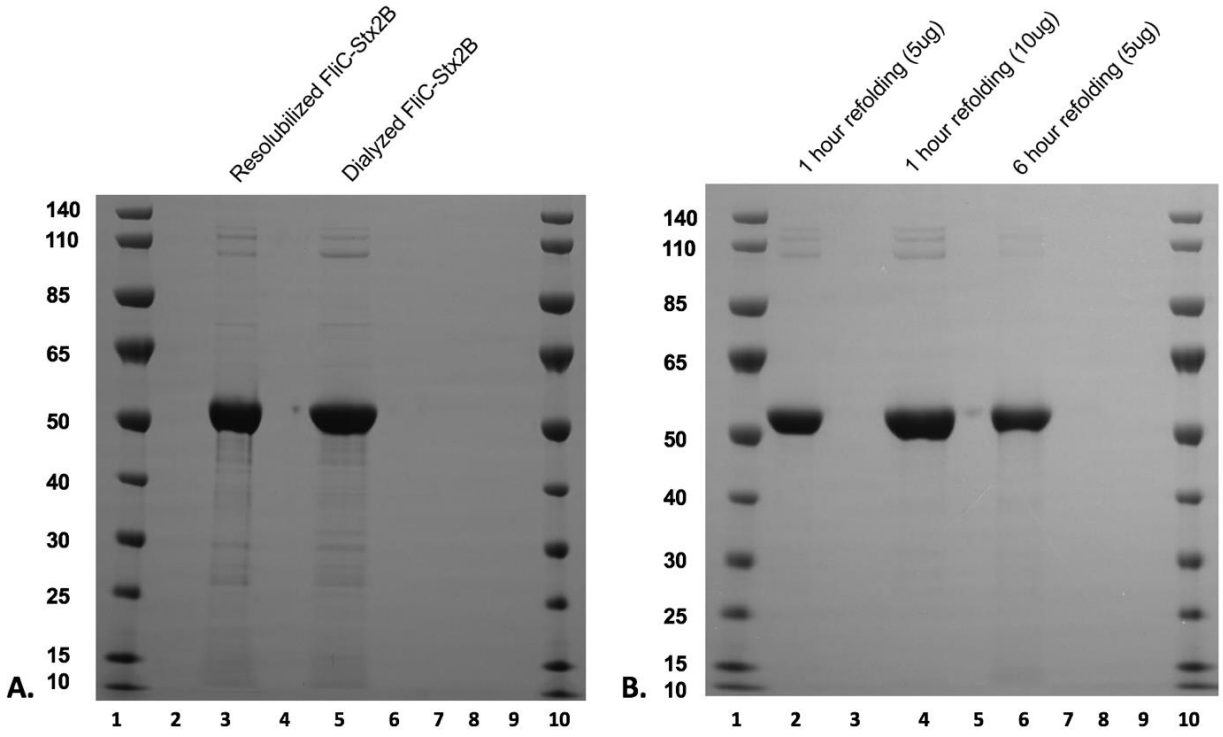

Figure 3.23 Resolubilized, refolded, & on-column purified FliC-Stx2B
(A) Dialyzed FliC-Stx2B. *Lanes 1 & 10) Page-Ruler Protein Ladder. Lane 3) Resolubilized FliC-Stx2B using 2M Gnd-HCl. Lane 5) Dialyzed & refolded resolubilized FliC-Stx2B.* ***(B) On-Column purified FliC-Stx2B.*** *Lanes 1 & 10) Page-Ruler Protein Ladder. Lane 2) 1-hour on-column refolded FliC-Stx2B purified protein. Lane 4) 1-hour on-column refolded FliC-Stx2B purified protein. Lane 6) 6-hour on-column refolded FliC-Stx2B purified protein. Samples were treated with 6M Gnd-HCl prior to nickel column purification.*

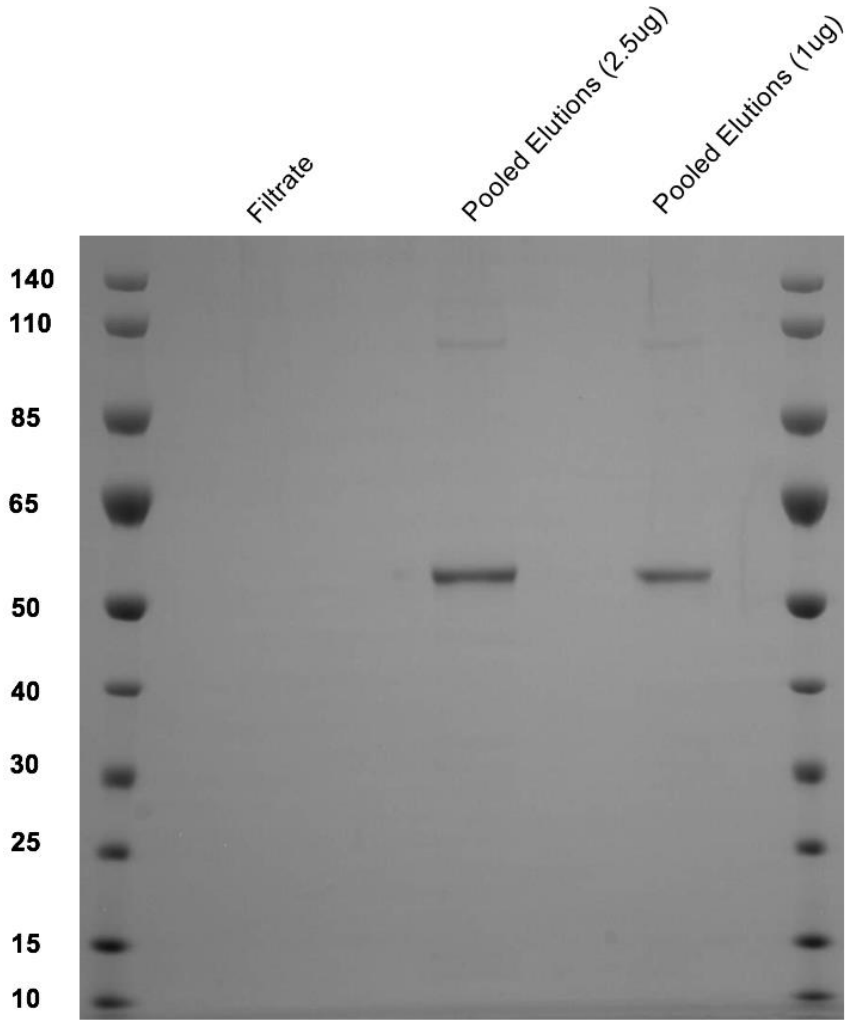

Figure 3.24 Dialysis refolded FliC-Stx2B purified samples
Resolubilized & refolded FliC-Stx2B samples purified using nickel column affinity.

3.13 Dialyzed FliC-Stx2B Western Blot & Indirect ELISA analysis

In order to determine both purity & biological activity for the FliC-Stx2B fusion protein, a Western blot and indirect ELISA was conducted on both resolubilized and dialyzed samples (Fig. 3.25 & 3.26). Western blot analysis seen in Fig. 3.25A & 3.25B (lanes 3, 5, 7, & 9) show positive biological activity against anti-Stx2B monoclonal antibodies. This is also seen across a

concentration gradient from 10ug-2.5ug in dialyzed FliC-Stx2B samples. Higher protein bands seen previously in Fig. 3.23A were also identified as containing the Stx2B epitope (Fig. 3.25).

Indirect ELISA analysis (Fig. 3.26) shows positive biological activity for both resolubilized and dialysis refolded FliC-Stx2B samples across a concentration gradient of 250ug to 3.9ug. Biological profiles between both sample types were similar in activity.

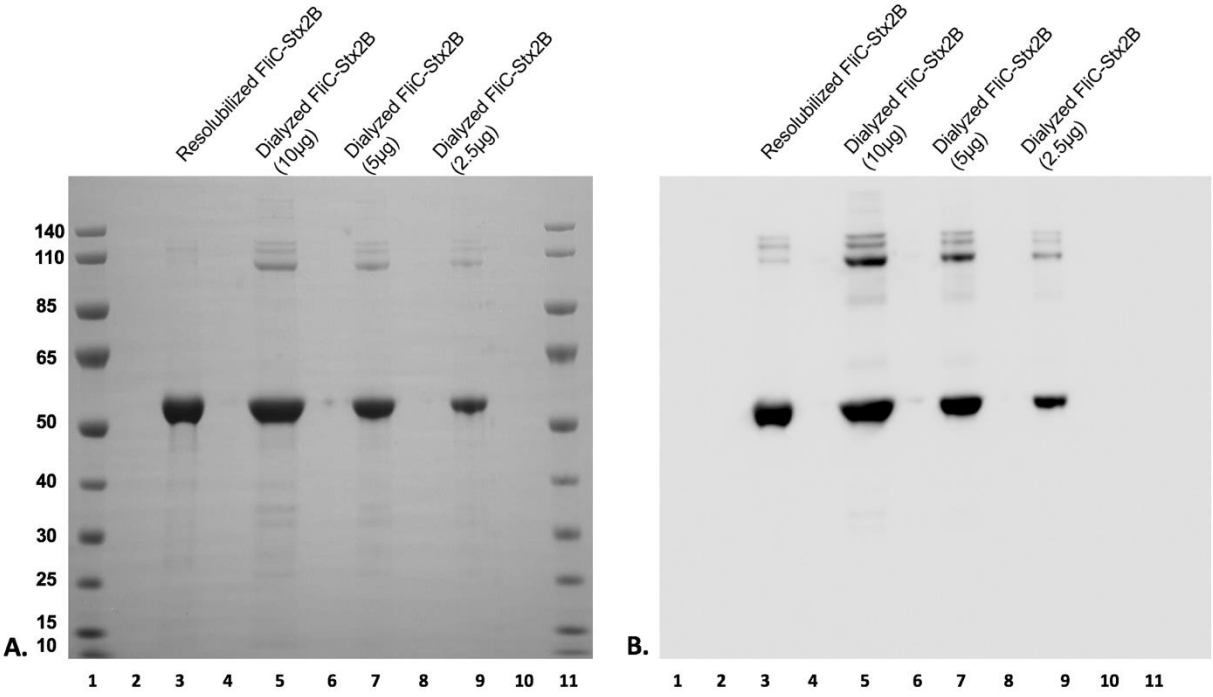

Figure 3.25 SDS-PAGE & Western Blot for resolubilized & purified dialyzed FliC-Stx2B
(A) *Lanes 1 & 11) Page-Ruler protein ladder. Lane 3) Resolubilized FliC-Stx2B. Lane 5) Dialyzed FliC-Stx2B (10ug). Lane 7) Dialyzed FliC-Stx2B (5ug). Lane 9) Dialyzed FliC-Stx2B (2.5ug).* ***(B)*** *All lanes correspond to (A). Anti-Stx2B primary mAb was used at a ratio of 1: 1,000.*

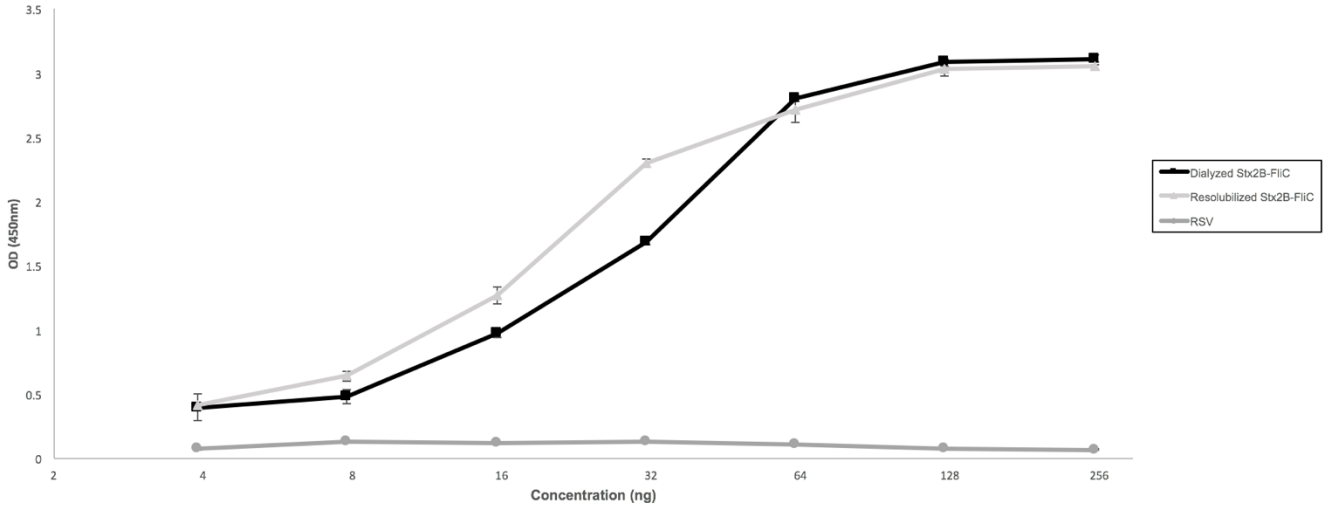

Figure 3.26 FliC-Stx2B resolubilized & dialysis refolded indirect ELISA

Resolubilized & dialysis refolded FliC-Stx2B protein samples tested over a concentration range of 250ng-3.9ng.

3.14 Native-FliC

Cells containing Native-FliC, inserted into the host plasmid pJ404, were expressed then separated into both soluble and insoluble fractions (Fig. 3.27). Expression of Native-FliC is seen in equal parts for both soluble and insoluble fractions, however does not appear in uninduced samples.

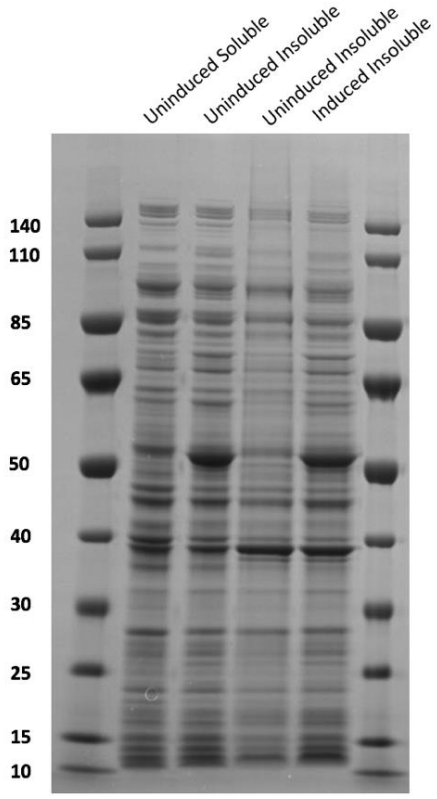

Figure 3.27 Native-FliC soluble & insoluble induction samples

3.15 Insoluble Native-FliC clarification & resolubilization

Native FliC cell pellet sample was processed the same way described for FliC-Stx2B, and then clarified to remove excess proteins and inclusion bodies (Fig. 3.28). Following the detergent washes in lanes 3 & 4, the resolubilized Native-FliC insoluble protein lane shows an increased

reduction in non-desired protein. The corresponding Western blot confirms the activity of Native-FliC (Fig. 3.28) while showing no positive banding against purified FliC-Stx2B.

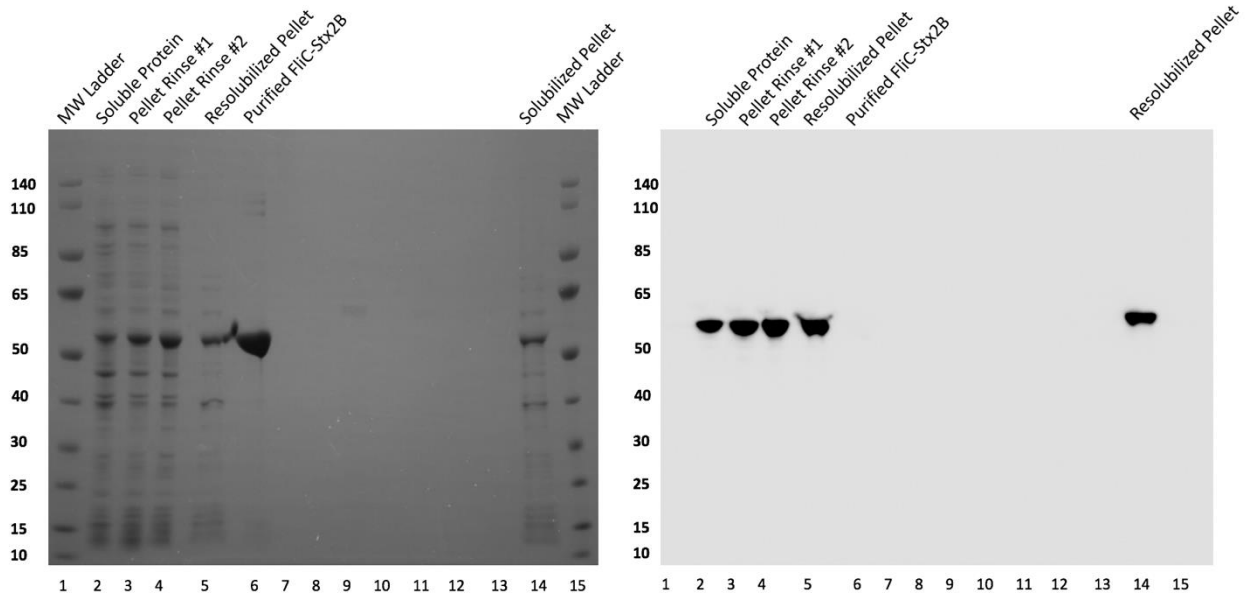

Figure 3.28 SDS-PAGE & Western Blot (anti-FliC) for insoluble Native-FliC cell clarification

SDS-PAGE: *Lanes 1 & 15) Page-Ruler® protein ladder. Lane 2) Soluble protein fraction. Lane 3 & 4) Pellet detergent washes 1 & 2. Lane 5) Resolubilized Native-FliC insoluble protein. Lane 6) Purified FliC-Stx2B.* ***Western Blot:*** *All lanes correspond to SDS-PAGE.*

3.16 Native-FliC on-column refolding & purification

Purification of resolubilized Native-FliC was conducted using AKTA® FPLC systems using the same parameters as the aforementioned FliC-Stx2B purification, however at a lower imidazole concentration gradient (5-100mM imidazole). It was observed (Fig. 2.29) that elution of nickel column bound Native-FliC began at 30mM imidazole and produced pure protein banding at ~60mM imidazole during the elution gradient, when using a 0.3mL/min flow rate.

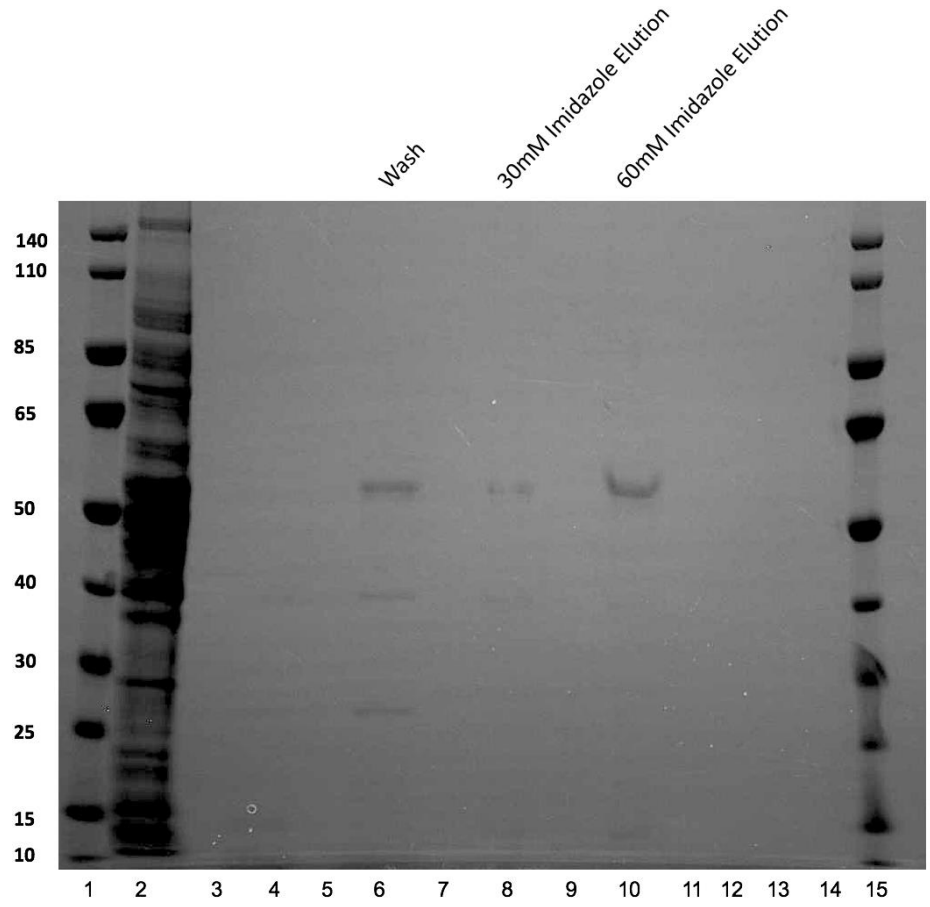

Figure 3.29 SDS-PAGE for Native-FliC AKTA© FPLC Purification

Lanes 1 & 15) Page-Ruler protein ladder. Lane 2) Resolubilized Native-FliC insoluble protein. Lane 6) 5mM Imidazole wash. Lane 8) 30mM imidazole elution. Lane 10) 60mM imidazole elution.

4 CONCLUSIONS

4.1 mRFP

In silico design for mRFP was proven successful following PCR amplification (Fig. 3.1) producing large quantities of mRFP DNA from the host plasmid pSB1AC3. The high concentration of amplified DNA yield further allowed sufficient working material for subsequent down-stream applications such as; restriction digest, ligation, and transformation. This is attributed to the high primer specificity generated during *In silico* design, ensuring that melting temperatures were within the appropriate accuracy range based upon their G-C base pair content.

Transformation of mRFP recirularized DNA samples were successful and yielded numerous cream-colored colonies, indicative of *E. coli* growth (Fig. 3.2). On selective control plates, no colonies were visible on plates containing solely electro-competent *E. coli* cells. No growth was also seen on plates inoculated with pJ404 plasmid DNA subjected to restriction enzyme double digest without the addition of DNA ligase. The presence of no growth with samples excluding DNA ligase illustrates that recircularization of the linearized plasmid did not occur during ligation, indicating efficient ligation of pJ404 vector plasmid and insert mRFP DNA.

Colony PCR data supports this assessment (Fig. 3.3) as gene specific banding appeared at ~700bp, similar to previously amplified mRFP DNA banding migration patterns. However, during protein expression, no fluorescence was observed. The transformant colonies also did not show any signs of fluorescence when subjugated to UV radiation at 240nm. Due to these results, it was presumed that fluorescence produced by mRFP was intrinsically weak and was unable to functionally emit observable levels.

4.2 Stx2B-1N *in silico* verification

Previous work conducted on amplification of the toxoid gene of interest, Stx2B, from the host plasmid provided very small amounts of working insert DNA. Because of this, a redesign on previous *in silico* work was conducted in order to maximize starting DNA concentrations for subsequent experiments. Stx2B *in silico* gene analysis uncovered a competitive upstream SpeI restriction enzyme cut site located in host plasmid pJ204. Targeted insertion of Stx2B into synthetic FliC has the gene of interest located in the N' terminus of synthetic FliC, between NcoI & SpeI restriction enzyme cut sites. Because of this, a competitive binding site for the Stx2B reverse primer was introduced due to SpeI being located on both the downstream end of the gene and the primer itself.

In an attempt to optimize, PCR parameters were changed in order to enhance primer binding. These changes included; extending primer length, decreasing the concentration of template DNA over a gradient, and increasing the previous annealing temperature to 64°C. Each change was designed to increase specificity of the primers to template DNA during the annealing step, thus allowing primers to bind only to the specified region and not the competitive upstream restriction cut site. As shown in Fig. 3.4, decreasing the concentration of template DNA for PCR proved successful in producing a single amplified band, as a gradient like effect was seen when going down from 500ng to 100ng of template DNA. With these parameter changes established, high yields of concentrated amplicon DNA was produced for subsequent experiments for transformation.

4.3 Stx2B-1N transformation & analysis

With the higher yields of concentrated amplicon DNA for restriction enzyme digest and ligation, subsequent transformation and selective plating produced positive transformant

colonies. Colonies which grew on the selective LB plates with ampicillin exhibited similar growth characteristics, such as color & shape, as those seen with mRFP transformation.

A quadrant colony PCR was conducted on several colonies per quadrant per plate for each molar ligation ratio (1:3 and 1:8) and yielded expected results (Fig. 3.6). Each quadrant, for each plate tested, showed Stx2B amplification from the transformant colonies. Thus, indicating that per quadrant tested, there was at least one colony that contained the Stx2B toxoid gene insert.

Following these results, isolated colony PCR on several of the colonies that were used in quadrant colony PCR would be tested individually for PCR verification and to ensure no false positives (Fig. 3.7). The Stx2B toxoid gene insert again appeared on the gel following PCR, indicating that the Stx2B gene was inserted into host plasmid pJ404, which contains the histidine tagged synthetic FliC backbone. Restriction enzyme digest conducted on Stx2B-1N produced the gene of insert at the expected banding migration as seen in comparison to previous samples. DNA sequencing conducted at Georgia State University also confirmed Stx2B gene insertion at the correct location with no frame shifts or alterations to the *in silico* design.

4.4 Stx2B-1N induction & purification analysis

Induction on the Shiga-like toxoid containing *E. coli* cells (Fig. 3.13; Appendix A.3, A12-A14) showed that expression of the gene of interest was found primarily in insoluble fractions. Higher rates of gene expression were also seen at an optimal temperature of 37°C, and at an inducer concentration of 1.0mM Isopropyl β-D-1-thiogalactopyranoside (IPTG).

Initial analysis conducted on clarified induced cell samples for purification (Fig. 3.8) showed that secretion of the recombinant protein, Stx2B-1N, maintains higher levels in the

soluble cell-associated fractions as opposed to insoluble fractions (Fig. 3.8 & 3.9). The presence of Stx2B-1N within the soluble intracellular fractions indicate that despite the addition of a 19 mer signal peptide ('MKKMFIAVLFALVSVNAMA'), a type 3 secretion system motif, the associated protein remains primarily within the soluble cell fraction and not within extracellular supernatant. This suggests that the induced rate for protein expression is either insufficient for translocation, or that Stx2B-1N remains adhered to the cellular transmembrane space during translocation. Moreover, during nickel column purification, eluted fractions for clarified Stx2B-1N contained competitive non-specific protein which also demonstrated affinity for the column (Fig. 3.8).

Because of this, troubleshooting techniques for enhanced fusion protein binding against nickel columns, and subsequent elution, were analyzed (Fig. 3.9). Enhancements to protein binding & elution was attempted through the usage of varying concentrations of imidazole in the binding buffer. Salt concentrations were increased from 2mM, to 5mM & 20mM of imidazole, respectfully (Fig. 3.9A & 3.9B). A decrease in excess non-specific protein during elution using 20mM of imidazole (Fig. 3.9B) was observed in comparison to elution with the addition of only 5mM of imidazole (Fig. 3.9A). The increase in imidazole enables previously competitive proteins, within a 20mM imidazole charged nickel column, to be removed during wash steps. However, this did not completely remove the remaining interfering proteins.

4.5 Stx2B-1N fermentation analysis

In order to produce large quantities of *E. coli* cell paste, containing the shiga-like toxoid subunit linked to synthetic FliC, a fed-batch fermentation was conducted and induced with IPTG for five hours. The cell paste, grown in ECAM synthetic media, was then processed into a

workable refined lysate and analyzed by SDS-PAGE & Western blot for protein expression levels.

As it is seen in Fig. 3.10A & 3.10B, the protein of interest was expressed at a molecular weight of ~55kda, when using anti-FliC antibodies, throughout all the fractions during the clarification process. Another band, located at a molecular weight of ~38kda, was also seen and expressed at higher levels then the recombinant protein Stx2B-1N while appearing distinctly on the corresponding Western Blot.

In order to isolate the expressed recombinant protein, several clarification steps were applied to the fermentation cell paste in order to remove non-desired proteins (Fig. 3.10). The SDS-PAGE ran on all sample fractions during homogenization, PEG 3350 precipitation, and Triton X-114 2-phase separation showed little removal of excess non-specific protein banding. Furthermore, the Western blot against anti-FliC antibodies showed an incremental decrease in the amount of Stx2B-1N recombinant protein throughout PEG precipitation and two-phase separation (Fig. 3.9B). Interestingly, the most prominent band on the Western blot was the ~38kda protein band which became incrementally prominent during the separation phase.

Analysis of the putative bands seen on the Western blot was conducted by Maldi-Tof MS/MS at Georgia State University's protein core facilities department and confirmed the presence of Stx2B-1N. Whereas the ~38kda protein was identified as an outer membrane protein (OMP) commonly associated with *E. coli* cell fractions.

4.6 FliC-Stx2B *in silico* design & transformation verification

Previously, Stx2B-1N has shown expression in LB, TB, & *E. coli* Adaptation Mediums, respectfully. However, this level of expression appeared basal in comparison to other

recombinant protein expression levels pertaining to Stx2B. In order to enhance the level of expression a new clone series was designed and inserted into vector plasmid pJ404, containing synthetic FliC, into the C-terminal D0 domain in order to enhance hexa-histidine tag presentation during the purification process, and is aptly named FliC-Stx2B.

More importantly as described above, FliC-Stx2B was designed & cloned with the exclusion of its native signal peptide motif to further enhance protein expression. It has been shown empirically by other researchers that the inclusion of the signal peptide can alter protein expression making it non-ideal for large yields following purification (Skinner & Jackson, 1998; Leung, *et al.*, 2002)

As described above, the toxoid subunit Stx2B was inserted into host plasmid pJ404 into the N' terminal end of synthetic FliC with the concurrent omission of its' signal peptide motif, and addition of flanking restriction enzyme cut sites & hexa-histidine tag. Restriction enzyme digest, ligation, & transformation were conducted and produced transformant colonies which were verified to contain the Stx2B toxoid subunit by isolated colony PCR & restriction enzyme digest (Fig. 3.11 & 3.12).

4.7 FliC-Stx2B induction & clarification analysis

As it is seen Fig. 3.13, a small-scale flask induction was conducted using both Stx2B-1N and FliC-Stx2B expressing *E. coli* (BL21) cells in ECAM with induced IPTG concentrations of 0.4 & 1.0mM. When analyzing the processed samples, the desired proteins appeared mainly in the insoluble fractions in both clones. In addition, both 0.4mM & 1.0mM IPTG induced culture samples showed qualitatively the same level of expression, whereas the uninduced fractions did not contain the protein of interest indicating tight promoter control.

Separate FliC-Stx2B expressing *E. coli* cultures were also induced (Fig. 3.14) using the same concentrations of IPTG; however, grown in LB, TB, & ECAM for preliminary induction analysis. Expression of FliC-Stx2B, which has a molecular weight of ~53kda, is found mainly in the insoluble fraction although it is also seen in the soluble fractions, however very slight.

The level of expression seen in ECAM flask work in comparison to Stx2B-1N induced culture samples also appears to be qualitatively more significant. Suggesting that the removal of the signal peptide sequence could potentially have an effect in the recombinant protein's translocation, post-expression (Selyunin & Mukhopadhyay, 2015). Another correlation presented is the decrease in prominence of non-desired protein bands when comparing uninduced & induced FliC-Stx2B samples. Specifically, this decrease is observed with an outer membrane protein (Omp), ~38kDa, commonly seen within induced insoluble samples.

In order to isolate and purify insoluble FliC-Stx2B, processing methods needed to focus on resolubilization and removal of any inclusion bodies or improperly folded protein. This was achieved by using a detergent wash method, using medium to saturating levels of detergents such as Urea and Guanidine Hydrochloride (Fig. 3.15 & 3.16). By washing the insoluble pellet, separated from the soluble protein fraction, it was shown that removal of non-desired proteins increased following each wash step performed. Interestingly, following the detergent washes, removal of most non-desired proteins was achieved when resolubilizing the insoluble pellet sample in guanidine hydrochloride rich binding buffer, leaving an almost pure sample of FliC-Stx2B prior to protein purification, (Appendix A.3, A16-A20).

However, it is important to note that with each wash step performed removal of FliC-Stx2B also occurred. The banding pattern for resolubilized pellet samples on the SDS-PAGEs

also migrate slightly higher as a result of the extra salt concentration provided by Guanidine Hydrochloride.

In order to determine whether or not the processed samples contained biological epitope activity, a Western blot was conducted alongside the corresponding SDS-PAGE (Fig. 3.16). Results showed that expressed FliC-Stx2B contains biological activity for anti-Stx2B antibodies in all fractions, with the exception of the separated soluble fraction. This further supports the theory that the exclusion of Stx2B's native signal peptide may lead to sequestration of the protein in insoluble cytoplasmic compartments within the cell, as opposed to other translocation pathways. Polymer FliC-Stx2B protein complexes were also observed on the Western blot at ~110-140kDA. These bands however began to decrease after subsequent detergent washes during cell clarification, and with the inclusion of reducing agents during sample processing for SDS-PAGE.

4.8 FliC-Stx2B on-column purification time studies & *in vitro* analysis

Since the isolated protein following cell clarification was treated with medium to high concentrations of denaturing detergents, a refolding step to properly refold the denatured proteins while adhered to the nickel column was conducted using AKTA® FPLC systems. With the addition of the hexa-histidine tag to the synthetic FliC construct, refolding and purification could be done simultaneously, allowing for a more rapid throughput in regard to purification times. Analyzed elution samples show purified FliC-Stx2B elution at 60-80% of the step-wise elution gradient (Fig. 3.17 & 3.19; Appendix A.3, A21-A23). Additionally, each refolding time-point purification showed protein elution at the same 60-80% illustrating consistent elution

characteristics for FliC-Stx2B. Yields for solubilized pellet samples (prior-AKTA® FPLC) and de-salted purified FliC-Stx2B showed ~70% retention of the desired protein.

Following elution, pure two-hour refolded FliC-Stx2B samples were subjected to *in vitro* analysis utilizing indirect-ELISA to quantitatively determine their biological activity against pre-purification non-refolded FliC-Stx2B. This would in effect determine the refolding efficiency while the recombinant protein is bound to the nickel column. As it is shown in Fig. 3.18, purified FliC-Stx2B shows a higher rate of activity per concentration of sample tested. It also shows levels of saturation at roughly 0.00625ng & 150ng (low and high). This data suggests that refolding of the solubilized protein is necessary in order to activate higher levels of Stx2B epitope affinity.

One & six-hour refolded FliC-Stx2B samples were also subjugated to *in vitro* analysis following elution (Fig. 3.19) to quantitatively determine their biological activity. Compared test samples included FliC-Stx2B refolding time-points and negative control RSV-N, which utilizes the same synthetic FliC platform but does not contain the Stx2B toxoid. Comparing the refolding efficiencies of refolded his-tagged FliC-Stx2B protein bound to the HisTrap nickel column overtime further characterizes FliC-Stx2B's biological activity profile.

As it is seen in Fig. 3.19 & 3.20, purified 1 hour refolded FliC-Stx2B shows a higher rate of activity per sample concentration tested than samples subjugated to 6 hours. It also shows levels of saturation at roughly 7.8ng & 125ng (low and high). This data suggests that refolding times necessary for biological activity retention can be relatively short, and as low as 1 hour. Furthermore, biological activity needed for adaptive immunity, seen between refolding time-point samples, did not show any significant decrease indicating a faster throughput FliC-Stx2B production.

Moreover, preliminary activation of TLR5 receptors which are associated with APC maturation and pro-inflammatory cytokine response (Fig. 3.21) showed comparable TLR5 activation against the known agonist control flagellin protein FljB. The fusion protein, FliC-Stx2B, utilizes both an innate (synthetic FliC) and adaptive (Shiga toxoid 2, subunit B) immune system component for a potential humoral affect. By using a two-pronged approach, the innate response activating component of FliC-Stx2B may initiate innate cell maturation; allowing a humoral response through antigenic presentation on APCs and subsequent T cell maturation to occur, (Leigh, *et al.* 2014; Osterhaus, 2014; Sabag & Lorberboum-Galski, 2014; Song, *et al.* 2014, Tarahomojoo, 2014). Activation and maturation of T cells specifically against the epitopic portions of FliC-Stx2B may then produce antibodies directly targeted against the attachment pentamer forming protein Stx2B, (Sandvig, 2000; Houdouin, *et al.*, 2004; Fuller, *et al.*, 2011; Scheutz, *et al.*, 2012).

4.9 FliC-Stx2B dialysis refolding, purification, & *in vitro* analysis

Protein expression of the FliC-Stx2B fusion protein has been seen in previous works, enhanced by the removal of the signal peptide motif associated with the B subunit of Stx2. This expression, in comparison to previous FliC fusion protein Stx2B-1N, shows a higher rate of recombinant protein production when induced during cell culturing. FliC-Stx2B remains primarily an insoluble protein following separation of soluble and insoluble cell fractions (Fig. 3.13 & 3.14). However, the presence of non-desired protein is still present, and further processing is necessary. A resolubilization procedure conducted on insoluble fractions (Fig. 3.15, 3.16, & 3.22) using varying concentrations of detergents illustrated that isolation of FliC-Stx2B is possible and efficient. When comparing samples treated with either 2M or 6M Guanidine

hydrochloride in the binding buffer little variation is seen qualitatively on SDS-PAGE (Fig. 3.22). In order to return FliC-Stx2B to an intrinsic form without the addition of on-column refolding, dialysis refolding methods were used (Fig. 3.23).

Little difference was seen qualitatively on SDS-PAGE between resolubilized & dialyzed FliC-Stx2B with both samples exhibiting 90% FliC-Stx2B band presence (Fig. 3.23). It has been previously reported that FliC-Stx2B polymerizes and forms complexes which migrate higher on SDS-PAGE. In comparison, on-column purified FliC-Stx2B produced protein samples at ~98% purity when taking account of higher molecular weight polymerized proteins (Fig. 3.23B). In order to confirm the presence of polymerized FliC-Stx2B and other proteins containing the Stx2B epitope domain, a Western blot was conducted using anti-Stx2B monoclonal antibodies (Fig. 3.25A & 3.25B). As previously theorized, higher molecular weight polymerized protein bands seen (Fig. 3.25A) were confirmed for having biological activity against Stx2b mAbs (Fig. 3.25B). This further supports the isolation & resolubilization methods used for FliC-Stx2B processing. Interestingly, bands appearing at ~60 & ~90kDa also appeared on the Western blot, while lower molecular weight bands did not.

Biological activity for resolubilized & dialysis refolded FliC-Stx2B samples were further supported by showing positive anti-Stx2b activity along a varying concentration gradient on an indirect ELISA (Fig. 3.26). The data seen is consistent amongst both samples, indicating that FliC-Stx2b (when resolubilized with 2M Guanidine hydrochloride) contains a similar biological activity profile when compared to its refolded form. In previous studies, ELISA data gathered on resolubilized samples, using 6M Guanidine hydrochloride, illustrated a diminished biological activity profile in comparison to nickel column refolded & purified samples (Fig. 3.20). With these data, it can be theorized that using a detergent such as Guanidine hydrochloride, at a

concentration of 2M for protein resolubilization, is sufficient in isolating the FliC-Stx2B fusion protein while also maintaining its biological activity throughout the process.

4.10 Native-FliC resolubilization & purification

Native-FliC, inserted into vector plasmid pJ404, was also resolubilized using the same parameters as FliC-Stx2B above. Applying the same detergent wash method described above, 6M guanidine hydrochloride, induced Native-FliC *E. coli* cells were disrupted, clarified, and analyzed on SDS-PAGE & Western blot (Fig. 3.27). Unlike with FliC-Stx2B, Native-FliC expression is seen in both the soluble and insoluble fractions, making the starting material needed for cell clarification significantly less in flask work. Despite this however, removal of non-desired proteins throughout detergent washes and final resolubilization was seen (Fig. 3.28). Prior to purification, a Western blot against Native-FliC showed biological activity in both soluble and insoluble fractions, confirming the presence of the protein (Fig. 3.29).

The resolubilized pellet sample produced during the detergent wash method was used for purification and passed through a nickel column using the same conditions as FliC-Stx2B purification. Previous Native-FliC purifications showed protein being washed off the nickel column when imidazole concentrations were at 20mM. Because of this, imidazole concentrations for Native-FliC samples were reduced to 5mM, and elution concentrations were reduced to a gradient of 5-100mM imidazole. Using these characteristics, resolubilized Native-FliC was eluted at a concentration of ~30-60mM imidazole during the elution gradient (Fig. 3.29).

4.11 Summary

In summary, this work outlines the development of process methodology for the design, production, & characterization of a recombinant based fusion protein containing immunity activating FliC & a shiga-like toxoid subunit B protein. The methodology presented herein may also directly be applied to other similar fusion based protein constructs located in cellular insoluble inclusion body fractions. The developed process overview is as follows; *in silico* design, induction studies, clarification & isolation, on-column & dialysis refolding purifications, qualitative analysis, & *in vitro* analysis.

The removal of Stx2B's intrinsic signal peptide led to a significant increase in starting material when induced, indicating fusion protein retention in the cytoplasm. A modified detergent wash method, utilizing guanidine hydrochloride, removed ~90-95% non-desired proteins while retaining FliC-Stx2B biological activity following refolding by dialysis or on-column purification. Interestingly, samples resolubilized with 6M guanidine hydrochloride illustrated a lower activity profile against anti-Stx2B antibodies then samples processed with 2M guanidine hydrochloride. Purified protein yields ranged from 40-78%, and produced significant amounts of FliC-Stx2B that was further characterized to be biologically active against anti-Stx2B antibodies & TLR5 receptors.

Future approaches to optimize this work should focus on further characterizing purification parameters such as nickel based, hydrophobic interaction, or size exclusion columns. Linear elution gradients conducted during purification will help to characterize elution time points/parameters, and further increase purified protein yields. Alternative methods for isolation and purification will also aid in streamlining workflow and preventing bottlenecking during production.

REFERENCES

Andersen-Nissen E, Smith KD, Strobe KL, Barrett SLR, Cookson BT, Logan SM, et al. Evasion of Toll-like receptor 5 by flagellated bacteria. Proc Natl Acad Sci USA. 2005 Jun 28;102(26):9247–52.

Bates JT, Graff AH, Phipps JP, Grayson JM, Mizel SB. Enhanced Antigen Processing of Flagellin Fusion Proteins Promotes the Antigen-Specific CD8+ T Cell Response Independently of TLR5 and MyD88. The Journal of Immunology. 2011 Jun 1;186(11):6255–62.

Boyd, Sarah, "Design and Production of a Recombinant FliC-Antigen Co-Expression Platform for Increased Vaccine E cacy." Dissertation, Georgia State University, 2014. h p://scholarworks.gsu.edu/biology_diss/142

Brussow H, Canchaya C, Hardt W-D. Phages and the Evolution of Bacterial Pathogens: from Genomic Rearrangements to Lysogenic Conversion. Microbiology and Molecular Biology Reviews. 2004 Sep 1;68(3):560–602.

Chaucheyras-Durand F, Faqir F, Ameilbonne A, Rozand C, Martin C. Fates of Acid-Resistant and Non-Acid-Resistant Shiga Toxin-Producing Escherichia coli Strains in Ruminant Digestive Contents in the Absence and Presence of Probiotics. Appl Environ Microbiol. 2010 Feb 1;76(3):640–7.

Cohen D, Green MS, Block C, Rouach T, Ofek I. Serum antibodies to lipopolysaccharide and natural immunity to shigellosis in an Israeli military population. J Infect Dis. 1988 May;157(5):1068–71.

Donnelly MA, Steiner TS. Two Nonadjacent Regions in Enteroaggregative Escherichia coli Flagellin Are Required for Activation of Toll-like Receptor 5. Journal of Biological Chemistry. 2002 Oct 25;277(43):40456–61.

Eaves-Pyles TD, Wong HR, Odoms K, Pyles RB. Salmonella flagellin-dependent proinflammatory responses are localized to the conserved amino and carboxyl regions of the protein. J Immunol. 2001 Dec 15;167(12):7009–16.

Feng P. Shiga Toxin-Producing Escherichia coli (STEC) in Fresh Produce—A Food Safety Dilemma. Microbiology Spectrum [Internet]. 2014 Aug 15 [cited 2017 Sep 22];2(4). Available from: http://www.asmscience.org/content/journal/microbiolspec/10.1128/microbiolspec.EHEC-0010-2013

Filloux A. A Variety of Bacterial Pili Involved in Horizontal Gene Transfer. Journal of Bacteriology. 2010 Jul 1;192(13):3243–5.

Fraser ME, Chernaia MM, Kozlov YV, James MNG. Crystal structure of the holotoxino from Shigella dysenteriae at 2.5 |[Aring]| resolution. Nature Structural & Molecular Biology. 1994 Jan 1;1(1):59–64.

Fuller CA, Pellino CA, Flagler MJ, Strasser JE, Weiss AA. Shiga Toxin Subtypes Display Dramatic Differences in Potency. Infection and Immunity. 2011 Mar 1;79(3):1329–37.

Garg AX, Suri RS, Barrowman N, Rehman F, Matsell D, Rosas-Arellano MP, et al. Long-term renal prognosis of diarrhea-associated hemolytic uremic syndrome: a systematic review, meta-analysis, and meta-regression. JAMA. 2003 Sep 10;290(10):1360–70.

Gupta SK, Bajwa P, Deb R, Chellappa MM, Dey S. Flagellin A Toll-Like Receptor 5 Agonist as an Adjuvant in Chicken Vaccines. Clinical and Vaccine Immunology. 2014 Mar 1;21(3):261–70.

He X, Kong Q, Patfield S, Skinner C, Rasooly R. A New Immunoassay for Detecting All Subtypes of Shiga Toxins Produced by Shiga Toxin-Producing E. coli in Ground Beef. PLOS ONE. 2016 Jan 29;11(1):e0148092.

Herman KM, Hall AJ, Gould LH. Outbreaks attributed to fresh leafy vegetables, United States, 1973–2012. Epidemiol Infect. 2015 Oct;143(14):3011–21.

Ho NK, Henry AC, Johnson-Henry K, Sherman PM. Pathogenicity, host responses and implications for management of enterohemorrhagic Escherichia coli O157:H7 infection. Can J Gastroenterol. 2013;27(5):281–5.

Houdouin V, Catherine D, Mariani P, Brahimi N, Loirat C, Bourrillon A, et al. A Pediatric Cluster of Shigella dysenteriae Serotype 1 Diarrhea with Hemolytic Uremic Syndrome in 2 Families from France. Clinical Infectious Diseases. 2004 May 1;38(9):e96–9.

Huang J, Motto DG, Bundle DR, Sadler JE. Shiga toxin B subunits induce VWF secretion by human endothelial cells and thrombotic microangiopathy in ADAMTS13-deficient mice. Blood. 2010 Nov 4;116(18):3653–9.

Johannes L, JoS W. Shiga toxins--from cell biology to biomedical applications. Nat Rev Microbiol. 2010 Feb;8(2):105–16.

Kaper JB, Nataro JP, Mobley HLT. Pathogenic Escherichia coli. Nat Rev Micro. 2004 Feb;2(2):123–40.

Kotloff KL, Nataro JP, Blackwelder WC, Nasrin D, Farag TH, Panchalingam S, et al. Burden and aetiology of diarrhoeal disease in infants and young children in developing countries (the Global Enteric Multicenter Study, GEMS): a prospective, case-control study. The Lancet. 2013 Jul 20;382(9888):209–22.

Lamberti LM, Bourgeois AL, Fischer Walker CL, Black RE, Sack D. Estimating Diarrheal Illness and Deaths Attributable to Shigellae and Enterotoxigenic Escherichia coli among Older Children, Adolescents, and Adults in South Asia and Africa. Vinetz JM, editor. PLoS Neglected Tropical Diseases. 2014 Feb 13;8(2):e2705.

Lanata CF, Fischer-Walker CL, Olascoaga AC, Torres CX, Aryee MJ, Black RE, et al. Global Causes of Diarrheal Disease Mortality in Children <5 Years of Age: A Systematic Review. Sestak K, editor. PLoS ONE. 2013 Sep 4;8(9):e72788.

Leigh ND, Bian G, Ding X, Liu H, Aygun-Sunar S, Burdelya LG, et al. A Flagellin-Derived Toll-Like Receptor 5 Agonist Stimulates Cytotoxic Lymphocyte-Mediated Tumor Immunity. Piccirillo CA, editor. PLoS ONE. 2014 Jan 14;9(1):e85587.

Leung PHM, Peiris JSM, Ng WWS, Yam WC. Polyclonal Antibodies to Glutathione S-Transferase- Verotoxin Subunit A Fusion Proteins Neutralize Verotoxins. Clinical and Vaccine Immunology. 2002 May 1;9(3):687–92.

Lindsay B, Ochieng JB, Ikumapayi UN, Toure A, Ahmed D, Li S, et al. Quantitative PCR for Detection of Shigella Improves Ascertainment of Shigella Burden in Children with Moderate-to-Severe Diarrhea in Low-Income Countries. Journal of Clinical Microbiology. 2013 Jun 1;51(6):1740–6.

Liu F, Yang J, Zhang Y, Zhou D, Chen Y, Gai W, et al. Recombinant flagellins with partial deletions of the hypervariable domain lose antigenicity but not mucosal adjuvancy. Biochemical and Biophysical Research Communications. 2010 Feb;392(4):582–7.

Livio S, Strockbine NA, Panchalingam S, Tennant SM, Barry EM, Marohn ME, et al. Shigella Isolates From the Global Enteric Multicenter Study Inform Vaccine Development. Clin Infect Dis. 2014 Oct 1;59(7):933–41.

Lu Y, Swartz JR. Functional properties of flagellin as a stimulator of innate immunity. Scientific Reports. 2016 Jan 12;6:srep18379.

Mani S, Wierzba T, Walker RI. Status of vaccine research and development for Shigella. Vaccine. 2016 Jun;34(26):2887–94.

Martinez-Becerra FJ, Kissmann JM, Diaz-McNair J, Choudhari SP, Quick AM, Mellado-Sanchez G, et al. Broadly Protective Shigella Vaccine Based on Type III Secretion Apparatus Proteins. Infect Immun. 2012 Mar 1;80(3):1222–31.

Mead P. Food-Related Illness and Death in the United States Reply to Dr. Hedberg. Emerging Infectious Diseases. 1999 Dec;5(6):841–2.

Miyake T, Demerec M. Salmonella–Escherichia Hybrids. Nature. 1959 Jun 6;183(4675):1586–1586.

Miyake, T. (1962). Exchange of Genetic Material between Salmonella Typhimurium and Escherichia Coli K-12. *Genetics*, *47*(8), 1043–1052.

Mizel SB, Bates JT. Flagellin as an Adjuvant: Cellular Mechanisms and Potential. The Journal of Immunology. 2010 Nov 15;185(10):5677–82.

Osterhaus A. Faculty of 1000 evaluation for Safety and immunogenicity of a recombinant M2e-flagellin influenza vaccine (STF2.4xM2e) in healthy adults. [Internet]. 2014 May [cited 2017 Apr 21]. Available from: http://f1000.com/prime/718384268#eval793495081

Pennington H. Escherichia coli O157. The Lancet. 2010 Oct 23;376(9750):1428–35.

Pore D, Chakrabarti MK. Outer membrane protein A (OmpA) from Shigella flexneri 2a: A promising subunit vaccine candidate. Vaccine. 2013 Aug 12;31(36):3644–50.

Pozsgay V, Chu C, Pannell L, Wolfe J, Robbins JB, Schneerson R. Protein conjugates of synthetic saccharides elicit higher levels of serum IgG lipopolysaccharide antibodies in mice than do those of the O-specific polysaccharide from Shigella dysenteriae type 1. PNAS. 1999 Apr 27;96(9):5194–7.

Sabag O, Lorberboum-Galski H. Combining flagellin and human Î²-defensin-3 to combat bacterial infections. Frontiers in Microbiology [Internet]. 2014 Dec 9 [cited 2017 Apr 21];5. Available from: http://journal.frontiersin.org/article/10.3389/fmicb.2014.00673/abstract

Saitoh T, Iyoda S, Yamamoto S, Lu Y, Shimuta K, Ohnishi M, et al. Transcription of the ehx Enterohemolysin Gene Is Positively Regulated by GrlA, a Global Regulator Encoded within the Locus of Enterocyte Effacement in Enterohemorrhagic Escherichia coli. J Bacteriol. 2008 Jul;190(14):4822–30.

Sandvig K. NEW EMBO MEMBERS' REVIEW: Entry of ricin and Shiga toxin into cells: molecular mechanisms and medical perspectives. The EMBO Journal. 2000 Nov 15;19(22):5943–50.

Scheutz F, Teel LD, Beutin L, Pierard D, Buvens G, Karch H, et al. Multicenter Evaluation of a Sequence-Based Protocol for Subtyping Shiga Toxins and Standardizing Stx Nomenclature. Journal of Clinical Microbiology. 2012 Sep 1;50(9):2951–63.

Selyunin AS, Mukhopadhyay S. A conserved structural motif mediates retrograde trafficking of Shiga toxin types 1 and 2. Traffic. 2015 Dec;16(12):1270–87.

Skinner L, Jackson M. Inhibition of prokaryotic translation by the Shiga toxin enzymatic subunit. Microbial Pathogenesis. 1998 Feb;24(2):117–22.

Song L, Liu G, Umlauf S, Liu X, Li H, Tian H, et al. A rationally designed form of the TLR5 agonist, flagellin, supports superior immunogenicity of Influenza B globular head vaccines. Vaccine. 2014 Jul;32(34):4317–23.

Sperandio V, Pacheco AR. Shiga toxin in enterohemorrhagic E.coli: regulation and novel anti-virulence strategies. Front Cell Infect Microbiol [Internet]. 2012 [cited 2017 Sep 24];2. Available from: http://journal.frontiersin.org/article/10.3389/fcimb.2012.00081/full

Stein PE, Boodhoo A, Tyrrell GJ, Brunton JL, Read RJ. Crystal structure of the cell-binding B oligomer of verotoxin-1 from E. coli. Nature. 1992 Feb 20;355(6362):748–50.

Tarahomjoo S. Utilizing bacterial flagellins against infectious diseases and cancers. Antonie van Leeuwenhoek. 2014 Feb;105(2):275–88.

Tarr PI, Gordon CA, Chandler WL. Shiga-toxin-producing Escherichia coli and haemolytic uraemic syndrome. Lancet. 2005 Mar 19;365(9464):1073–86.

Tu W, Cai K, Gao X, Xiao L, Chen R, Shi J, et al. Improved production of holotoxin Stx2 with biological activities by using a single-promoter vector and an auto-induction expression system. Protein Expr Purif. 2009 Oct;67(2):169–74.

Venkatesan MM, Ranallo RT. Live-attenuated Shigella vaccines. Expert Review of Vaccines. 2006 Oct 1;5(5):669–86.

Yang J, Yan R, Roy A, Xu D, Poisson J, Zhang Y. The I-TASSER Suite: protein structure and function prediction. Nat Meth. 2015 Jan;12(1):7–8.

Yang S-C, Lin C-H, Aljuffali IA, Fang J-Y. Current pathogenic Escherichia coli foodborne outbreak cases and therapy development. Arch Microbiol. 2017 Aug 1;199(6):811–25.

Yoon S -i., Kurnasov O, Natarajan V, Hong M, Gudkov AV, Osterman AL, et al. Structural Basis of TLR5-Flagellin Recognition and Signaling. Science. 2012 Feb 17;335(6070):859–64.

APPENDICES

Appendix A

Appendix A.1 Construct design

Restriction Enzyme Cut Site Legend
NcoI EcoRI XbaI SpeI BamHI HindIII XhoI NotI AatII AvrII Buffer bases

Sequence after F1 and R1 primers:
GGATCCATGAAGAAGATGTTTATGGCGGTTTTATTTGCATTAGCTTCTGTTAATGCAATGGCGGCGG
ATTGTGCTAAAGGTAAAATTGAGTTTTCCAAGTATAATGAGGATGACACATTTACAGTGAAGGTTG
ACGGGAAAGAATACTGGACCAGTCGCTGGAATCTGCAACCGTTACTGCAAAGTGCTCAGTTGACAG
GAATGACTGTCACAATCAAATCCAGTACCTGTGAATCAGGCTCCGGATTTGCTGAAGTGCAGTTTAA
TAATGACACTAGT

F1: 5' – GGATCCATGAAGAAGATGTTTATGGCGGTT – 3'
R1: 5' –ACTAGTGTCATTATTAAACTGCACTTCAGC – 3'

Sequence after F2 and R2C (C' Terminus) primers:
CCATGGAAGGATCCATGAAGAAGATGTTTATGGCGGTTTTATTTGCATTAGCTTCTGTTAATGCAAT
GGCGGCGGATTGTGCTAAAGGTAAAATTGAGTTTTCCAAGTATAATGAGGATGACACATTTACAGT
GAAGGTTGACGGGAAAGAATACTGGACCAGTCGCTGGAATCTGCAACCGTTACTGCAAAGTGCTCA
GTTGACAGGAATGACTGTCACAATCAAATCCAGTACCTGTGAATCAGGCTCCGGATTTGCTGAAGT
GCAGTTTAATAATGACACTAGT**TAG**GCGGCCGC

F2: 5' – CCATGGAAGGATCCATGAAGAAGATG – 3'
R2C: 5' – GCGGCCGC**CTA**ACTAGTGTCATTATT – 3'

Sequence After F3 and R3C (C' Terminus) primers:
TCTTGCTTAACTCCATGGAAGGATCCATGAAGAAGATGTTTATGGCGGTTTTATTTGCATTAGCTTCT
GTTAATGCAATGGCGGCGGATTGTGCTAAAGGTAAAATTGAGTTTTCCAAGTATAATGAGGATGAC
ACATTTACAGTGAAGGTTGACGGGAAAGAATACTGGACCAGTCGCTGGAATCTGCAACCGTTACTG
CAAAGTGCTCAGTTGACAGGAATGACTGTCACAATCAAATCCAGTACCTGTGAATCAGGCTCCGGA
TTTGCTGAAGTGCAGTTTAATAATGACACTAGT**TAG**GCGGCCGCAATGATATTTAT

F3: 5' – TCTTGCTTAACTCCATGGAAGGATCCATG – 3'
R3C: 5' – ATAAATATCATTGCGGCCGC**CTA**ACTAGT – 3'

A 1 Stx2B step wise PCR primer* in silico *design.

CCCGTAGAAAAGATCAAAGGATCTTCTTGAGATCCTTTTTTTCTGCGCGTAATCTGCTGCTTGCAAA
CAAAAAAACCACCGCTACCAGCGGTGGTTTGTTTGCCGGATCAAGAGCTACCAACTCTTTTTCCGAA
GGTAACTGGCTTCAGCAGAGCGCAGATACCAAATACTGTTCTTCTAGTGTAGCCGTAGTTAGCCCAC
CACTTCAAGAACTCTGTAGCACCGCCTACATACCTCGCTCTGCTAATCCTGTTACCAGTGGCTGCTG
CCAGTGGCGATAAGTCGTGTCTTACCGGGTTGGACTCAAGACGATAGTTACCGGATAAGGCGCAGC
GGTCGGGCTGAACGGGGGGTTCGTGCACACAGCCCAGCTTGGAGCGAACGACCTACACCGAACTGA
GATACCTACAGCGTGAGCTATGAGAAAGCGCCACGCTTCCCGAAGGGAGAAAGGCGGACAGGTAT
CCGGTAAGCGGCAGGGTCGGAACAGGAGAGCGCACGAGGGAGCTTCCAGGGGGAAACGCCTGGTA
TCTTTATAGTCCTGTCGGGTTTCGCCACCTCTGACTTGAGCGTCGATTTTTGTGATGCTCGTCAGGGG
GGCGGAGCCTATGGAAAAACGCCAGCAACGCGGCCTTTTTACGGTTCCTGGCCTTTTGCTGGCCTTT
TGCTCACATGTTCTTTCCTGCGTTATCCCCTGATTCTGTGGATAACCGTATTACCGCCTTTGAGTGAG
CTGATACCGCTCGCCGCAGCCGAACGACCGAGCGCAGCGAGTCAGTGAGCGAGGAAGCGGAAGGC
GAGAGTAGGGAACTGCCAGGCATCAAACTAAGCAGAAGGCCCCTGACGGATGGCCTTTTTGCGTTT
CTACAAACTCTTTCTGTGTTGTAAAACGACGGCCAGTCTTAAGCTCGGGCCCCCTGGGCGGTTCTGA
TAACGAGTAATCGTTAATCCGCAAATAACGTAAAAACCCGCTTCGGCGGGTTTTTTTATGGGGGGA
GTTTAGGGAAAGAGCATTTGTCAGAATATTTAAGGGCGCCTGTCACTTTGCTTGATATATGAGAATT
ATTTAACCTTATAAATGAGAAAAAAGCAACGCACTTTAAATAAGATACGTTGCTTTTTCGATTGATG
AACACCTATAATTAAACTATTCATCTATTATTTATGATTTTTTGTATATACAATATTTCTAGTTTGTTA
AAGAGAATTAAGAAAATAAATCTCGAAAATAATAAAGGGAAAATCAGTTTTTGATATCAAAATTAT
ACATGTCAACGATAATACAAAATATAATACAAACTATAAGATGTTATCAGTATTTATTATCATTTAG
AATAAATTTTGTGTCGCCCTTAATTGTGAGCGGATAACAATTACGAGCTTCATGCACAGTGAAATCA
TGAAAAATTTATTTGCTTTGTGAGCGGATAACAATTATAATATGTGGAATTGTGAGCGCTCACAATT
CCACAACGGTTTCCCTCTAGAAATAATTTTGTTTAACTTTTAGGAGGTAAAACACCATGGGAATTCG
GTCTAGAACTAGTGCAGCCGGCCAGGCGATTGCGAATCGTTTTACGGCGAACATCAAGGGTCTGAC
CCAAGCCTCTCGTAATGCAAATGATGGTATTAGCATCGCACAAACCACCGAAGGCGCGCTGAACGA
GATCAACAATAACTTGCAACGTGTCCGTGAGCTGGCAGTTCAGAGCGCGAACAGCACGAATAGCCA
GTCCGATTTGGACAGCATCCAGGCGGAGATTACGCAACGTTTGAACGAAATCGACCGCGTCAGCGG
TCAAACGCAGTTTAATGGTGTGAAAGTTCTGGCCCAGGATAACACCCTGACGATTCAGGTTGGCGC
AAACGACGGTGAAACGATTGATATTGACCTGAAGCAGATCAACAGCCAAACCCTGGGTCTGGACAC
CCTGAACGTGCAACAAAAGTATAAGGTGTCGGACACGGCCGCTACCGTGACCGGCGACGTCGATAC
TACGATTGCTGGGCCCAATAGTACTTTTAAAGCTAGCGCTACTGGTCTTGGTGAGCTCGACCAGAAA
ATTGATCATATGTTAAAATTTGATGATCAATTGGGAAAATATTACGCCCCGCGGACCGTTACGGGGG
GACGATCGAAAGATGGCTATTATACCGGTTCCGTTGATAAGACGGCATGCGAGGTGACTCTTGCTGT
GCACGCGACTTCCCCGCTTACGCGTGGACTACCTGCGACAAGATCTGAGGATGTGAAAAATCCTAG
GGTTGCCAACGCTGACCTGACCGAGGCGAAAGCGGCGCTGACCGCAGCGGGCGTTACTGGTACCGC
AAGCGTTGTGAAAATGAGCTACACCGACAATAATGGTAAAACTATCGATGGCGGTCTGGCGGTCAA
AGTCGGCGACGACTACTATTCCGCCACCCAGAACAAAGACGGCAGCATCAGCATTAACACTACGAA
ATACACCGCAGATGACGGCACGAGCAAAACGGCACTGAATAAGCTGGGCGGTGCGGATGGTAAGA
CCGAAGTTGTTAGCATTGGTGGTAAAACCTATGCCGCGTCCAAGGCAGAGGGTCACAATTTCAAGG
CGCAGCCGGATCTGGCGGAAGCTGCAGCGACCACGACCGAGAATCCGTTGCAGAAGATTGATGCGG
CGCTGGCACAGGTCGATACGCTGCGCTCTGACCTGGGTGCCGTACAAAACCGTTTCAATAGCGCGA
TCACCAATCTGGGCAACACCGTGAACAATCTGACCTCTGCTCGCAGCCGTATTGAGGGATCCGCGG
ATTGTGCTAAAGGTAAAATTGAGTTTTCCAAGTATAATGAGGATGACACATTTACAGTGAAGGTTG
ACGGGAAAGAATACTGGACCAGTCGCTGGAATCTGCAACCGTTACTGCAAAGTGCTCAGTTGACAG
GAATGACTGTCACAATCAAATCCAGTACCTGTGAATCAGGCTCCGGATTTGCTGAAGTGCAGTTTAA
TAATGACCATCACCATCATCACCATCTCGAGTAGGCGGCCGCAAGCCCCAAGGGCGACACCCCATA
ATTAGCCCGGGCGAAAGGCCCAGTCTTTCGACTGAGCCTTTCGTTTTATTTGATGCCTGGCAGTTCC
CTACTCTCGCATGGGGAGTCCCCACACTACCATCGGCGCTACGGCGTTTCACTTCTGAGTTCGGCAT
GGGGTCAGGTGGGACCACCGCGCTACTGCCGCCAGGCAAACAAGGGGTGTTATGAGCCATATTCAG
GTATAAATGGGCTCGCGATAATGTTCAGAATTGGTTAATTGGTTGTAACACTGACCCCTATTTGTTT
ATTTTTCTAAATACATTCAAATATGTATCCGCTCATGAGACAATAACCCTGATAAATGCTTCAATAA
TATTGAAAAAGGAAGAATATGAGTATTCAACATTTCCGTGTCGCCCTTATTCCCTTTTTTGCGGCATT
TTGCCTTCCTGTTTTTGCTCACCCAGAAACGCTGGTGAAAGTAAAAGATGCTGAAGATCAGTTGGGT
GCACGAGTGGGTTACATCGAACTGGATCTCAACAGCGGTAAGATCCTTGAGAGTTTTCGCCCCGAA
GAACGTTTTCCAATGATGAGCACTTTTAAAGTTCTGCTATGTGGCGCGGTATTATCCCGTATTGACG
CCGGGCAAGAGCAACTCGGTCGCCGCATACACTATTCTCAGAATGACTTGGTTGAGTACTCACCAGT

CACAGAAAAGCATCTTACGGATGGCATGACAGTAAGAGAATTATGCAGTGCTGCCATAACCATGAG
TGATAACACTGCGGCCAACTTACTTCTGACAACGATCGGAGGACCGAAGGAGCTAACCGCTTTTTTG
CACAACATGGGGGATCATGTAACTCGCCTTGATCGTTGGGAACCGGAGCTGAATGAAGCCATACCA
AACGACGAGCGTGACACCACGATGCCTGTAGCGATGGCAACAACGTTGCGCAAACTATTAACTGGC
GAACTACTTACTCTAGCTTCCCGGCAACAATTAATAGACTGGATGGAGGCGGATAAAGTTGCAGGA
CCACTTCTGCGCTCGGCCCTTCCGGCTGGCTGGTTTATTGCTGATAAATCCGGAGCCGGTGAGCGTG
GTTCTCGCGGTATCATCGCAGCGCTGGGGCCAGATGGTAAGCCCTCCCGTATCGTAGTTATCTACAC
GACGGGGAGTCAGGCAACTATGGATGAACGAAATAGACAGATCGCTGAGATAGGTGCCTCACTGAT
TAAGCATTGGTAAGCGGCGCGCCATCGAATGGCGCAAAACCTTTCGCGGTATGGCATGATAGCGCC
CGGAAGAGAGTCAATTCAGGGTGGTGAATATGAAACCAGTAACGTTATACGATGTCGCAGAGTATG
CCGGTGTCTCTTATCAGACCGTTTCCCGCGTGGTGAACCAGGCCAGCCACGTTTCTGCGAAAACGCG
GGAAAAAGTGGAAGCGGCGATGGCGGAGCTGAATTACATTCCCAACCGCGTGGCACAACAACTGG
CGGGCAAACAGTCGTTGCTGATTGGCGTTGCCACCTCCAGTCTGGCCCTGCACGCGCCGTCGCAAAT
TGTCGCGGCGATTAAATCTCGCGCCGATCAACTGGGTGCCAGCGTGGTGGTGTCGATGGTAGAACG
AAGCGGCGTCGAAGCCTGTAAAGCGGCGGTGCACAATCTTCTCGCGCAACGCGTCAGTGGGCTGAT
CATTAACTATCCGCTGGATGACCAGGATGCCATTGCTGTGGAAGCTGCCTGCACTAATGTTCCGGCG
TTATTTCTTGATGTCTCTGACCAGACACCCATCAACAGTATTATTTTCTCCCATGAGGACGGTACGCG
ACTGGGCGTGGAGCATCTGGTCGCATTGGGTCACCAGCAAATCGCGCTGTTAGCGGGCCCATTAAG
TTCTGTCTCGGCGCGTCTGCGTCTGGCTGGCTGGCATAAATATCTCACTCGCAATCAAATTCAGCCG
ATAGCGGAACGGGAAGGCGACTGGAGTGCCATGTCCGGTTTTCAACAAACCATGCAAATGCTGAAT
GAGGGCATCGTTCCCACTGCGATGCTGGTTGCCAACGATCAGATGGCGCTGGGCGCAATGCGCGCC
ATTACCGAGTCCGGGCTGCGCGTTGGTGCGGATATCTCGGTAGTGGGATACGACGATACCGAAGAT
AGCTCATGTTATATCCCGCCGTTAACCACCATCAAACAGGATTTTCGCCTGCTGGGGCAAACCAGCG
TGGACCGCTTGCTGCAACTCTCTCAGGGCCAGGCGGTGAAGGGCAATCAGCTGTTGCCAGTCTCACT
GGTGAAAAGAAAAACCACCCTGGCGCCCAATACGCAAACCGCCTCTCCCCGCGCGTTGGCCGATTC
ATTAATGCAGCTGGCACGACAGGTTTCCCGACTGGAAAGCGGGCAGTGACTCATGACCAAAATCCC
TTAACGTGAGTTACGCGCGCGTCGTTCCACTGAGCGTCAGAC

A 2 FliC-Stx2B in pJ404 plasmid nucleotide sequence (5492 bp)

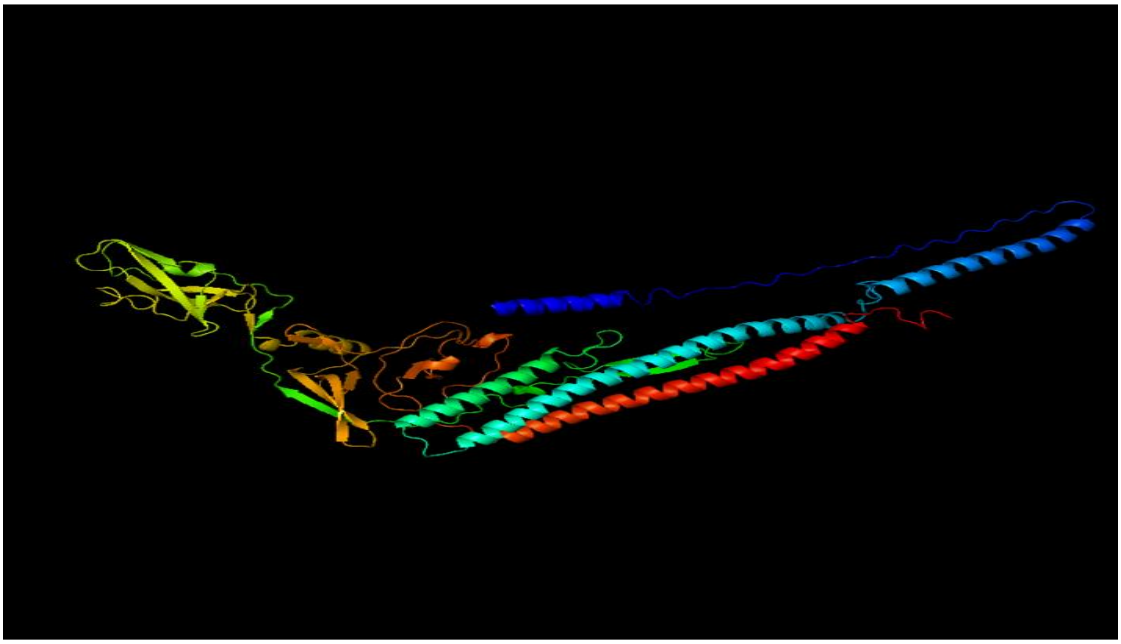

A 3 Stx2B-1N bioinformatic predicted protein structure (Yang, 2015)

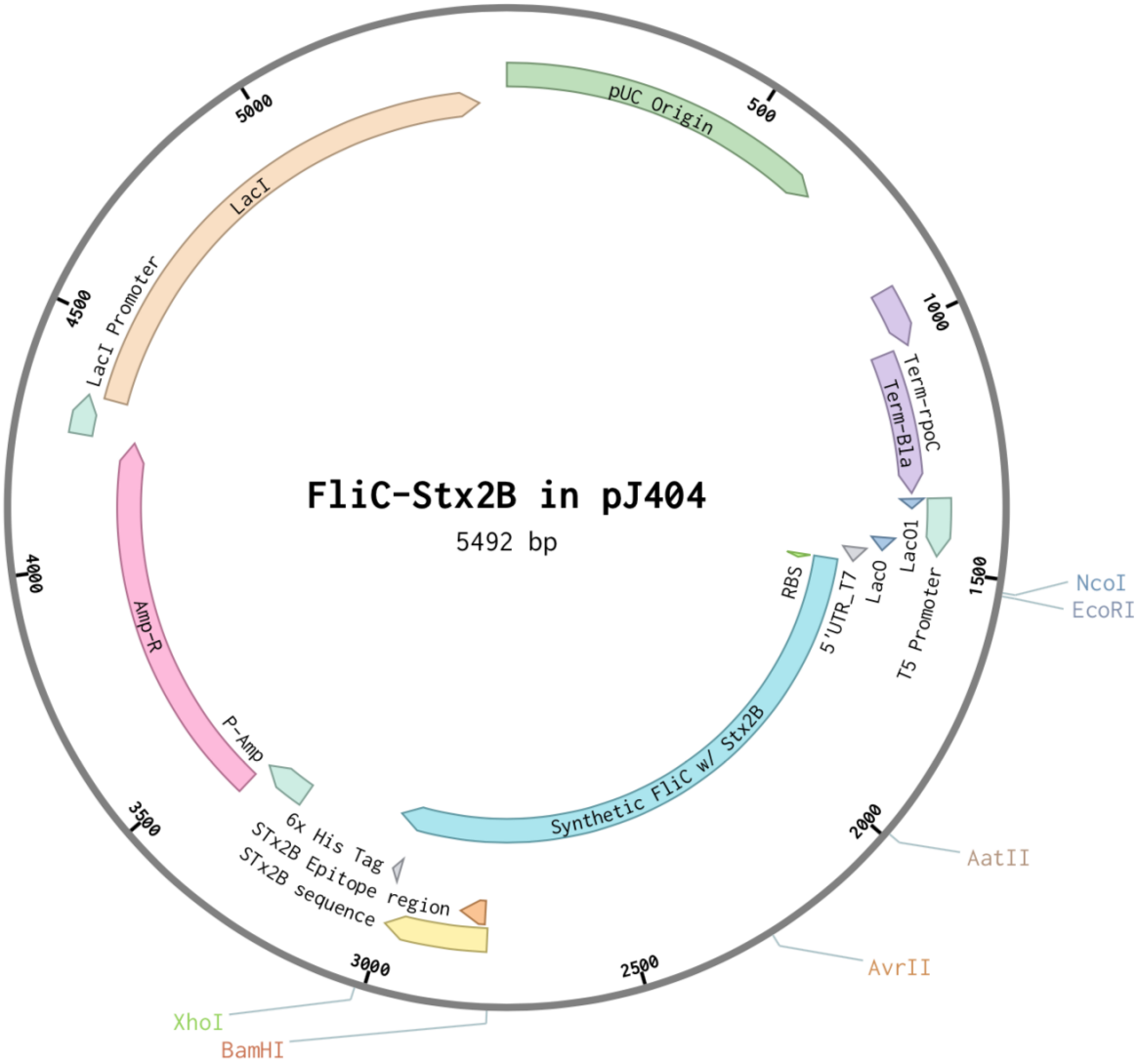

A 4 FliC-Stx2B in pJ404 plasmid map (Benchling®)

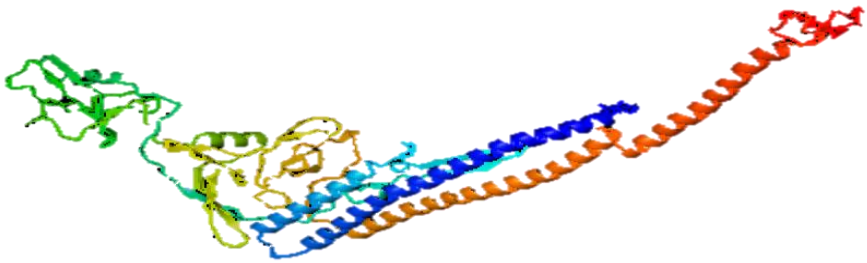

A 5 FliC-Stx2B bioinformatic predicted protein structure, (Yang 2015)

Appendix A.2 Reaction volumes

A 6 mRFP PCR volumes

mRFP Template DNA	13.75µL
mRFP Forward primer	2µL
mRFP Reverse primer	2 µL
Master Mix Buffer	25µL
Nuclease free water	9.25µL
Total Volume	50µL

A 7 mRFP and pJ404 digest volumes

mRFP		**pJ404**	
Nco1	1µL	Nco1	1µL
EcoR1	2µL	EcoR1	2µL
Neb 3.1 buffer	5µL	Neb 3.1 buffer	5µL
DNA	2.5 µL	DNA	10 µL
Nuclease free water	39.5 µL	Nuclease free water	35 µL

A 8 mRFP/pJ404 ligation volumes.

Linearized pj404 vector DNA	100ng (1µL)
Insert DNA	5 µL
5x Rapid Ligation Buffer	4 µL
T4 DNA ligase	1 µL
Nuclease free water	9 µL
Total volume	20 µL

A 9 Step wise PCR parameters for Stx2b plasmid (pJ204).

Template DNA	1µg
Forward primer	2µL
Reverse primer	2 µL
Master Mix Buffer	25µL
Nuclease free water	—
Total Volume	50µL

A 10 PCR parameters for Stx2B-1N primers at varying DNA concentrations.

1) 100ng DNA		**2) 300ng DNA**		**3) 500ng DNA**	
STx2Bfwd	1µL	STx2Bfwd	1µL	STx2Bfwd	1µL
STx2Brev	1µL	STx2Brev	1µL	STx2Brev	1µL
Master Mix	25µL	Master Mix	25µL	Master Mix	25µL
Template DNA (STx2B/pJ204) 100ng DNA	1.2µL	Template DNA (STx2B/pJ204) 300ng DNA	3.5µL	Template DNA (STx2B/pJ204) 500ng DNA	5.7µL
ddiH2O	21.8µL	ddiH2O	19.5µL	ddiH2O	17.3µL
Total	50µL	Total	50µL	Total	50µL

A 11 Stx2B-1N ligation volumes.

vector DNA	50ng
Insert DNA	1.75 µL
5x Rapid Ligation Buffer	4 µL
T4 DNA ligase	1 µL
Nuclease free water	4.63 µL
Total volume	20 µL

Appendix A.3 Protein work

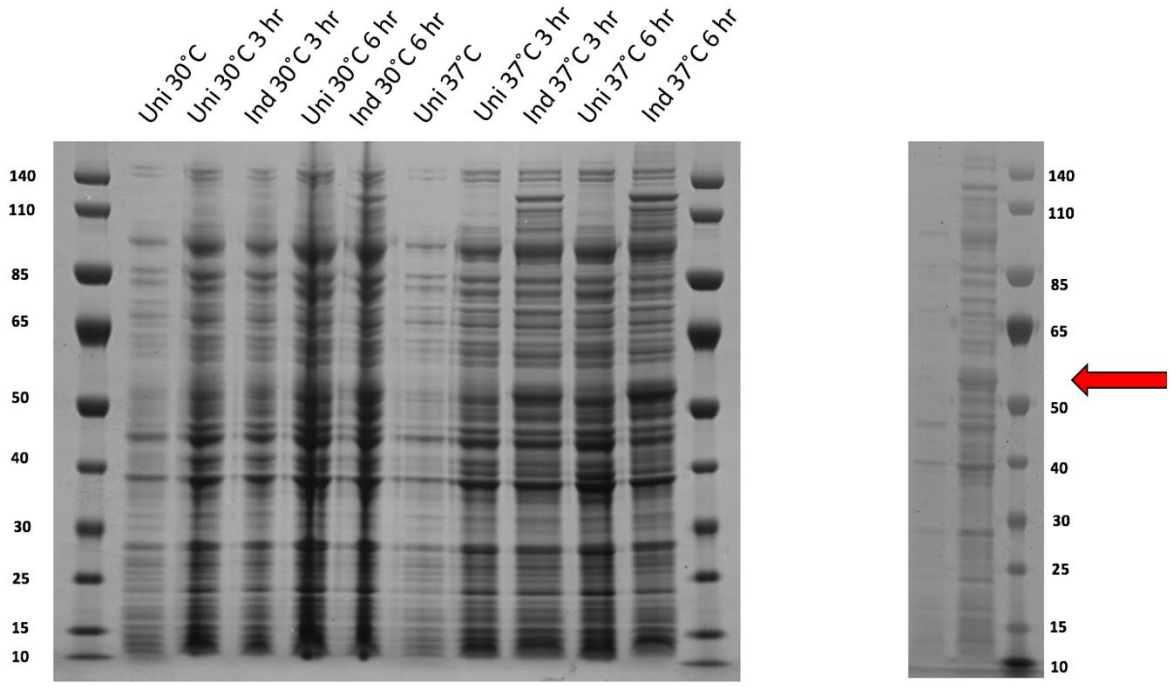

A 12 STx2B-1N induction using 0.1mM IPTG.

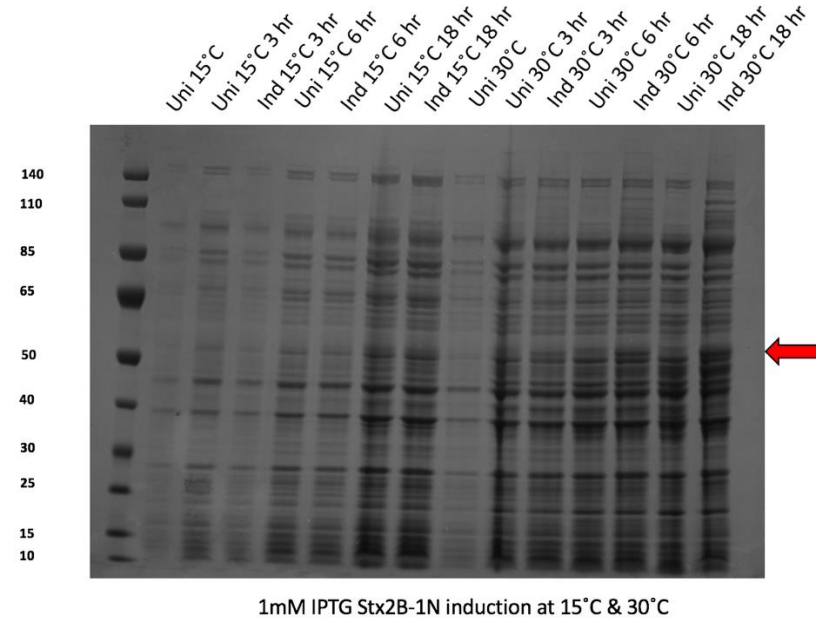

A 13 STx2B-1N induction using 1.0mM IPTG.

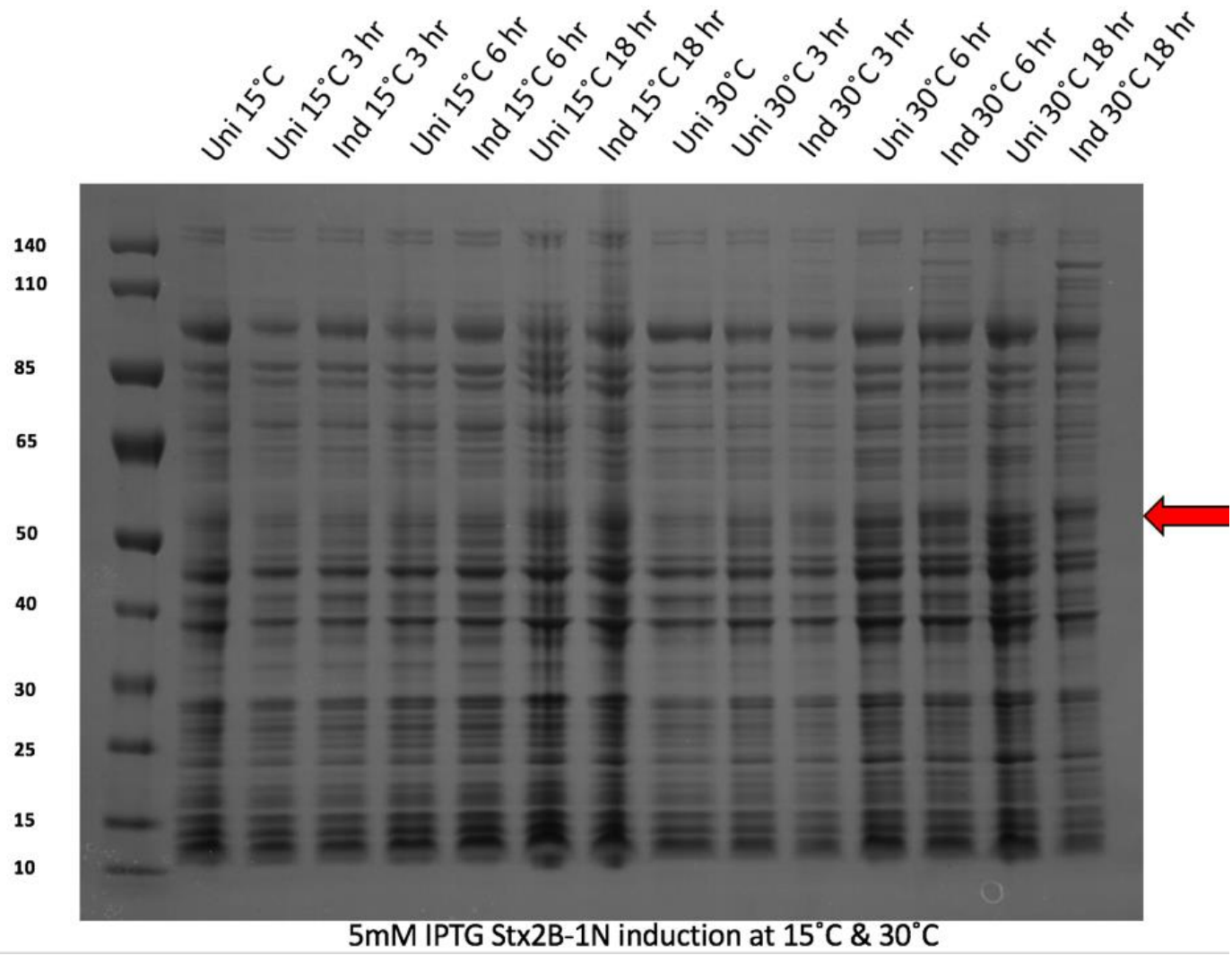

A 14 STx2B-1N induction using 5.0mM IPTG.

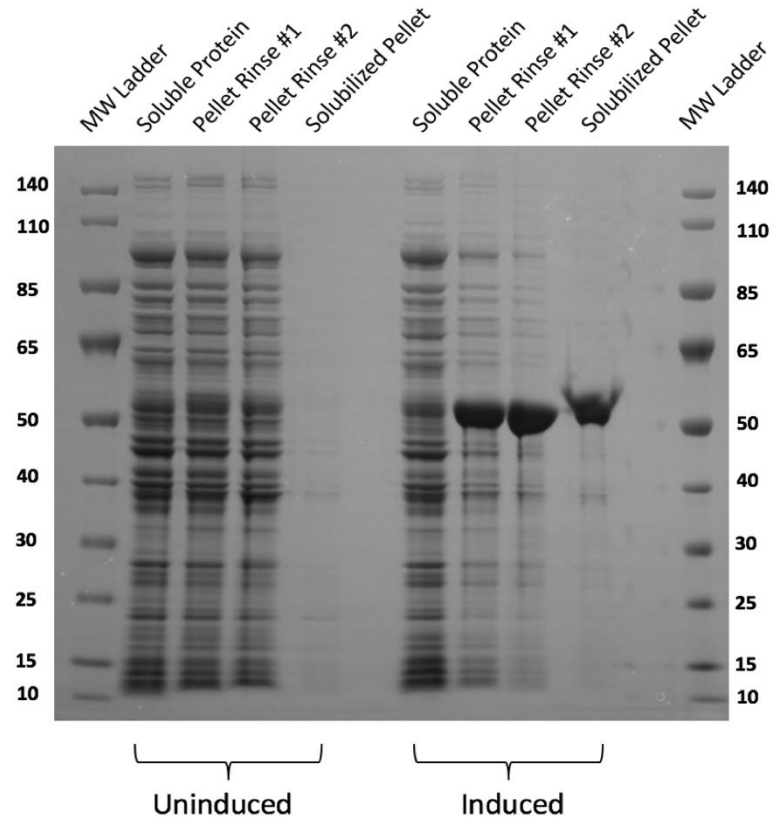

A 15 FliC-Stx2B expression & resolubilization.

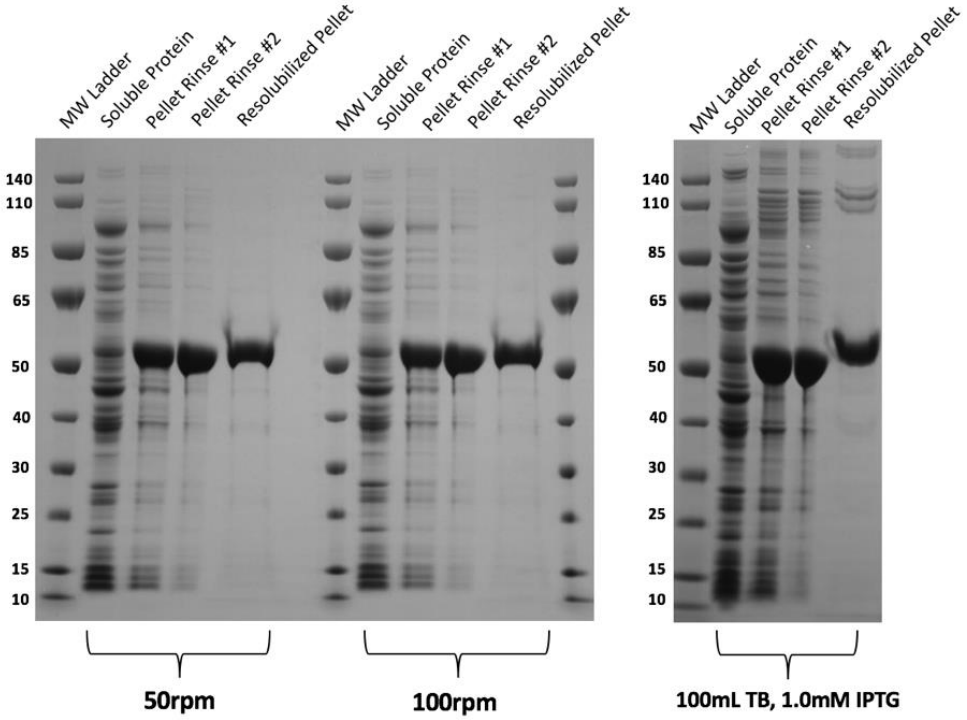

A 16 FliC-Stx2B resolubilized using 50rpm & 100rpm agitation.

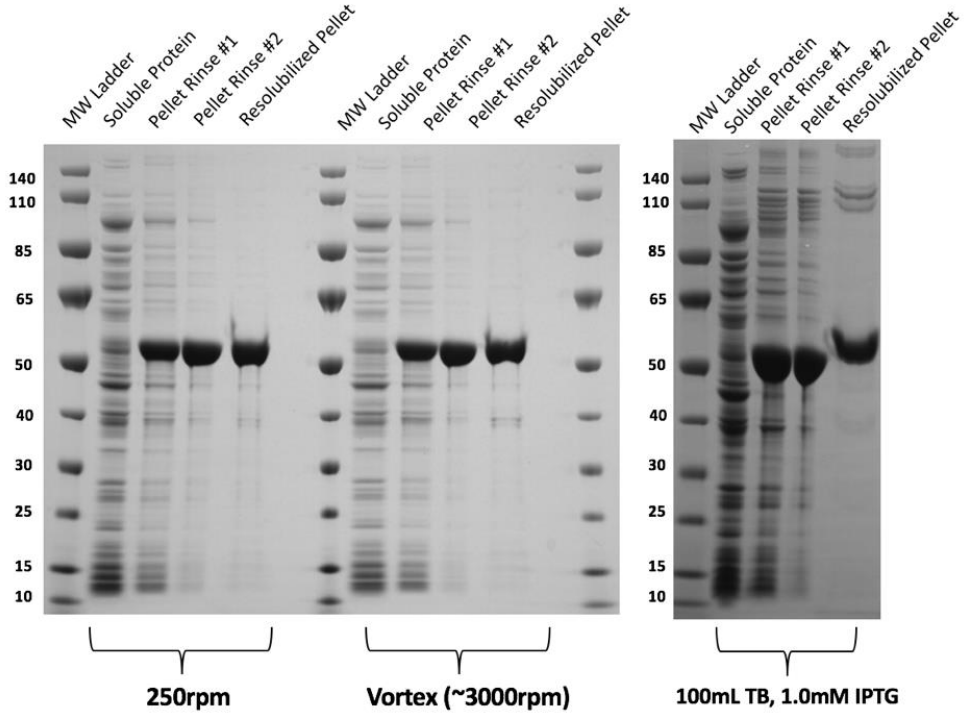

A 17 FliC-Stx2B resolubilized using 250rpm & ~3000rpm agitation.

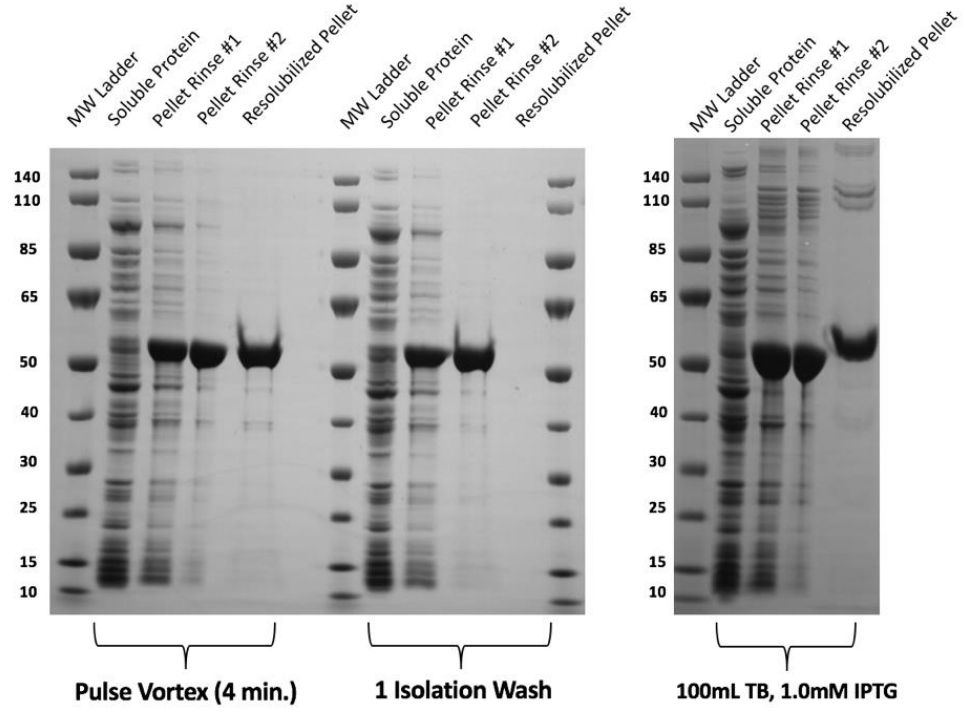

A 18 FliC-Stx2B resolubilized using pulse vortex agitation & single isolation wash.

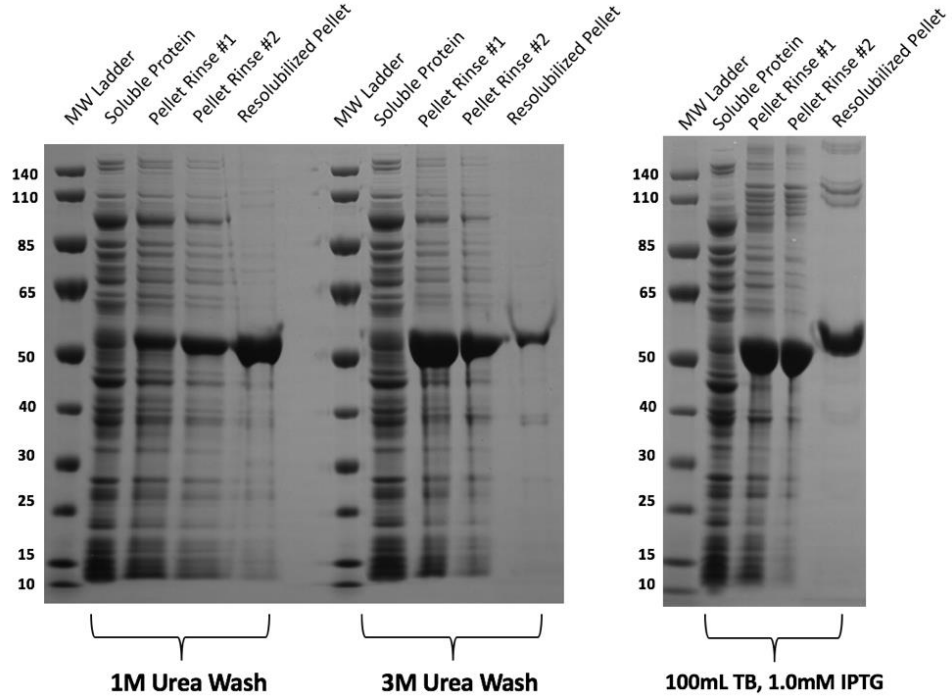

A 19 FliC-Stx2B resolubilized using 1M or 3M urea detergent washes.

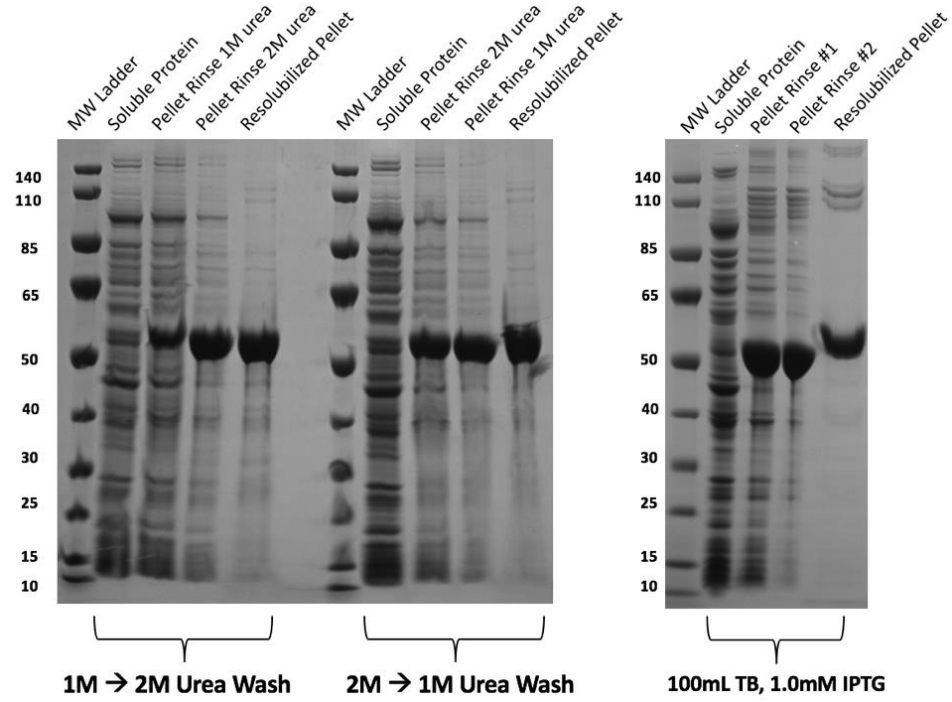

A 20 FliC-Stx2B resolubilized using detergent wash concentrations.

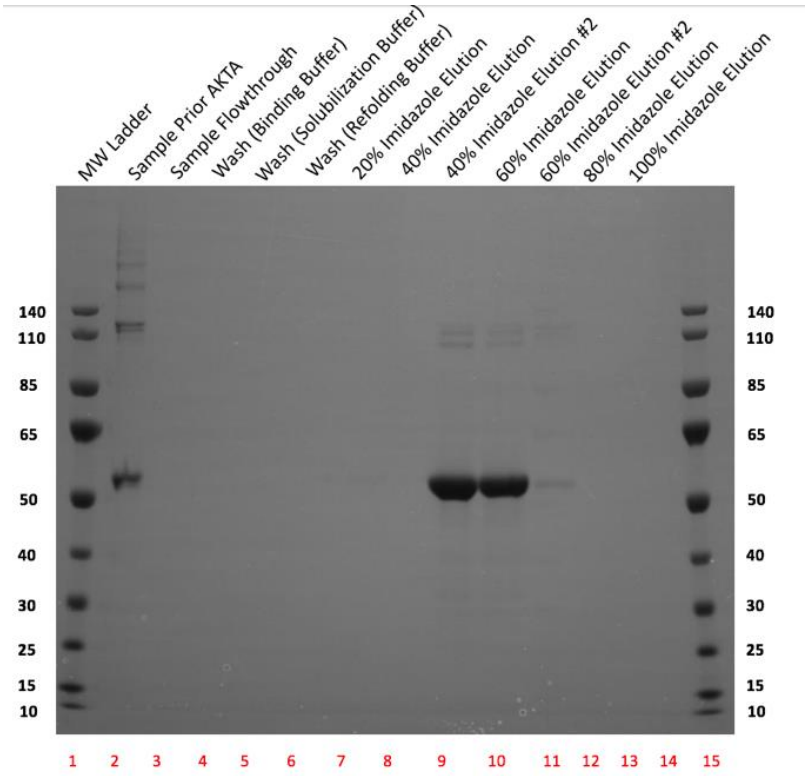

A 21 One-hour refolded FliC-Stx2B purification.

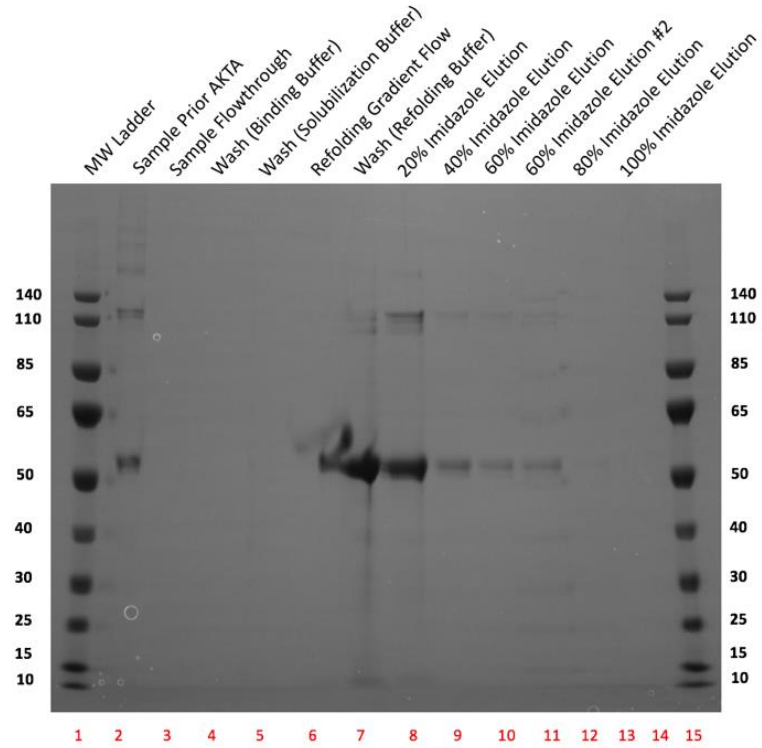

A 22 Three-hour refolded FliC-Stx2B purification.

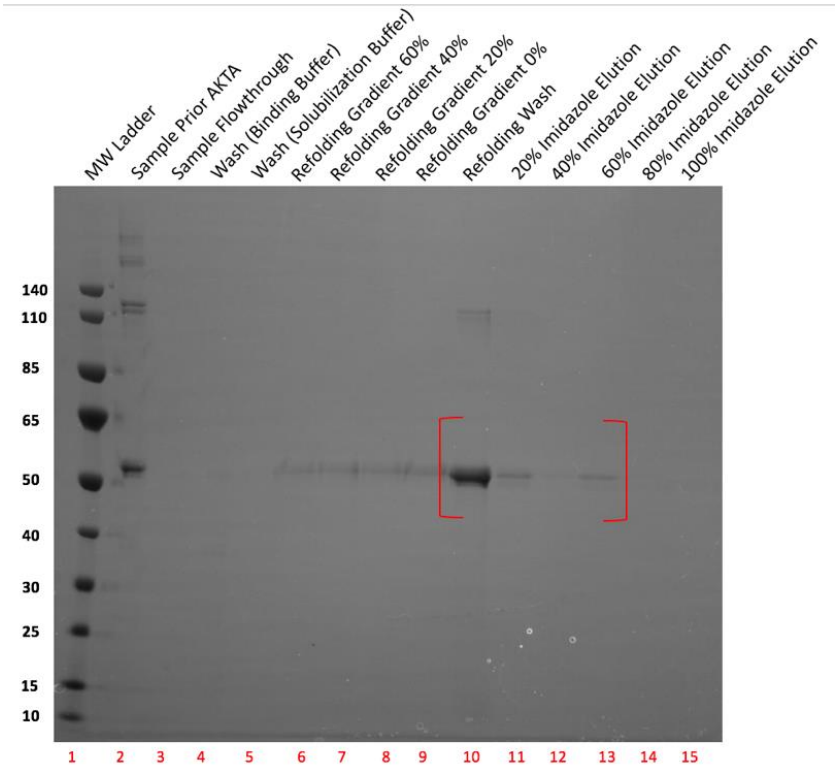

A 23 Six-hour refolded FliC-Stx2B purification.

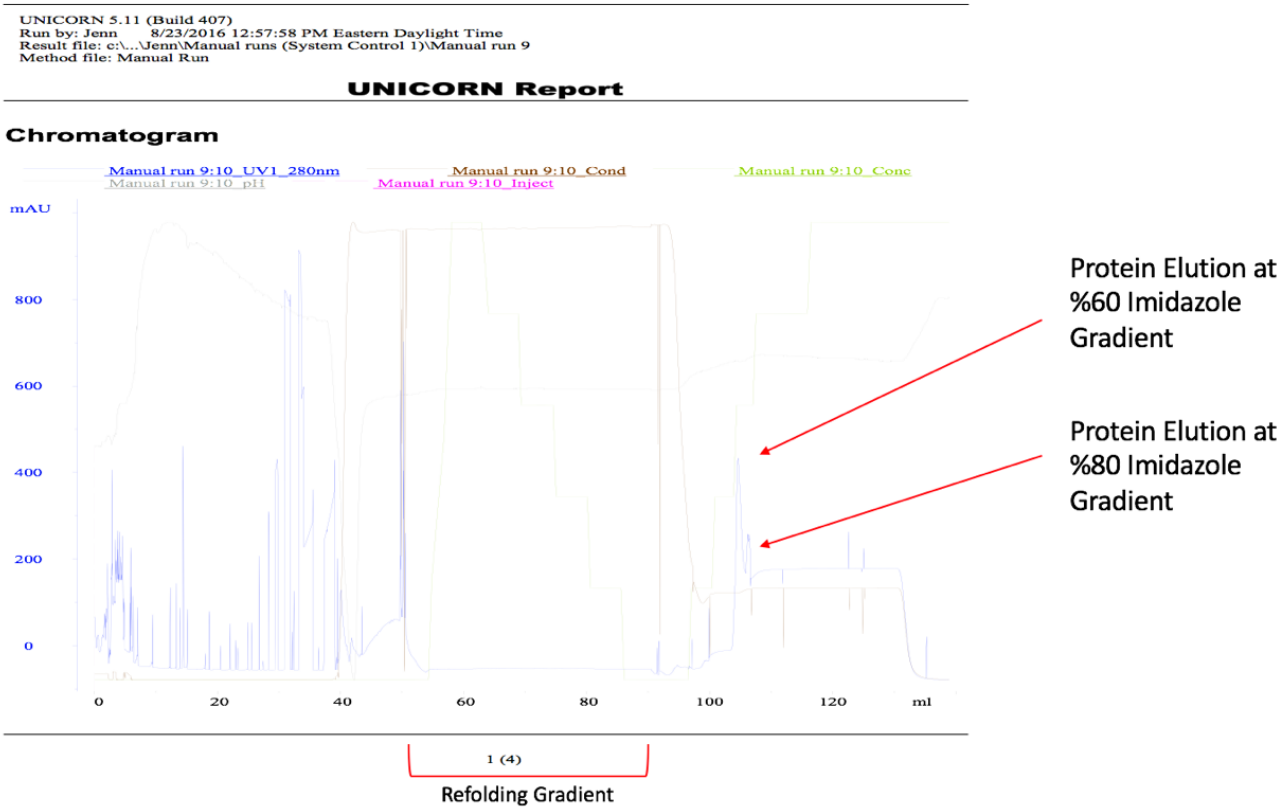

A 24 FliC-Stx2B refolding purification AKTA® FPLC chromatogram.

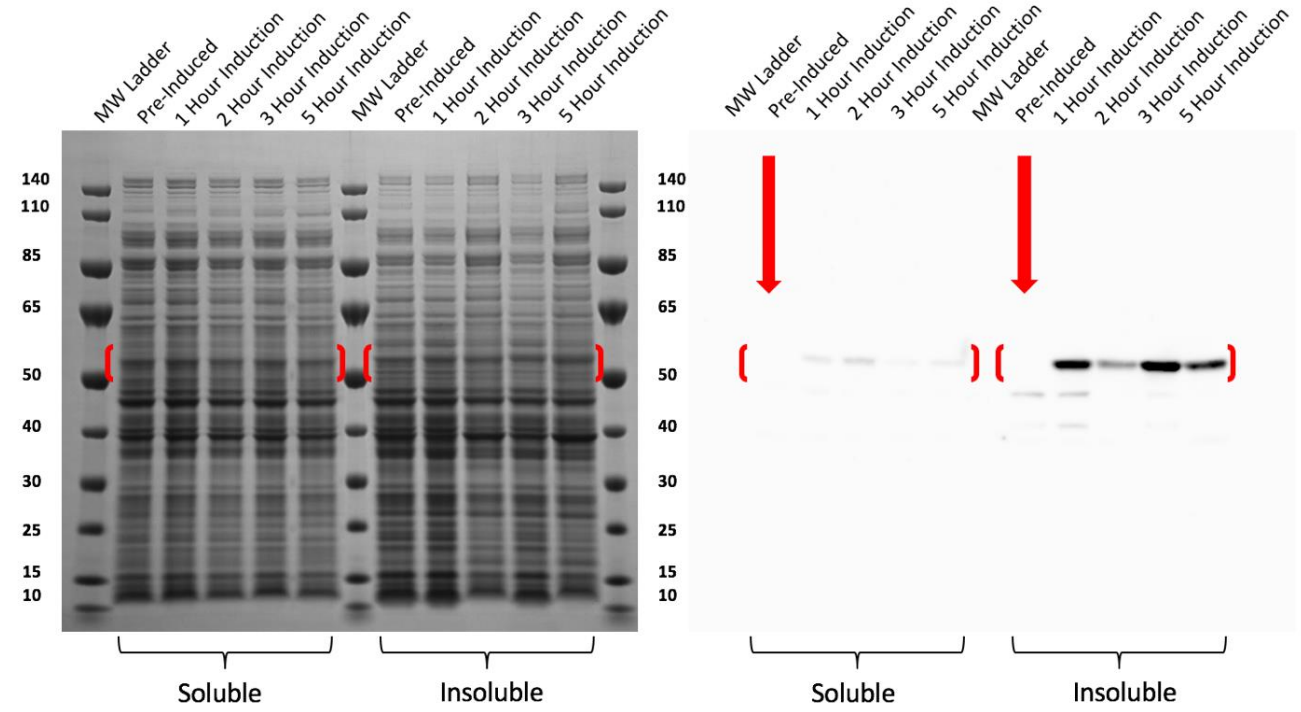

A 25 FliC-Stx2B fed-batch fermentation in ECAM.

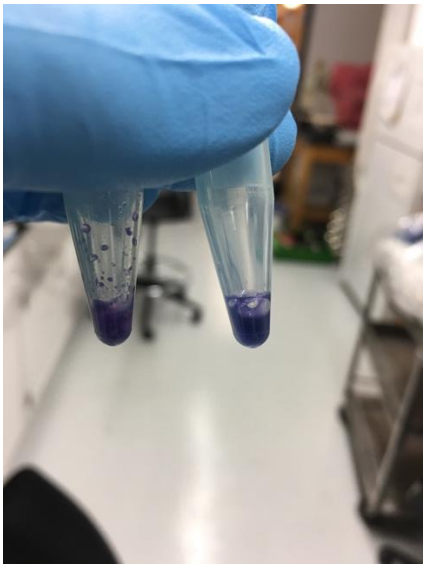

A 26 LDS test for guanidine hydrochloride retention.

Appendix A.4 Media & Buffer list

Media:

SOB (1L)

20g Tryptone
5g Yeast extract
0.5g NaCl
2.4g Magnesium sulfate anhydrous
286mg Potassium chloride
diH2O
pH 6.8-7.0

Luria Broth (1L)

10g Tryptone
10g NaCl
5g Yeast extract
diH2O
pH 7.0

Terrific Broth (1L)

12g Tryptone
24g Yeast extract
4mL Glycerol
2.31 g Potassium phosphate monobasic
12.54g Potassium phosphate dibasic
diH2O
pH 7.0

***E. coli* adaptation media (1L)**

7.8g KH_2PO_4
1.0g Citric acid
2.33g $(NH_4)_2SO_4$
1mL Trace metal solution
1mL Thiamine HCl solution
40mL Glucose stock solution
13mL $MgSO_4$ solution
0.5mlL CaC_{12} solution
50mg Carbenicillin
34mg Chloramphenicol
diH2O
pH 7.2

Buffers:

Super Q equilibration buffer (1L)

20mM Tris
diH2O
pH 7.2

B80 Lysis buffer (1L)

50mM Tris
125mM NaCl
10mM EDTA
4% Sucrose
diH2O
pH 8.0

Pellet resuspension buffer (B57, 1L)

100mM Tris
8M Urea
diH2O
pH 8.0

Resuspension buffer (1L)

20mM Tris
diH2O
pH 8.0

Isolation buffer (1L)

2M Urea
20mM Tris
0.5M NaCl
2% Triton X-100
diH2O
pH to 8.0

Binding buffer (1L)

6M Guanidine Hydrochloride
20mM Tris
0.5M NaCl
20mM Imidazole
1mM DTT
diH2O
pH 8.0

Solubilization buffer (1L)

6M Urea
20mM Tris
0.5M NaCl
20mM Imidazole
1mM DTT
diH2O
pH 8.0

Refolding buffer (1L)

20mM Tris
0.5M NaCl
20mM Imidazole
1mM DTT
diH2O
pH 8.0

Elution buffer (1L)

20mM Tris
0.5M NaCl
0.5M Imidazole
1mM DTT
diH2O
pH 8.0

PBST (1L)

0.05% Tween 20 in Phosphate-buffered saline
diH2O
pH 7.4

50X TAE (1L)

242g Tris base
57.1mL Glacial acetic acid
100mL EDTA (500mM)
diH2O
pH 8.0

ELISA substrate solutions:

ELISA Coating buffer (1L)

1.5g Sodium Carbonate anhydrous
2.93g Sodium Bicarbonate
diH2O
pH 9.6

ELISA Wash buffer (1L)

8.0g Sodium Chloride
0.2g Potassium Chloride
1.15g Sodium Phosphate dibasic anhydrous
0.2g Potassium Phosphate monobasic
0.05% Tween 20
5% Nonfat dry milk
diH2O
pH 7.4

ELISA Blocking buffer (1L)

5% Non-fat dry milk in PBST
diH2O
pH 7.4

TBST solution buffer (1L)

20mM Tris-HCl
0.15mM NaCl
1% Triton X-100
diH2O
pH 7.4

TBST-Milk solution buffer (1L)

20mM Tris-HCl
0.15mM NaCl
1% Triton X-100
5% nonfat dry milk
diH2O
pH 7.4